THEORETISCHE CHEMIE

SS 2010

INTRODUCTION TO MCTDH

LECTURE NOTES

Prof. Dr. Hans-Dieter Meyer

LaTeXversion: Dr. Daniel Peláez-Ruiz

July 2011, revised: June 2013, March 2014, April 2016, April 2017, October 2018

To download this manuscript open the MCTDH web site:
http://mctdh.uni-hd.de
then click on *Literature Downloads* and then on *intro_MCTDH*
Or use the direct link:
http://www.pci.uni-heidelberg.de/tc/usr/mctdh/lit/intro_MCTDH.pdf

Contents

List of Figures

Abbreviations

CAP Complex Absorbing Potential

CDVR Correlation Discrete Variable Representation

CI Configuration Interaction

CMF Constant Mean Field

CPU Central Process Unit

D Dimension

DF Dirac-Frenkel

DOF Degree Of Freedom

DVR Discrete Variable Representation

EOM Equation Of Motion

FBR Finite Basis Representation

FD Filter Diagonalization

GB Gigabyte

GS Ground State

IR Infrared

KB Kilobyte

MB Megabyte

MCTDH Multiconfiguration Time-Dependent Hartree

ML-MCTDH Multi-Layer Multiconfiguration Time-Dependent Hartree

PB Petabyte

PDE Partial Differential Equation

PES Potential Energy Surface

RPA Ramdon-Phase Approximation

SE Schrödinger Equation

SIL Short Iterative Lanczos

SPF Single Particle Function

SPP Single Particle Potential

TB Terabyte

TD Time Dependent

TD-DVR Time-Dependent Discrete Variable Representation

TDH Time-Dependent Hartree

TDHF Time-Dependent Hartree-Fock

TDSE Time Dependent Schrödinger Equation

TIH Time-Independent Hartree

TISE Time Independent Schrödinger Equation

VP Variational Principle

WF Wave Function

WP Wave Packet

Chapter 1

Introduction to Quantum Dynamics

1.1 Time-dependent versus time-independent methods

If the Hamiltonian is time-dependent, *e.g.* because there is a coupling to an external electromagnetic field, the time-dependent (TD) version of the Schrödinger equation (TDSE) obviously must be used[1,2]

$$i\dot{\Psi}(\boldsymbol{q},t) = \hat{H}(t)\Psi(\boldsymbol{q},t) \tag{1.1}$$

However, one often deals with systems where the Hamiltonian is time-independent. When solving those problems, why engage the seemingly complicated TD version of the Schrödinger equation, why not turn to the time-independent (TI) one?

$$\hat{H}\Psi_n(\boldsymbol{q}) = E_n\Psi_n(\boldsymbol{q}) \tag{1.2}$$

In the time-dependent Schrödinger equation there appears one more variable, the time. But mathematically the TDSE is a simpler equation than the time-independent one. The TDSE is an initial value problem of a first order differential equation, a very simple mathematical problem except that it is of very high, in fact infinite, dimensionality. The TISE poses an eigenvalue problem which is more complicated. The dimensionality of both problems is the same, provided one uses identical discretization schemes (basis sets, grids, etc.). Which method, TD or TI, is more appropriate, depends on the problem to be solved. The TDSE may need to be solved over a long time interval and the TISE may have to provide many eigenstates. If only the ground-state (GS) is desired (this is not a dynamical problem, though) then the TISE is the obvious method of choice. However, even for obtaining a ground state wavefunction the TD method is quite often used, although with a slight modification: propagation in imaginary time, the so called relaxation method. We will discuss this later.

[1] Except for purely periodic interactions when one may use the Floquet-Theorem to transform the problem to a time-independent one.

[2] We use a unit system with $\hbar = 1$ throughout.

The TD method is of advantage if the propagation time needed is rather short. Obviously, the numerical effort increases, at least linearly, with propagation time. Hence, scattering and half-scattering processes are particularly well suited for being treated within the TD picture. Firstly, because the interaction time is finite and often rather short. And secondly, because one has to deal with continua. The inclusion of continua makes the solution of the TISE much harder. The SE has to be solved with respect to complicated boundary conditions. The eigenvalue equation

$$H\Psi_E = E\Psi_E \tag{1.3}$$

is then solved for a set of fixed energies (every energy is an eigenvalue, we are in a continuum), usually by solving spatial differential equations on a grid.

In the TD world, however, one propagates a wavepacket (WP), and there is no difference in propagating a wavepacket which is a superposition of bound-states to a superposition of continuum states. It is the same propagation algorithm but possibly on longer grids.

Let us draw some pictures of scattering or half-scattering problems.:

- Photodissociation:

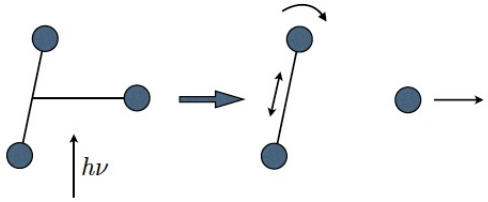

- Inelastic scattering:

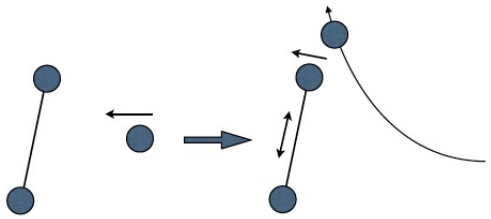

- Reactive scattering:

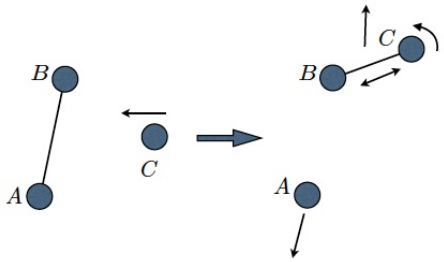

It can be easily seen that the TD method requires three steps:

(1) Preparation of the initial state $\Psi(0)$.

(2) Propagation: $\Psi(0) \rightarrow \Psi(t)$.

(3) Analysis: $\Psi(t) \rightarrow$ observables (cross-sections, spectra, etc.).

1.2 Initial state

We discuss by two typical examples how to choose an initial state.

1.2.1 Photoexcitation and Photodissociation

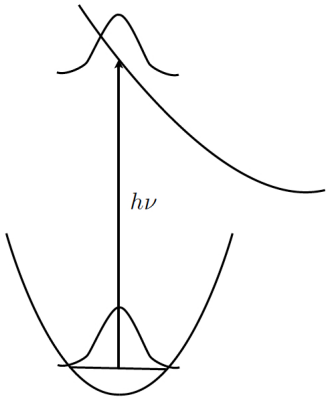

Figure 1.1: Photodissociation initial step.

When studying photoexcitation or photodissociation, the initial state is the vibrational ground state (GS) of the electronic ground state potential energy surface (PES) placed on an excited state PES (Condon approximation, see Fig.1.1). In a more general case, the initial state is the GS multiplied with a dipole operator surface.

1.2.2 Inelastic scattering, reactive scattering

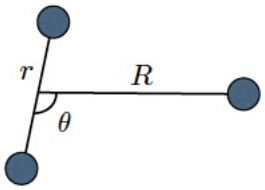

Figure 1.2: Definition of Jacobi coordinates for a triatomic molecule.

For inelastic or reactive scattering, one may take a Hartree product as initial state

$$\Psi(t=0;\theta,r,R) = \Psi_1(\theta)\ \Psi_2(r)\ \Psi_3(R) \tag{1.4}$$
$$\Psi_1(\theta) = \text{const.} \times P_j(cos\theta)$$
$$\Psi_2(r) = \text{eigenfunction of vibrational Hamiltonian which includes a centrifugal potential)}$$
$$\Psi_3(R) = \text{many choices possible, usually gaussian times plane wave}$$

This makes it clear that we obtain only information with respect to the initial state. *E.g.* if in the inelastic scattering problem the initial state is chosen such, that the diatom is in its ($j = 0$, $v = 0$) quantum state, then we can obtain only the cross sections

$$\sigma(E,(0,0) \ \rightarrow \ (j'',v'')) \tag{1.5}$$

To obtain the cross sections

$$\sigma(E,(j',v') \ \rightarrow \ (j'',v'')) \tag{1.6}$$

one has to run a propagation with a wavepacket initially in (j', v'). Furthermore, the initial state of relative motion, $\Psi_3(R)$, its velocity distribution, determines the energy range investigated.

To discuss this more formally, we inspect the S-matrix. With a TI method one always computes the full S-matrix for one energy

$$S(E) = \begin{pmatrix} \vdots & & \cdots & \\ & \ddots & & \vdots \\ \vdots & \ddots & & \\ & & \cdots & \end{pmatrix} \tag{1.7}$$

whereas a TD method generates one column of the S-matrix for a range of energies.

$$S(E) = \begin{pmatrix} & \Psi(0) & \\ & | & \\ & | & \\ & | & \end{pmatrix} \tag{1.8}$$

That only one column is generated is not a disadvantage, it is in fact an advantage! For large systems one does not want to know all state-to-state cross sections or, more generally, all quantum information. Only a selected set of information is wanted. Using the TD picture it is much easier to concentrate on the desired observables as compared to the TI picture.

Turning to the numerical representation of a WP we note another advantage of the TD picture and this one is probably the most important one for approximate methods. The TD WP (at each instant of time), is less structured and hence easier to represent compared to eigenstates (except for the GS). Time Dependent Hartree (TDH) is known to yield better eigenenergies than TIH. In electronic structure theory TDHF is is known to be equivalent to the Random-Phase Appromixation (RPA) which contains some correlation.

To give another example. In the the $70s$, Heller introduced Gaussian WP propagation. He wrote the WP as

$$\Psi(x,t) = \exp[-\alpha(t)\cdot(x-x_0(t))^2 - ip_0(t)\cdot(x-x_0(t)) + \gamma(t)] \tag{1.9}$$

and derived EOM for the parameters α, x_0, p_0, and γ.

This is a simple, crude method, but for several systems it provides useful information; spectra, etc. While approximating a time-dependent WP by a Gaussian may work reasonably well, approximating eigenstates by a Gaussian is useless. Only the GS can be approximated by a single Gaussian.

1.3 Analysis

We want to give some examples for the analysis step

$$\Psi(t) \rightarrow \text{observables}$$

1.3.1 Power spectrum

$$\sigma(E) = \big\langle \Psi \big| \delta(E-H) \big| \Psi \big\rangle \tag{1.10}$$

If the spectrum is discrete, we can insert the completeness relation

$$\mathbf{1} = \sum_n \big|\Psi_n\big\rangle\big\langle\Psi_n\big|$$

where

$$H\Psi_n = E\Psi_n$$

then

$$\begin{aligned}\sigma(E) &= \sum_{n,m} \langle\Psi|\Psi_n\rangle\langle\Psi_n|\delta(E-H)\ |\Psi_m\rangle\langle\Psi_m|\Psi\rangle \\ &= \sum_{n,m} \langle\Psi|\Psi_n\rangle\ \delta(E-E_n)\ \delta_{n,m}\langle\Psi_m|\Psi\rangle \\ &= \sum_n |C_n|^2\ \delta(E-E_n) \end{aligned} \tag{1.11}$$

with

$$C_n = \langle\Psi_n|\Psi\rangle \tag{1.12}$$

and hence

$$\Psi = \sum_n C_n\ \Psi_n \tag{1.13}$$

Turning to the time-dependent picture, we use the Fourier representation of the δ-function

$$\delta(E) = \frac{1}{2\pi}\int_{-\infty}^{\infty} e^{iEt}\ dt \tag{1.14}$$

$$\begin{aligned}\sigma(E) &= \frac{1}{2\pi}\int_{-\infty}^{\infty} \langle\Psi|e^{i(E-H)t}|\Psi\rangle\ dt \\ &= \frac{1}{2\pi}\int_{-\infty}^{\infty} e^{iEt}\ \langle\Psi|\Psi(t)\rangle dt \\ &= \frac{1}{2\pi}\int_{-\infty}^{\infty} e^{iEt}\ a(t) dt \end{aligned} \tag{1.15}$$

with the autocorrelation function

$$a(t) = \langle\Psi|e^{-iHt}|\Psi\rangle = \langle\Psi|\Psi(t)\rangle \tag{1.16}$$

The integration over negative time is cumbersome, but can easily be avoided. If the Hamiltonian is hermitian, one finds

$$a(-t) = \langle\Psi|e^{iHt}|\Psi\rangle = \langle e^{-iHt}\ \Psi|\Psi\rangle = \langle\Psi|e^{-iHt}|\Psi\rangle^* = [a(t)]^* \tag{1.17}$$

Thus

$$\int_{-\infty}^{0} e^{iEt}\ a(t)\ dt = \int_0^{\infty} e^{-iEt}\ a(-t)\ dt = \int_0^{\infty} [e^{iEt}\ a(t)]^*\ dt \tag{1.18}$$

$$\sigma(E) = \frac{1}{2\pi}\int_0^{\infty} \big([e^{iEt}\ a(t)]^* + e^{iEt}\ a(t)\big) dt = \frac{1}{\pi} Re \int_0^{\infty} e^{iEt}\ a(t)\ dt \tag{1.19}$$

More tricks are possible

$$\begin{aligned} a(t) &= \langle\Psi|e^{-iHt}|\Psi\rangle \\ &= \langle e^{iH^\dagger t/2}\ \Psi|e^{-iHt/2}\ \Psi\rangle \\ &= \langle\big(e^{-iH^{\dagger *}t/2}\ \Psi^*\big)^*|e^{-iHt/2}\ \Psi\rangle \\ &= \langle\Psi(t/2)^*|\Psi(t/2)\rangle \end{aligned} \tag{1.20}$$

where the last step requires a real initial state ($\Psi^* = \Psi$) and a symmetric Hamiltonian

$$H = H^T = H^{\dagger^*} \tag{1.21}$$

This so-called $t/2$-trick is very useful because it provides an autocorrelation function which is twice as long as the propagation. In general, one wants to use both, Eq. (1.19) and Eq. (1.20). This requires a real-symmetric Hamiltonian. Fortunately, real-symmetric Hamiltonians augmented with a complex absorbing potential (CAP) are not excluded. A closer analysis shows that the sign of a CAP has to be inverted when propagating in negative time. This keeps Eq. (1.17-1.19) valid even for CAP augmented real-symmetric Hamiltonians.

One will never be able to perform the propagation up to $t = \infty$ but will stop at some finite time T. Rather than replacing the upper integral limit by T, we introduce a window function $g(t)$

$$\sigma_g(E) = \frac{Re}{\pi} \int_0^\infty e^{iEt}\ g(t)\ a(t)\ dt = \frac{1}{2\pi} \int_{-\infty}^\infty e^{iEt}\ g(t)\ a(t)\ dt \tag{1.22}$$

and require

$$0 \le g(t) \le 1, \quad g(0) = 1, \quad g(t) = 0 \text{ for } |t| > T, \quad g(t) = g(-t) \tag{1.23}$$

As well known, the Fourier transform of a product of two functions is equal to the convolution of the Fourier transforms of the two functions. *I.e.*

$$\begin{aligned} \sigma_g(E) &= (\sigma * \tilde{g})(E) \\ &= \int \sigma(\epsilon)\ \tilde{g}(E-\epsilon)\ d\epsilon \\ &= \int \sigma(E-\epsilon)\ \tilde{g}(\epsilon)\ d\epsilon \end{aligned}$$

where

$$\tilde{g}(\epsilon) = \frac{1}{2\pi} \int_{-\infty}^\infty e^{i\epsilon t}\ g(t)\ dt$$

The proof is simple, we use

$$\delta(\tau - t) = \frac{1}{2\pi} \int e^{i(\tau-t)\epsilon}\ d\epsilon \tag{1.24}$$

$$\begin{aligned} \sigma_g(E) &= \frac{1}{2\pi} \int_{-\infty}^\infty e^{iEt}\ g(t)\ a(t)\ dt \\ &= \frac{1}{2\pi} \int\int e^{iEt}\ g(\tau)\ a(t)\ \delta(\tau - t)\ dt\ d\tau \\ &= \frac{1}{(2\pi)^2} \int\int\int e^{iEt}\ a(t)\ e^{-i\epsilon t}\ e^{i\epsilon\tau}\ g(\tau)\ d\tau\ dt\ d\epsilon \\ &= \frac{1}{2\pi} \int\int e^{i(E-\epsilon)t}\ a(t)\ \tilde{g}(\epsilon)\ dt\ d\epsilon \\ &= \int \sigma(E-\epsilon)\ \tilde{g}(\epsilon)\ d\epsilon \end{aligned} \tag{1.25}$$

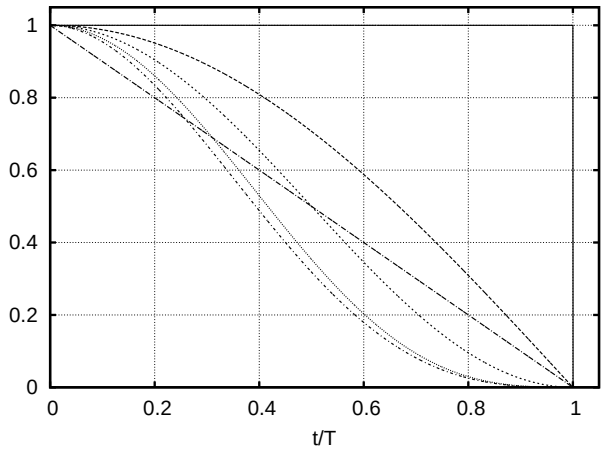

Figure 1.3: Window functions g_0, g_1, g_2, g_3 and, to be discussed below, g_0' and g_1'. The straight line is g_0' whereas g_1' is the lowest curve in the plot.

We now can choose g to have compact support, *i.e.*

$$g(t) = 0 \qquad \text{if } |t| > T \tag{1.26}$$

In particular, we inspect the three window functions

$$g_k(t) = cos^k\left(\frac{\pi t}{2T}\right)\theta\big(1 - \frac{|t|}{T}\big) \tag{1.27}$$

for $k = 0, 1, 2, 3$. These are displayed in Fig. 1.3

Fourier-transforming the (time) window functions g_k yield the energy window functions $\tilde{g}_k$

$$\tilde{g}_0(\omega) = \frac{\sin(\omega T)}{\pi\omega} \tag{1.28}$$

$$\tilde{g}_1(\omega) = \frac{2T\cos(\omega T)}{(\pi - 2\omega T)\ (\pi + 2\omega T)} \tag{1.29}$$

$$\tilde{g}_2(\omega) = \frac{\pi\sin(\omega T)}{2\omega\ (\pi - \omega T)(\pi + \omega T)} \tag{1.30}$$

$$\tilde{g}_3(\omega) = \frac{12\pi^2 T\cos(\omega T)}{(\pi - 2\omega T)\ (\pi + 2\omega T)(3\pi - 2\omega T)\ (3\pi + 2\omega T)} \tag{1.31}$$

The oscillations caused by the box-filter ($k = 0$) are known as Gibbs phenomena. To avoid or at least lessen those we use in general g_1 or g_2. As shown in Fig. 1.4 the better filter leads to broader lines. The energy window functions $\tilde{g}_k$ are normalized as $\int \tilde{g}_k(\omega)\, d\omega = 1$. For better visibility, however, they are renormalized in Fig. 1.4 at their maxima.

For the convenience of the reader we provide the full widths at half maximum (FWHM) of the window functions $\tilde{g}_k$. (The filter functions $\tilde{g}'$ will be discussed below.) The entries in Table 1.1 are to be divided by the length of the autocorrelation function to yield the FWHM.

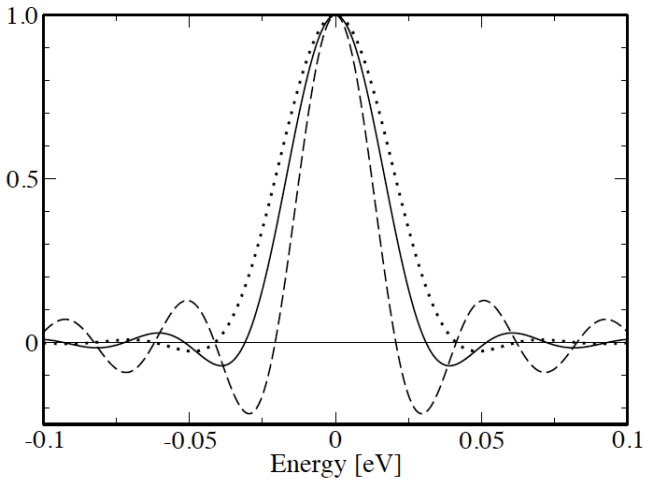

Figure 1.4: Energy window functions. Reduction of the Gibbs phenomenon by application of time window functions: (i) $\tilde{g}_0$, dashed line; (ii) $\tilde{g}_1$, solid line; (iii) $\tilde{g}_2$, dotted line. The length of the autocorrelation function is $T = 100$ fs

$\tilde{g}_0$	$\tilde{g}_1$	$\tilde{g}_2$	$\tilde{g}_3$	$\tilde{g}'_0$	$\tilde{g}'_1$	unit
2.49	3.38	4.14	4.78	3.66	4.91	eV fs
20.1	27.3	33.2	38.6	29.5	39.6	cm^{-1} ps

Table 1.1: FWHM values of the window functions $\tilde{g}_k$ times the length of the autocorrelation function. Remember that the length of the autocorrelation function is twice the propagation time, if the t/2-trick, Eq.(1.20), is used.

As well known, the Fourier transform of the convolution of two functions equals the product of the Fourier transforms of the functions (cf. Eqs.(1.24,1.25)). A self-convolution of a filter function thus leads to a filter in ω-space which is a square and hence non-negative, a very desirable property. We define

$$g'(t) = \frac{a}{2T} \int g(\tau) g(2t - \tau) d\tau \ , \tag{1.32}$$

where a is a normalization factor to be chosen such that $g'(0) = 1$. *I.e.* $a = 2T/\int [g(\tau)]^2 d\tau$. One has to use $2t$ rather than t as shift to ensure that the new function, g', has again the support $[-T, T]$. The Fourier transform reads

$$\tilde{g}'(\omega) = \frac{a\pi}{2T} \left[\tilde{g}(\frac{\omega}{2})\right]^2 \ , \tag{1.33}$$

where the appearance of $\omega/2$ is a consequence of the use of $2t$ in Eq.(1.32). This doubles the width of the filter, but the squaring reduces the widths and the overall increase in width is about $\sqrt{2}$. Applying the procedure just described to

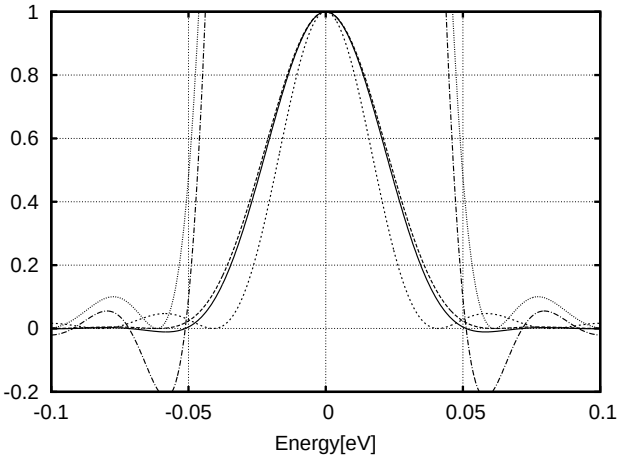

Figure 1.5: Energy window functions, second set. (i) $\tilde{g}_3$, solid line; (ii) $\tilde{g}'_0$, dotted line; (iii) $\tilde{g}'_1$, dashed line. For $\tilde{g}_3$ and $\tilde{g}'_1$ the wings of the filters are also shown 20 times enlarged. The length of the autocorrelation function is $T = 100$ fs.

g_0 and g_1 yields

$$g'_0(t) = (1 - |t|/T)\,\theta(T - |t|) \tag{1.34}$$

$$g'_1(t) = \left[\left(1 - \frac{|t|}{T}\right)\cos(\frac{\pi t}{T}) + \frac{1}{\pi}\sin(\frac{\pi|t|}{T})\right]\theta(T - |t|)\,, \tag{1.35}$$

and their Fourier transforms read

$$\tilde{g}'_0(\omega) = \frac{T}{2\pi}\,\frac{\sin^2(\omega T/2)}{(\omega T/2)^2} \tag{1.36}$$

$$\tilde{g}'_1(\omega) = \frac{4\pi T\,\cos^2(\omega T/2)}{(\pi - \omega T)^2\,(\pi + \omega T)^2}\,. \tag{1.37}$$

It should be emphasized again, that the $\tilde{g}'$ filters are non-negative. In particular, $\tilde{g}'_1$ is an almost ideal filter with only very small wing-oscillations. See Fig.1.5 However, it is the broadest of all filters discussed.

The power spectrum, although very useful, is an academic quantity. Let us turn to real spectra, *e.g.* absorption spectra.[3]

$$I(\omega) = \frac{\pi\omega}{3c\epsilon_0\hbar^2}\sum_n \left|\langle\Psi_n^{(f)}|\mu|\Psi_0^{(i)}\rangle\right|^2\,\delta(\hbar\omega + E_0^{(i)} - E_n^{(f)}) \tag{1.38}$$

μ is the transition operator, usually the dipole operator (μ has three components. As the molecule freely rotates one averages over the three intensities).
For electronic spectra one often adopts the Condon approximation and sets $\mu = 1$. $\Psi_n^{(f)}$ and $E_n^{(f)}$ are the exact eigenstates and energies of the final PES and similar for the superscript (i), which refers to the initial electronic state.

[3] Usually $\hbar = 1$, but here we reintroduce $\hbar$.

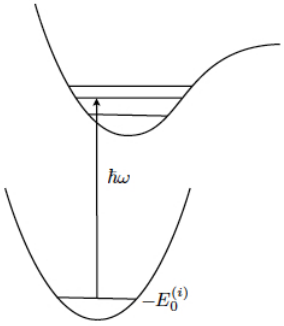

Figure 1.6: Electronic transition.

On the other hand, infrared spectroscopy is characterized by the initial and final electronic states been identical, $i = f$.

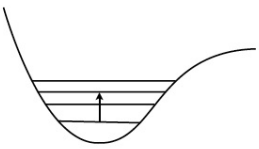

Figure 1.7: Infrared absorption.

We now rearrange the sum

$$\begin{aligned}
&\sum_n \left\langle \Psi_0^{(i)} \middle| \mu^\dagger \middle| \Psi_n^{(f)} \right\rangle \delta(\hbar\omega + E_0^{(i)} - E_n^{(f)}) \left\langle \Psi_n^{(f)} \middle| \mu \middle| \Psi_0^{(i)} \right\rangle \\
&= \left\langle \Psi_0^{(i)} \middle| \mu^\dagger \ \delta(\hbar\omega + E_0^{(i)} - H) \ \mu \middle| \Psi_0^{(i)} \right\rangle \\
&= \left\langle \Psi_\mu \middle| \delta(\hbar\omega + E_0^{(i)} - H) \middle| \Psi_\mu \right\rangle
\end{aligned} \tag{1.39}$$

with $\Psi_\mu = \mu \left| \Psi_0^{(i)} \right\rangle$.

Hence

$$I(\omega) = \frac{\pi\omega}{3c\epsilon_0\hbar^2} \sigma_{\text{Power},\Psi_\mu}(\hbar\omega + E_0^{(i)}) \tag{1.40}$$

Most of the observables one wants to compute are determined by a Fourier transform of some correlation function.

1.4 Autocorrelation functions

The wave function may consist of a discrete and a continuous part:

$$\Psi = \sum_n C_n \varphi_n + \int_{E_c}^{\infty} C(E) \ \varphi_E \ dE \tag{1.41}$$

with

$$\begin{aligned} H\varphi_n &= E_n\varphi_n \qquad (E_n \le E_c,\ E_c \text{ is the threshold for continuum}) \\ H\varphi_E &= E\varphi_E \qquad (E > E_c) \end{aligned}$$

and

$$\langle\varphi_n|\varphi_m\rangle = \delta_{n,m} \quad \langle\varphi_n|\varphi_E\rangle = 0 \quad \langle\varphi_E|\varphi_{E'}\rangle = \delta(E-E') \tag{1.42}$$

$$C_n = \langle\varphi_n|\Psi\rangle, \quad C(E) = \langle\varphi_E|\Psi\rangle \qquad (C(E) = 0 \text{ for } E \le E_c) \tag{1.43}$$

The power spectrum

$$\sigma(E) = \langle\Psi|\delta(E-H)|\Psi\rangle \tag{1.44}$$

is then given by

$$\sigma(E) = \sum_n |C_n|^2\ \delta(E-E_n) + |C(E)|^2 \tag{1.45}$$

Switching to the time-dependent picture, we write the wave function as

$$\Psi(t) = \sum_n C_n\ \varphi_n\ e^{-iEt} + \int_{E_c}^{\infty} C(\epsilon)\ \varphi_\epsilon\ e^{-i\epsilon t}\ d\epsilon \tag{1.46}$$

The autocorrelation function then becomes

$$a(t) = \langle\Psi(0)|\Psi(t)\rangle = \sum_n |C_n|^2\ e^{-iE_nt} + \int_{E_c}^{\infty} |C(\epsilon)|^2 e^{-i\epsilon t} d\epsilon \tag{1.47}$$

and the power spectrum in terms of the autocorrelation function is given by Eq. (1.19) or, when using a window function, by Eq. (1.22). It is illustrative to show some autocorrelation functions and the spectra generated from them.

The autocorrelation function of the photodissociation of NOCl vanishes quickly (Fig.1.8). Figure 1.9 shows two spectra generated from this autocorrelation function, one using the window g_0 and the other using g_2. (The spectrum generated with window g_1 lies in between). As the autocorrelation goes to zero, there are no artifacts caused by the Gibbs phenomenon and the window g_0 performs well. The filters g_1 and g_2 wash out the structure of the spectrum and hence should not be used in the present case.

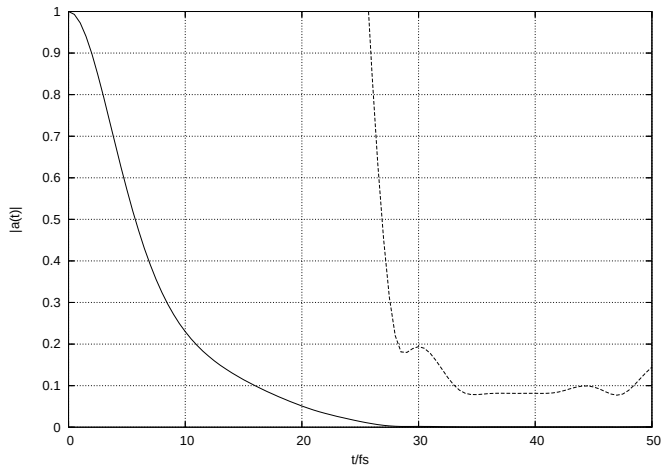

Figure 1.8: Absolute value of the autocorrelation function of the photodissociation process $NOCl \rightarrow NO + Cl$. The dashed line displays $100 \cdot |a(t)|$.

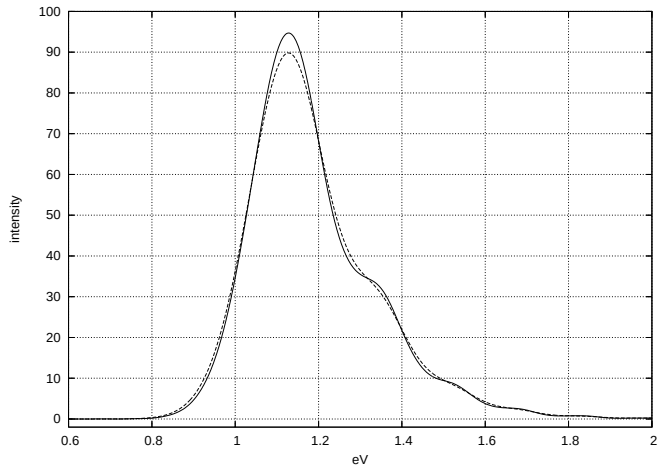

Figure 1.9: Power spectrum generated from the autocorrelation function Fig. 1.8. The full and dashed line spectra were generated with the window g_0 and g_2 respectively.

As a next example, we discuss the autocorrelation and spectrum of photoexcited pyrazine. This is a molecule with 24 degrees of freedom and very complicated dynamics as a conical intersection couples the S_1 and S_2 electronic states. Due to this, an enormous large number of vibrational (or more precisely vibronic) states contribute to the sum in Eq. (1.47).

Although this is a bounded system with no contribution from a continuum, the autocorrelation drops quickly, due to destructive interference in the sum in Eq. (1.47). After 50 fs the autocorrelation oscillates around ~ 0.015 but does not decrease further. This is shown in Fig. 1.10.

The spectra generated from this autocorrelation using different window functions are shown in Fig. 1.11. Using the g_0 window the spectrum shows strong negative parts caused by the Gibbs phenomenon. The spectrum in the middle, which is generated with the g_1 window is much clearer, and the g_2 generated spectrum is even smoother. However, it almost washes out some small oscillations, *e.g.* between 2.3 and 2.4 eV. Hence, the g_1 window seems to be the best choice in this case.

The unphysical negative parts of a spectrum originate from two causes. The first cause is the Gibbs phenomenon, *i.e.* the chopping of the autocorrelation function at $t = T$. For this the window functions were introduced and going from g_0 to g_1 and g_2 will substantially reduce this artifact (see Fig. 1.4). The other cause is an inaccurate autocorrelation function. Small errors in the autocorrelation may lead to small negative parts in the spectrum. These errors are only weakly modified by the window function. In such a case, a more accurate propagation helps.

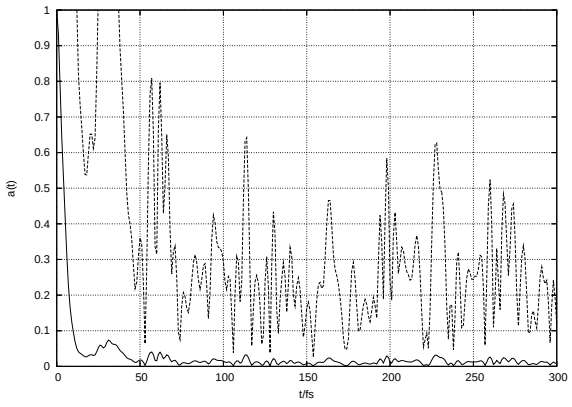

Figure 1.10: Absolute value of the autocorrelation function of the photoexcited pyrazine. The dashed line shows the autocorrelation enlarged by a factor of 20.

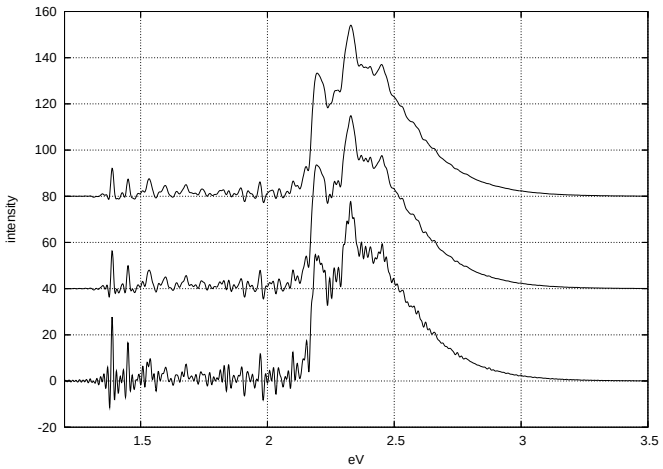

Figure 1.11: Pyrazine spectra generated from the autocorrelation function (Fig.1.10) using the window functions g_0, g_1, and g_2, respectively. (bottom to top)

As third example, we discuss the (bending) excitation of water (Figs.1.12 and 1.13) show the autocorrelation function and spectrum for this model. This is a bound state problem where only a few eigenstates contribute. The autocorrelation function is oscillatory but does not decay. Generating the spectrum with the g_0 window leads to strong artificial oscillations, a beautiful demonstration of the Gibbs phenomenon. The g_1 spectrum (middle) is much improved but in this case the g_2 spectrum (top) is clearly the best.

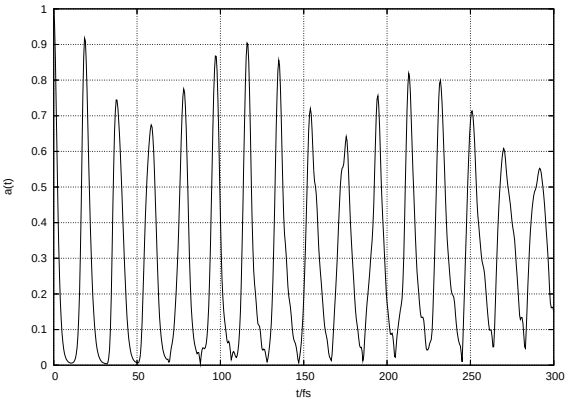

Figure 1.12: Oscillatory autocorrelation function for H_2O.

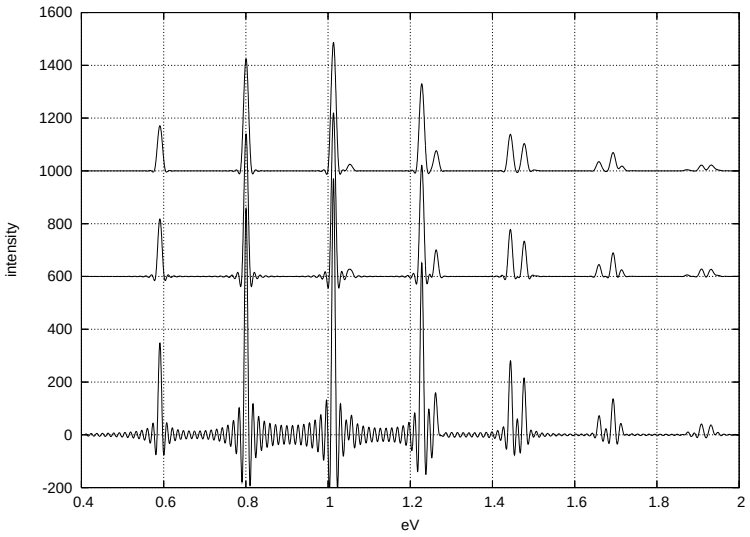

Figure 1.13: Spectrum of H_2O for different window functions. The spectrum is generated from the autocorrelation function displayed in Fig. 1.12. The spectrum obtained with the window functions g_1 and g_2 are shifted upwards by 600 and 1000 units, respectively.

Chapter 2

Standard method and TDH

2.1 Variational Principles

There are three well-known time-dependent variational principles

- Dirac-Frenkel:

$$\langle \delta\Psi | H - i\frac{\partial}{\partial t} | \Psi \rangle = 0 \tag{2.1}$$

- McLachlan:

$$\delta \|\theta - H\Psi\|^2 = 0 \quad (\|\theta - H\Psi\|^2 = min) \tag{2.2}$$

  where θ is varied and $i\dot{\Psi} = \theta$

- Lagrange:

$$\delta \int_{t_1}^{t_2} \langle \Psi | H - i\frac{\partial}{\partial t} | \Psi \rangle dt = 0 \tag{2.3}$$

  with the condition that the variation of the integrand vanishes for $t = t_1$ and $t = t_2$.

McLachlan's principle is equivalent to

$$\mathrm{Im}\langle \delta\Psi | H - i\frac{\partial}{\partial t} | \Psi \rangle = 0 \tag{2.4}$$

if the variational spaces of Ψ and $\dot{\Psi}$ are identical, *i.e.*

$$\{\delta\dot{\Psi}\} = \{\delta\Psi\} \tag{2.5}$$

Analogously, Lagrange's principle implies

$$\mathrm{Re}\langle \delta\Psi | H - i\frac{\partial}{\partial t} | \Psi \rangle = 0 \tag{2.6}$$

If all parameters are complex analytic then $i\delta\Psi$ is an allowed variation when $\delta\Psi$ is an allowed variation and all the variational principles discussed are identical! Hence we use Dirac-Frenkel, which is the simplest. For more details see Appendix B.

Theorem
The equations of motion derived from the Dirac-Frenkel variational principle conserve both norm and energy, if the Hamiltonian is Hermitian and time-independent, $\frac{\partial}{\partial t}H = 0$, and if the model wavefunction Ψ itself is contained in the space of the allowed variations: $\Psi \in \{\delta\Psi\}$.

In order to prove this theorem, first an expression for the time derivative of the expectation value of the nth moment of the Hamiltonian is derived:

$$\begin{aligned}\frac{d}{dt}\langle\Psi\,|\,H^n\,|\,\Psi\rangle &= \langle\dot\Psi\,|\,H^n\,|\,\Psi\rangle + \langle\Psi\,|\,H^n\,|\,\dot\Psi\rangle \\ &= 2\,\mathrm{Re}\,\langle\Psi\,|\,H^n\,|\,\dot\Psi\rangle \\ &= -2\,\mathrm{Im}\,\langle H^n\Psi\,|\,-i\,\frac{\partial}{\partial t}\,|\,\Psi\rangle \\ &= -2\,\mathrm{Im}\,\langle H^n\Psi\,|\,H - i\,\frac{\partial}{\partial t}\,|\,\Psi\rangle\,. \end{aligned} \tag{2.7}$$

The transformation of the last line was performed by addition of the real expectation value $\langle\Psi\,|\,H^{n+1}\,|\,\Psi\rangle$.

For $n = 0$ Eq. (2.7) proves the conservation of norm:

$$\frac{d}{dt}\langle\Psi\,|\,1\,|\,\Psi\rangle = -2\,\mathrm{Im}\,\langle\Psi\,|\,H - i\,\frac{\partial}{\partial t}\,|\,\Psi\rangle = 0\,, \tag{2.8}$$

as Eq. (2.1) ensures that $\langle\Psi\,|\,H - i\,\frac{\partial}{\partial t}\,|\,\Psi\rangle$ vanishes because $\delta\Psi = \Psi$ is an allowed variation by the assumption $\Psi \in \{\delta\Psi\}$. This assumption is valid if the model ansatz for Ψ contains a parameter which controls its length, *e.g.* if there are linear parameters. This is true for both TDH and MCTDH.

The case $n = 1$ demonstrates the conservation of energy:

$$\begin{aligned}\frac{d}{dt}\langle\Psi\,|\,H\,|\,\Psi\rangle &= -2\,\mathrm{Im}\,\langle H\Psi\,|\,H - i\,\frac{\partial}{\partial t}\,|\,\Psi\rangle \\ &= -2\,\mathrm{Im}\Big[\Big\langle\Big(H - i\,\frac{\partial}{\partial t}\Big)\,\Psi\Big|\,\Big(H - i\,\frac{\partial}{\partial t}\Big)\,\Psi\Big\rangle + \Big\langle i\,\frac{\partial}{\partial t}\Psi\Big|H - i\,\frac{\partial}{\partial t}\Big|\Psi\Big\rangle\Big] \\ &= 2\,\mathrm{Re}\,\Big\langle\frac{\partial}{\partial t}\Psi\Big|H - i\,\frac{\partial}{\partial t}\Big|\Psi\Big\rangle \\ &= 0\,, \end{aligned} \tag{2.9}$$

since $\delta\Psi = \frac{\partial}{\partial t}\Psi$ is always an allowed variation, $\dot\Psi \in \{\delta\Psi\}$, because $\dot\Psi = \sum\dot\lambda_k\,\partial\Psi/\partial\lambda_k$, where λ_k formally denote the parameters of the model wavefunction.

Finally, $n = 2$ yields the energy variance:

$$\begin{aligned}
\frac{d}{dt}\langle\Psi\,|\,H^2\,|\,\Psi\rangle &= -2\,\mathrm{Im}\,\langle H^2\Psi\,|\,H - i\,\frac{\partial}{\partial t}\,|\,\Psi\rangle \\
&= -2\,\mathrm{Im}\Big[\Big\langle\Big(H - i\,\frac{\partial}{\partial t}\Big)\,\Psi\Big|H\Big|\Big(H - i\,\frac{\partial}{\partial t}\Big)\,\Psi\Big\rangle \qquad (2.10)\\
&\qquad + \Big\langle i\,\frac{\partial}{\partial t}\Psi\Big|H\Big(H - i\,\frac{\partial}{\partial t}\Big)\,\Big|\Psi\Big\rangle\Big] \\
&= -2\,\mathrm{Im}\,\Big\langle i\,\frac{\partial}{\partial t}\Psi\Big|H\Big(H - i\,\frac{\partial}{\partial t}\Big)\,\Big|\Psi\Big\rangle \\
&= 2\,\mathrm{Re}\,\langle H\,\frac{\partial}{\partial t}\Psi\,|\,H - i\,\frac{\partial}{\partial t}\,|\,\Psi\rangle \\
&\neq 0 \quad \text{in general}\,, \qquad (2.11)
\end{aligned}$$

since, in general, $\delta\Psi = H\,\frac{\partial}{\partial t}\Psi$ is not an allowed variation, *i.e.* $H\,\frac{\partial}{\partial t}\Psi \notin \{\delta\Psi\}$.

All approaches to be discussed, standard method, TDH, and MCTDH, conserve norm and mean energy. If in an actual calculation these quantities are not conserved, this must be due to the numerics, in particular to the use of finite integrator step sizes. If norm and energy conservation is insufficient, one has to increase the integrator accuracy.

2.2 The standard method

The most direct way to solve the TDSE is to expand the WF into a product of TI basis set.

$$\Psi(q_1, q_2, \ldots, q_f, t) = \sum_{j_1\cdots j_f} C_{j_1\cdots j_f}(t)\;\chi^{(1)}_{j_1}(q_1)\cdots\chi^{(f)}_{j_f}(q_f) \qquad (2.12)$$

where the χ_j are orthonormal basis functions, *e.g.* harmonic oscillator (HO) functions, Legendre functions, plane waves, etc. In electronic structure theory this would be called a full-CI approach.

The goal is now to derive equations of motion for the coefficients C. For this, we employ the Dirac-Frenkel variational principle (VP), Eq. (2.1). Since the objects to be varied here are just numbers, the variation is a partial differentiation:

$$\delta\Psi = \sum_{l_1\cdots l_f} \frac{\partial\Psi}{\partial C_{l_1\cdots l_f}}\;\delta C_{l_1\cdots l_f} = \sum_{l_1\cdots l_f} \chi^{(1)}_{l_1}(q_1)\cdots\chi^{(f)}_{l_f}(q_f)\;\delta C_{l_1\cdots l_f} \qquad (2.13)$$

and

$$\dot\Psi = \sum_{j_1\cdots j_f} \dot C_{j_1\cdots j_f}\;\chi^{(1)}_{j_1}\cdots\chi^{(f)}_{j_f} \qquad (2.14)$$

Because the variations are independent one may set

$$\delta C_{l_1\cdots l_f} = \begin{cases} 1 & for \quad l_1\cdots l_f = l^{(0)}_1\cdots l^{(0)}_f \\ 0 & else \end{cases}$$

From $\langle \delta\Psi | H - i\frac{\partial}{\partial t} | \Psi \rangle = 0$, and replacing $l_\kappa^{(0)}$ by l_κ, we obtain

$$\langle \chi_{l_1} \cdots \chi_{l_f} | \sum_{j_1 \cdots j_f} C_{j_1 \cdots j_f} H \chi_{j_1} \cdots \chi_{j_f} \rangle = i \langle \chi_{l_1} \cdots \chi_{l_f} | \sum_{j_1 \cdots j_f} \dot{C}_{j_1 \cdots j_f} \chi_{j_1} \cdots \chi_{j_f} \rangle \tag{2.15}$$

or

$$\sum_{j_1 \cdots j_f} \langle \chi_{l_1} \cdots \chi_{l_f} | H | \chi_{j_1} \cdots \chi_{j_f} \rangle C_{j_1 \cdots j_f} = i \dot{C}_{l_1 \cdots l_f} . \tag{2.16}$$

Defining composite indices $J = (j_1, \ldots, j_f)$ and configurations $\chi_J = \prod_{\kappa=1}^{f} \chi_{j_\kappa}$, one arrives at the compact expression

$$\boxed{i\dot{C}_L = \sum_J \langle \chi_L | H | \chi_J \rangle \, C_J} \tag{2.17}$$

This is a very simple first order differential equation with constant coefficients. It has the formal solution (for time-independent Hamiltonians)

$$\boldsymbol{C}(t) = e^{-i\boldsymbol{H}t} \, \boldsymbol{C}(0) \tag{2.18}$$

where the bold faces shall indicate the vector and matrix form of coefficients and Hamiltonian, respectively. This differential equation is difficult to solve, because the number of coupled equations, its dimension, is large.

In general one needs at least 10 basis functions per degree of freedom. Hence, there are about 10^f coupled equations to be solved. Consider a molecule with 6 atoms, then there are $f = 3N - 6 = 12$ degrees of freedom, and 10^{12} coupled equations. This is not doable. In general only up to 4 atom systems ($6D$) may be treated by the standard method with today's computers. One hence has to resort to cleverer, but also more approximate methods.

2.3 The Time-dependent Hartree approach (TDH)

One of the simplest propagation methods is the TDH approach.

$$\Psi(q_1, q_2, \ldots, q_f, t) = a(t) \, \varphi_1(q_1, t) \cdots \varphi_f(q_f, t) \tag{2.19}$$

The representation is not unique because

$$\varphi_1 \cdot \varphi_2 = (\frac{\varphi_1}{b}) \cdot (\varphi_2 \cdot b) \tag{2.20}$$

holds for any complex constant $b \neq 0$.

The additional factor $a(t)$ increases the redundancy, but because of this coefficient there is now a free factor for each function φ_κ, called *single particle function* (SPF). All SPFs are now treated on the same footing. To arrive at unique equations of motion one has to introduce constraints, which remove the

non-uniqueness but do not narrow the variational space.[1]

If a function changes in time by a complex factor only, then this is equivalent to a time derivative which is always in the direction of the function itself

$$\dot{\varphi} \propto \varphi$$

To see this more explicitly, write

$$\varphi = \alpha \cdot \tilde{\varphi} \quad \text{with } \|\tilde{\varphi}\| = 1 \tag{2.21}$$
$$\dot{\varphi} = \dot{\alpha}\ \tilde{\varphi} + \alpha\ \dot{\tilde{\varphi}} \tag{2.22}$$

$$\langle\varphi|\dot{\varphi}\rangle = \alpha^* \dot{\alpha} + |\alpha|^2 \langle\tilde{\varphi}|\dot{\tilde{\varphi}}\rangle \tag{2.23}$$

This shows that we can prescribe $\langle\varphi|\dot{\varphi}\rangle$ any value, such a prescription will merely determine $\dot{\alpha}$.

Hence, we propose the constraints

$$i\langle\varphi_\kappa(t)|\dot{\varphi}_\kappa(t)\rangle = g_\kappa(t) \tag{2.24}$$

We would like to conserve the norm of the SPFs

$$\frac{d}{dt}\|\varphi_\kappa\|^2 = \frac{d}{dt}\langle\varphi_\kappa|\varphi_\kappa\rangle \tag{2.25}$$
$$= \langle\dot{\varphi}_\kappa|\varphi_\kappa\rangle + \langle\varphi_\kappa|\dot{\varphi}_\kappa\rangle \tag{2.26}$$
$$= 2Re\ \langle\varphi_\kappa|\dot{\varphi}_\kappa\rangle = 2Im\ g_\kappa \tag{2.27}$$

which implies that the norm is conserved if the constraints g_κ are real.

2.3.1 TDH equations

In the TDH approach, the WF is expressed as

$$\Psi(q_1, q_2, \ldots, q_f, t) = a(t) \prod_{\kappa=1}^{f} \varphi_\kappa(q_\kappa, t) = a(t) \cdot \Phi(t) \tag{2.28}$$

with the constraints:

$$i\langle\varphi_\kappa(t)|\dot{\varphi}_\kappa(t)\rangle = g_\kappa(t) \tag{2.29}$$

and with g_κ real, but otherwise arbitrary. Later, we will choose g_κ such that the EOM become as simple as possible. Without restriction we may choose the intial SPFs $\varphi_\kappa(t=0)$ to be normalised and Eq. (2.27) then tells us that they stay normalized for all times.

We are now ready to perform the variation.

$$\dot{\Psi} = \dot{a}(t) \prod_{\kappa=1}^{f} \varphi_\kappa(q_\kappa, t) + a(t) \sum_{\kappa=1}^{f} \dot{\varphi}_\kappa \prod_{\nu\neq\kappa}^{f} \varphi_\nu = \dot{a}(t)\ \Phi + a \sum_{\kappa=1}^{f} \dot{\varphi}_\kappa\ \Phi^{(\kappa)} \tag{2.30}$$

[1] *E.g.* the constraint $\dot{\varphi} = 0$ would dramatically narrow the variational space.

$$\delta\Psi = (\delta a)\cdot\Phi + a\sum_{\kappa=1}^{f}(\delta\varphi_\kappa)\ \Phi^{(\kappa)} \tag{2.31}$$

where we have used the definitions

$$\Phi = \prod_{\kappa=1}^{f}\varphi_\kappa \quad \text{and} \quad \Phi^{(\kappa)} = \prod_{\substack{\nu=1\\ \nu\neq\kappa}}^{f}\varphi_\nu \tag{2.32}$$

From the VP Eq. (2.1) follows

$$\begin{aligned}&\big\langle \delta a\ \Phi\big|H\big|a\,\Phi\big\rangle - i\big\langle \delta a\ \Phi\big|\dot a\,\Phi + a\sum_\kappa \dot\varphi_\kappa\ \Phi^{(\kappa)}\big\rangle\\ &+\sum_{\kappa=1}^{f}\Big\{\big\langle \delta\varphi_\kappa\ a\ \Phi^{(\kappa)}\big|H\big|a\ \Phi\big\rangle - i\Big\{\big\langle \delta\varphi_\kappa\ a\ \Phi^{(\kappa)}\big|\dot a\ \Phi + a\sum_{\kappa'}\dot\varphi_{\kappa'}\ \Phi^{(\kappa')}\big\rangle\Big\} = 0\end{aligned} \tag{2.33}$$

Since δa and all $\delta\varphi_\kappa$ are independent of each other, each line has to vanish individually.

δa :

$$(\delta a)^*\ a\big\langle\Phi\big|H\big|\Phi\big\rangle = i(\delta a)^*\ \dot a + i(\delta a)^*\ a\sum_\kappa\big\langle\Phi\big|\dot\varphi_\kappa\ \Phi^{(\kappa)}\big\rangle \tag{2.34}$$

Since

$$i\big\langle\Phi\big|\dot\varphi_\kappa\ \Phi^{(\kappa)}\big\rangle = i\big\langle\varphi_1\cdots\varphi_\kappa\cdots\varphi_f\big|\varphi_1\cdots\dot\varphi_\kappa\cdots\varphi_f\big\rangle = i\big\langle\varphi_\kappa\big|\dot\varphi_\kappa\big\rangle = g_\kappa\ , \tag{2.35}$$

follows

$$i\ \frac{\dot a}{a} = \big\langle\Phi\big|H\big|\Phi\big\rangle - \sum_\kappa g_\kappa \tag{2.36}$$

or, introducing[2]

$$E = \big\langle\Phi\big|H\big|\Phi\big\rangle = \frac{\big\langle\Psi\big|H\big|\Psi\big\rangle}{\big\langle\Psi\big|\Psi\big\rangle} \tag{2.37}$$

it follows

$$\boxed{i\ \dot a = (E - \sum_{\kappa=1}^{f} g_\kappa)\ a} \tag{2.38}$$

On the other hand, by varying a particular φ_κ, we obtain

$$\begin{aligned}\big\langle(\delta\varphi_\kappa)\ a\,\Phi^{(\kappa)}\big|H\big|a\ \Phi\big\rangle \quad &= \quad i\big\langle(\delta\varphi_\kappa)\ a\ \Phi^{(\kappa)}\big|\dot a\ \Phi\big\rangle +\\ &\quad i\big\langle(\delta\varphi_\kappa)\ a\,\Phi^{(\kappa)}\big|a\sum_{\nu=1}^{f}\dot\varphi_\nu\ \Phi^{(\nu)}\big\rangle\end{aligned} \tag{2.39}$$

[2]Note $E = E(t)$ in general.

Now

$$\begin{aligned}\left\langle (\delta\varphi_\kappa)\ a\,\Phi^{(\kappa)}\middle|H\middle|a\ \Phi\right\rangle &= |a|^2\left\langle (\delta\varphi_\kappa)\ \Phi^{(\kappa)}\middle|H\middle|\varphi_\kappa\ \Phi^{(\kappa)}\right\rangle \\ &= |a|^2\left\langle (\delta\varphi_\kappa)\middle|\left\langle \Phi^{(\kappa)}\middle|H\middle|\Phi^{(\kappa)}\right\rangle\middle|\varphi_\kappa\right\rangle \\ &= |a|^2\left\langle (\delta\varphi_\kappa)\middle|\mathcal{H}^{(\kappa)}\middle|\varphi_\kappa\right\rangle \end{aligned} \tag{2.40}$$

with the definition

$$\mathcal{H}^{(\kappa)} = \left\langle \Phi^{(\kappa)}\middle|H\middle|\Phi^{(\kappa)}\right\rangle \tag{2.41}$$

$\mathcal{H}^{(\kappa)}$ is called a *mean-field*. Note that it is an operator on the κ-th degree of freedom.

The second term of the Eq. (2.39) is transformed to

$$i\left\langle (\delta\varphi_\kappa)\, a\,\Phi^{(\kappa)}\middle|\dot{a}\ \Phi\right\rangle = i\dot{a}a^*\left\langle \delta\varphi_\kappa\middle|\varphi_\kappa\right\rangle = |a|^2\,(E-\sum_{\nu=1}^{f} g_\nu)\left\langle \delta\varphi_\kappa\middle|\varphi_\kappa\right\rangle \tag{2.42}$$

and the third term of (2.39)

$$\begin{aligned} i\left\langle (\delta\varphi_\kappa)\ a\ \Phi^{(\kappa)}\middle|a\sum_{\nu=1}^{f}\dot{\varphi}_\nu\ \Phi^{(\nu)}\right\rangle &= i|a|^2\left\langle \delta\varphi_\kappa\middle|\dot{\varphi}_\kappa\right\rangle + i|a|^2\sum_{\nu\neq\kappa}\left\langle \delta\varphi_\kappa\ \varphi_\nu\middle|\dot{\varphi}_\nu\ \varphi_\kappa\right\rangle \\ &= i|a|^2\left\langle \delta\varphi_\kappa\middle|\dot{\varphi}_\kappa\right\rangle + i|a|^2\left\langle \delta\varphi_\kappa\middle|\varphi_\kappa\right\rangle\cdot\sum_{\nu\neq\kappa}\left\langle \varphi_\nu\middle|\dot{\varphi}_\nu\right\rangle \\ &= i|a|^2\left\langle \delta\varphi_\kappa\middle|\dot{\varphi}_\kappa\right\rangle + |a|^2\left\langle \delta\varphi_\kappa\middle|\varphi_\kappa\right\rangle\sum_{\nu\neq\kappa} g_\nu \end{aligned} \tag{2.43}$$

(2.40) = (2.42) + (2.43) divided by $|a|^2$:

$$\begin{aligned}&\left\langle (\delta\varphi_\kappa)\middle|\mathcal{H}^{(\kappa)}\middle|\varphi_\kappa\right\rangle = \\ &(E-\sum_{\nu=1}^{f} g_\nu)\left\langle \delta\varphi_\kappa\middle|\varphi_\kappa\right\rangle + i\left\langle \delta\varphi_\kappa\middle|\dot{\varphi}_\kappa\right\rangle + \sum_{\nu\neq\kappa} g_\nu\left\langle \delta\varphi_\kappa\middle|\varphi_\kappa\right\rangle \end{aligned} \tag{2.44}$$

or

$$i\left\langle \delta\varphi_\kappa\middle|\dot{\varphi}_\kappa\right\rangle = \left\langle \delta\varphi_\kappa\middle|\mathcal{H}^{(\kappa)}\middle|\varphi_\kappa\right\rangle - (E-g_\kappa)\left\langle \delta\varphi_\kappa\middle|\varphi_\kappa\right\rangle \tag{2.45}$$

Since $\delta\varphi_\kappa$ is arbitrary, we finally arrive at

$$\boxed{\begin{aligned} i\ \dot{\varphi}_\kappa &= (\mathcal{H}^{(\kappa)} - E + g_\kappa)\ \varphi_\kappa \\ i\ \dot{a} &= (E-\sum_{\kappa=1}^{f} g_\kappa)\ a \end{aligned}} \tag{2.46}$$

Everything may be time-dependent.

If we multiply the first of the EOMs by $\left\langle \varphi_\kappa\right|$ we see that the constraint is obeyed (of course!),

$$i\left\langle \varphi_\kappa\middle|\dot{\varphi}_\kappa\right\rangle = \left\langle \varphi_\kappa\middle|\mathcal{H}^{(\kappa)}\middle|\varphi_\kappa\right\rangle - E + g_\kappa = g_\kappa \tag{2.47}$$

because

$$\langle\varphi_\kappa|\mathcal{H}^{(\kappa)}|\varphi_\kappa\rangle = \langle\varphi_\kappa\ \Phi^{(\kappa)}|H|\varphi_\kappa\ \Phi^{(\kappa)}\rangle = \langle\Phi|H|\Phi\rangle = E \tag{2.48}$$

We now have to decide what to take for g_κ. Remember that we can choose *any* function $g_\kappa(t)$ as long as it is real. The simplest choice is $g_\kappa \equiv 0$. This yields:

$$\boxed{\begin{aligned} a(t) &= a(0)\cdot exp\big(-i\int_0^t E(t')\ dt'\big) \\ i\ \dot\varphi_\kappa &= (\mathcal{H}^{(\kappa)} - E)\ \varphi_\kappa \\ &= \big(1 - |\varphi_\kappa\rangle\langle\varphi_\kappa|\big)\ \mathcal{H}^{(\kappa)}\ \varphi_\kappa \end{aligned}} \tag{2.49}$$

The very last line is introduced because of its similarity with the MCTDH EOM. It holds because of (2.48).

For hermitian time-independent Hamiltonians the Dirac-Frenkel variational principle ensures that the norm and the mean energy of the WP is conserved. Hence $E(t)$ is real and time-independent. For hermitian time-dependent Hamiltonians E will become time-dependent but stays real. For non-hermitian Hamiltonians E will become both complex and time-dependent.

Hence for hermitian Hamiltonians there are two other meaningful choices for g_κ, namely

$$g_\kappa = E \tag{2.50}$$

and

$$g_\kappa = E/f \tag{2.51}$$

Then[3]

$$\boxed{\begin{aligned} a(t) &= a(0)\cdot exp\big(i(f-1)\int_0^t E(t')\ dt'\big) \\ i\dot\varphi_\kappa &= \mathcal{H}^{(\kappa)}\ \varphi_\kappa \end{aligned}} \tag{2.52}$$

and

$$\boxed{\begin{aligned} a(t) &= a(0) \\ i\dot\varphi_\kappa &= \big(\mathcal{H}^{(\kappa)} - \left(\frac{f-1}{f}\right)\ E(t)\big)\ \varphi_\kappa \end{aligned}} \tag{2.53}$$

Hence the various choices of g_κ merely shift phase-factors from a to φ_κ and vice-versa.

The derivation of the EOM of the TDH method is now concluded.

[3] The TDH solution Ψ is always the same, only its representation differs.

The TDH solution is approximate because of the very restricted form of the wavefunction. To investigate the quality of a TDH solution, we adopt the idea of an effective Hamiltonian:

$$i\dot{\Psi} = H_{\text{eff}}\ \Psi \tag{2.54}$$

where Ψ denotes the TDH solution.

Using the last set of EOMs and remembering (since $\dot{a} = 0$ there)

$$\dot{\Psi} = a \sum_{\kappa} \dot{\varphi}_{\kappa}\ \Phi^{(\kappa)} \tag{2.55}$$

one readily finds[4]

$$\boxed{H_{\text{eff}} = \sum_{\kappa=1}^{f} \mathcal{H}^{(\kappa)}\ - (f-1)E} \tag{2.56}$$

The TDH solution is the exact solution of the TDSE using H_{eff} as Hamiltonian. To proceed, we split the Hamiltonian into separable and non-separable terms.

$$H = \sum_{\kappa=1}^{f} h^{(\kappa)} + V \tag{2.57}$$

where $h^{(\kappa)}$ operates only on the κ-th degree of freedom.

Example:

$$H = -\frac{1}{2m}\frac{\partial^2}{\partial x_1^2} - \frac{1}{2m}\frac{\partial^2}{\partial x_2^2} + \frac{1}{2}\ m\omega_1^2 x_1^2 + \frac{1}{2}\ m\omega_2^2 x_2^2 + \lambda\ x_1^2\ x_2^2 \tag{2.58}$$

$$\begin{aligned} h^{(1)}(x_1) &= -\frac{1}{2m}\frac{\partial^2}{\partial x_1^2} + \frac{1}{2}\ m\omega_1^2 x_1^2 \\ h^{(2)}(x_2) &= -\frac{1}{2m}\frac{\partial^2}{\partial x_2^2} + \frac{1}{2}\ m\omega_2^2 x_2^2 \\ V(x_1, x_2) &= \lambda\ x_1^2\ x_2^2 \end{aligned} \tag{2.59}$$

The mean-fields and the effective Hamiltonian can now be evaluated somewhat more explicitely

$$\begin{aligned} \mathcal{H}^{(\kappa)} &= \left\langle \Phi^{(\kappa)} \middle| H \middle| \Phi^{(\kappa)} \right\rangle \\ &= h^{(\kappa)}\ \left\langle \Phi^{(\kappa)} \middle| \Phi^{(\kappa)} \right\rangle + \sum_{\nu \neq \kappa} \left\langle \Phi^{(\kappa)} \middle| h^{(\nu)} \middle| \Phi^{(\kappa)} \right\rangle + \left\langle \Phi^{(\kappa)} \middle| V \middle| \Phi^{(\kappa)} \right\rangle \end{aligned} \tag{2.60}$$

or more compactly

$$\mathcal{H}^{(\kappa)} = h^{(\kappa)} + \sum_{\nu \neq \kappa} E^{(\nu)}_{\text{uncorr}} + v^{(\kappa)} \tag{2.61}$$

[4] Everything may be time-dependent.

with

$$E^{(\nu)}_{\rm uncorr} = \big\langle \Phi^{(\kappa)} \big| h^{(\nu)} \big| \Phi^{(\kappa)} \big\rangle = \big\langle \varphi^{(\nu)} \big| h^{(\nu)} \big| \varphi^{(\nu)} \big\rangle \tag{2.62}$$

$$E_{\rm uncorr} = \big\langle \Phi \big| \sum_{\nu} h^{(\nu)} \big| \Phi \big\rangle = \sum_{\nu} E^{(\nu)}_{\rm uncorr} \tag{2.63}$$

and

$$E_{\rm corr} = \big\langle \Phi \big| V \big| \Phi \big\rangle = \frac{\big\langle \Psi \big| V \big| \Psi \big\rangle}{\big\langle \Psi \big| \Psi \big\rangle} \tag{2.64}$$

Hence

$$E = \big\langle \Phi \big| H \big| \Phi \big\rangle = E_{\rm uncorr} + E_{\rm corr} \tag{2.65}$$

Before we continue, it may be helpful to give an example for $v^{(\kappa)}$,

$$v^{(1)}(x_1) = \big\langle \varphi_2 \cdots \varphi_f \big| V(x_1, \ldots, x_f) \big| \varphi_2 \cdots \varphi_f \big\rangle \tag{2.66}$$

For the 2D case it reads

$$v^{(1)}(x_1) = \int \big| \varphi_2(x_2) \big|^2 \; V(x_1, x_2) \; dx_2 \tag{2.67}$$

i.e. one averages the potential over the "other" degree of freedom. For the specific case

$$V = \lambda \; x_1^2 \; x_2^2 \tag{2.68}$$

one obtains

$$v^{(1)}(x_1) = \lambda \; x_1^2 \; \big\langle \varphi_2 \big| x_2^2 \big| \varphi_2 \big\rangle \tag{2.69}$$

which demonstrates that a product form leads to a great simplification!

We had derived the equation for the mean-fields

$$\mathcal{H}^{(\kappa)} = h^{(\kappa)} + v^{(\kappa)} + E_{\rm uncorr} - E^{(\kappa)}_{\rm uncorr} = h^{(\kappa)} + v^{(\kappa)} + \sum_{\nu \neq \kappa} E^{(\nu)}_{\rm uncorr} \tag{2.70}$$

$$\sum_{\kappa=1}^{f} \mathcal{H}^{(\kappa)} = \sum_{\kappa=1}^{f} \big(h^{(\kappa)} + v^{(\kappa)} \big) + (f-1) \; E_{\rm uncorr} \tag{2.71}$$

$$H_{\rm eff} = \sum_{\kappa=1}^{f} \mathcal{H}^{(\kappa)} - (f-1) \; E = \sum_{\kappa=1}^{f} \big(h^{(\kappa)} + v^{(\kappa)} \big) - (f-1) \; E_{\rm corr} \tag{2.72}$$

and

$$H - H_{\rm eff} = V - \sum_{\kappa=1}^{f} v^{(\kappa)} + (f-1) \; E_{\rm corr} \tag{2.73}$$

This makes it clear that TDH is exact, *i.e.* $H = H_{\rm eff}$, if $V \equiv 0$. In other words, if the Hamiltonian is separable.

To illuminate the errors introduced by TDH, let us consider a simple 2D example.

$$H = h^{(1)} + h^{(2)} + v_1(x_1) \cdot v_2(x_2) \tag{2.74}$$

$$E_{\rm corr} = \big\langle \varphi_1 \big| v_1 \big| \varphi_1 \big\rangle \cdot \big\langle \varphi_2 \big| v_2 \big| \varphi_2 \big\rangle \equiv \big\langle v_1 \big\rangle \; \big\langle v_2 \big\rangle \tag{2.75}$$

$$v^{(1)}(x_1) = v_1(x_1) \cdot \langle v_2 \rangle \tag{2.76}$$
$$v^{(2)}(x_2) = v_2(x_2) \cdot \langle v_1 \rangle \tag{2.77}$$

$$H - H_{\text{eff}} = v_1\ v_2 - v_2\ \langle v_1 \rangle - v_1\ \langle v_2 \rangle + \langle v_1 \rangle\ \langle v_2 \rangle \tag{2.78}$$

$$\boxed{H - H_{\text{eff}} = \big(v_1 - \langle v_1 \rangle\big)\big(v_2 - \langle v_2 \rangle\big)} \tag{2.79}$$

Hence the TDH-error is small, if the potential varies only little over the width of the wavepacket. In the (semi-)classical limit, when the wavefunction becomes a δ-function, TDH becomes exact! Quantum mechanics is so complicated because it is non-local.

In realistic applications, it is often the hard repulsion which limits the accuracy of TDH. This is demonstrated in Fig. 2.1. If the wave packet is close to the potential minimum, $v - \langle v \rangle$ takes only small values as indicated by the arrow on the right hand side. Close to the strongly repulsive wall, however $v - \langle v \rangle$ varies appreciably as the right hand side of the WP sees a much lower potential than its left hand side. Remember, however, that the TDH errors are caused by the non-separable parts of the Hamiltonians only. A separable strongly repulsive wall would not introduce TDH errors.

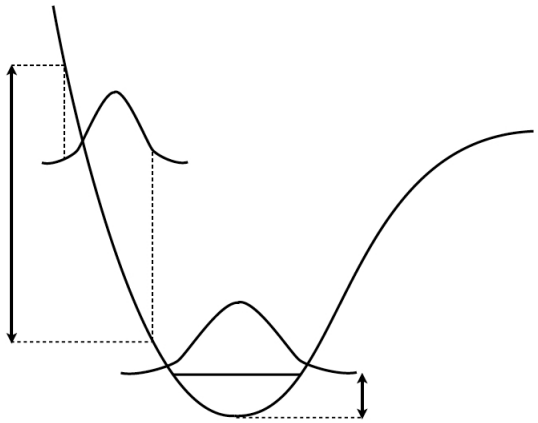

Figure 2.1: Visualization of $v - \langle v \rangle$. The arrows indicate the variation of the potential energy over the range of the wave packet.

TDH reduces an f-dimensional PDE to a set of f one-dimensional PDE. That is an enormous simplification. Assume we have 20 basis functions per DOF and 12 degrees of freedom. Then there are $20^{12} = 4 \cdot 10^{15}$ coupled differential equations to be solved for the standard method but only $12 \cdot 20 = 240$ equations for TDH. The first problem is undoable, the latter very simple. Well,

it would be very simple if there wouldn't be the integral problem.

At each time-step one has to evaluate the mean-fields $v^{(\kappa)}$ which are $(f-1)$ dimensional integrals

$$v^{(1)}(x_1) = \int \left|\phi^{(1)}(x_2,\ldots,x_f)\right|^2 V(x_1,\ldots,x_f)\; dx_2\cdots dx_f \tag{2.80}$$

If one would do these integrals directly, one would have to run f-times over the full product grid, which is undoable. One way out is to write the potential in product form

$$V(x_1,\ldots,x_f) = \sum_{r=1}^{s} v_{1,r}(x_1)\cdots v_{f,r}(x_f) \tag{2.81}$$

Then

$$v^{(1)}(x_1) = \sum_{r=1}^{s} v_{1,r}(x_1)\cdot\left\langle v_{2,r}\right\rangle\cdots\left\langle v_{f,r}\right\rangle \tag{2.82}$$

To do all the integral one has to run over $s\cdot f\cdot N$ grid points. If s is, say 1000, then we have for our example $1000\times 12\times 20 = 240,000$ operations, which is easily doable. A method, called *potfit*, which transforms a general potential to product form will be discussed later in more detail.

Chapter 3

The Multiconfiguration Time Dependent Hartree Method

3.1 MCTDH fundamentals

To overcome the limitations of TDH, we turn to a multi-configurational ansatz and write the WF as

$$\Psi(q_1,\ldots,q_f,t) = \sum_{j_1}^{n_1}\cdots\sum_{j_f}^{n_f} A_{j_1\ldots j_f}(t)\prod_{\kappa=1}^{f}\varphi_{j_\kappa}^{(\kappa)}(q_\kappa,t) \tag{3.1}$$

The number of "configurations", or "Hartree products", is given by the product $n_1\ldots n_f$. The SPFs, $\varphi_{j_\kappa}^{(\kappa)}(q_\kappa,t)$, are, as in the TDH approach, expressed in a time-independent basis set:

$$\varphi_{j_\kappa}^{(\kappa)}(q_\kappa,t) \quad = \quad \sum_{i_1=1}^{N_\kappa} c_{i_\kappa}^{(\kappa,j_\kappa)}(t)\;\chi_{i_\kappa}^{(\kappa)}(q_\kappa)\,, \tag{3.2}$$

where $\chi_{i_\kappa}^{(\kappa)}(q_\kappa)$ is a primitive basis functions, in general a DVR function, that depends on coordinate q_κ. If one sets in Eq. (3.1) $n_1 = n_2 = \ldots = n_f = 1$, one returns to the TDH approach. On the other hand, if $n_1 = N_1$, $n_2 = N_2$, ..., $n_f = N_f$, the MCTDH is equivalent to the standard approach since there is an unitary transformation between the primitive and SPF basis sets. Contrarily to the standard method, both the coefficients and the basis functions are time-dependent. Both are optimized using a variational principle. The SPFs adapt along the propagation of the wave packet and since $n_1, n_2, \ldots, n_f$ are, in general, smaller than $N_1, N_2, \ldots, N_f$, the number of equations to be solved is smaller and it is possible to treat larger systems. We are performing a contraction of the basis set since we have extracted a much smaller active space from the original space built by the primitive functions. MCTDH can be compared to the Multi-Configurational Self-Consistent Field (MCSCF) methods used in quantum chemistry to solve the time-independent electronic Schrödinger

equation. MCTDH is an MCSCF method but for the nuclear coordinates and time-dependent. If one uses MCTDH to solve the time-independent Schrödinger as discussed in Section 5 below, the algorithm will generate *vibrational orbitals* similar to the molecular orbitals for the electrons in quantum chemistry. Since we are solving the time-dependent Schrödinger equation here, we call the contracted basis functions *single particle functions* (SPFs) rather than orbitals. Note that, contrarily to the quantum chemistry methods, there is no exchange operator since we do not have to antisymmetrize the wavefunction. The wavefunction is antisymmetrized only if MCTDH is applied to a system of fermions as in the MCTDHF method. There, the MCTDH-wavefunction is expanded in Slater determinants rather than in Hartree products. In the same manner, if MCTDH is applied to a system of bosons, the wavefunction must be symmetrized leading to the MCTDHB method, where the MCTDH-wavefunction is expanded in permanents.

As in TDH, this ansatz is not unique. One may perform linear transformations among the SPFs (orbitals) and the inverse transformations on the coefficients (A-vector). Defining transformed SPFs and coefficients as

$$\begin{aligned} \tilde{\varphi}_{j_\kappa}^{(\kappa)} &= \sum_{l_\kappa} U_{j_\kappa l_\kappa}^{(\kappa)}\ \varphi_{l_\kappa}^{(\kappa)} \\ \tilde{A}_{j_1 \dots j_f} &= \sum_{l_1 \cdots l_f} A_{l_1 \dots l_f} (U^{(1)})_{l_1 j_1}^{-1} \cdots (U^{(f)})_{l_f j_f}^{-1} \end{aligned} \tag{3.3}$$

where $\boldsymbol{U}^{(\kappa)}$ denotes an arbitrary regular matrix, one obtains an unchanged total wavefunction in a different representation

$$\Psi = \sum_{j_1 \dots j_f} \tilde{A}_{j_1 \dots j_f}\ \tilde{\varphi}_{j_1} \cdots \tilde{\varphi}_{j_f} \tag{3.4}$$

As in TDH we need constraints to lift the ambiguity. As constraints we choose

$$i \langle \varphi_l^{(\kappa)} | \dot{\varphi}_j^{(\kappa)} \rangle = \langle \varphi_l^{(\kappa)} | \hat{g}^{(\kappa)} | \varphi_j^{(\kappa)} \rangle \tag{3.5}$$

with some arbitrary constraint operator $\hat{g}^{(\kappa)}$. The operator $\hat{g}^{(\kappa)}$ defines the transformation matrix $\boldsymbol{U}^{(\kappa)}$. In fact, after the equations of motion are derived one can show

$$i\ \dot{\boldsymbol{U}}^{(\kappa)} = \boldsymbol{g}^{(\kappa)^T}\ \boldsymbol{U}^{(\kappa)} \tag{3.6}$$

where

$$(\boldsymbol{g}^{(\kappa)})_{lj} = \langle \varphi_l^{(\kappa)} | \hat{g}^{(\kappa)} | \varphi_j^{(\kappa)} \rangle \tag{3.7}$$

A formal solution is hence

$$\boldsymbol{U}^{(\kappa)}(t) = \mathcal{T}\ \exp\Big(- i \int_0^t \boldsymbol{g}^{(\kappa)^T}(t')\ dt' \Big) \tag{3.8}$$

where $\mathcal{T}$ is the time-ordering operator, and $\boldsymbol{U}^{(\kappa)}$ is the transformation matrix from the SPFs computed with $\hat{g}^{(\kappa)} \equiv 0$ to those computed with $\hat{g}^{(\kappa)}$.

It is, of course, of great advantage if the SPFs are orthonormal. Orthonormality of the SPFs is not a restriction as one can always find a transformation

$\boldsymbol{U}^{(\kappa)}$ which orthogonalizes the SPFs. The overlap matrix is given by (dropping κ for the sake of simplicity)

$$S_{lj} = \langle \varphi_l | \varphi_j \rangle \tag{3.9}$$

and

$$\dot{S}_{lj} = \langle \varphi_l | \dot{\varphi}_j \rangle + \langle \dot{\varphi}_l | \varphi_j \rangle = -i \, (g_{lj} - g^*_{jl}) = -i \, (\boldsymbol{g} - \boldsymbol{g}^\dagger)_{lj}$$

Hence

$$\dot{\boldsymbol{S}} = 0 \qquad \text{if} \quad \boldsymbol{g} = \boldsymbol{g}^\dagger \tag{3.10}$$

and thus we require hermitian constraint operators.

If the initial WF, $\Psi(0)$, has orthornomal SPFs

$$S^{(\kappa)}_{lj}(0) = \langle \varphi^{(\kappa)}_l(0) | \varphi^{(\kappa)}_j(0) \rangle = \delta_{lj} \tag{3.11}$$

then it follows that the SPFs stay orthonormal for all times, because $\dot{\boldsymbol{S}}^{(\kappa)} = 0$ and hence $\boldsymbol{S}^{(\kappa)}(t) = \mathbf{1}$.

Before we derive the MCTDH equations of motion we have to introduce some notation:

- Composite indices:

  $J \equiv (j_1, \ldots, j_f)$
  $A_J \equiv A_{j_1 \cdots j_f}$

- Configuration or Hartree product:

  $\Phi_J \equiv \prod_{\kappa=1}^{f} \varphi^{(\kappa)}_{j_\kappa}$

Next we introduce single-hole functions. The WF Ψ lies, of course, in the space spanned by the SPFs and we can make use of completeness

$$\Psi = \sum_{l=1}^{n_\kappa} |\varphi^{(\kappa)}_l\rangle \langle \varphi^{(\kappa)}_l | \Psi \rangle_\kappa = \sum_{l=1}^{n_\kappa} \varphi^{(\kappa)}_l \; \Psi^{(\kappa)}_l \tag{3.12}$$

To make this clear, we write the single-hole function $\Psi^{(\kappa)}_l$ for the first DOF $\kappa = 1$

$$\Psi^{(1)}_l = \langle \varphi^{(1)}_l | \Psi \rangle = \sum_{j_2=1}^{n_2} \cdots \sum_{j_f=1}^{n_f} A_{l j_2 \cdots j_f} \; \varphi^{(2)}_{j_2} \cdots \varphi^{(f)}_{j_f} \tag{3.13}$$

For a general definition, we need an extended nomenclature:

- $J^\kappa \equiv (j_1, \ldots, j_{\kappa-1}, j_{\kappa+1}, \ldots, j_f)$
- $J^\kappa_l \equiv (j_1, \ldots, j_{\kappa-1}, l, j_{\kappa+1}, \ldots, j_f)$
- $\Phi_{J^\kappa} \equiv \prod_{\substack{\nu=1 \\ \nu\neq\kappa}}^{f} \varphi^{(\nu)}_{j_\nu}$

Then

$$\Psi^{(\kappa)}_l = \sum_{J^\kappa} A_{J^\kappa_l} \Phi_{J^\kappa} \tag{3.14}$$

The single-hole functions allow us to introduce mean-fields

$$\big\langle H \big\rangle^{(\kappa)}_{jl} = \big\langle \Psi^{(\kappa)}_j \big| H \big| \Psi^{(\kappa)}_l \big\rangle \tag{3.15}$$

Note that we have not only one mean-field for each degree of freedom, but a matrix of mean-fields!

Next, we introduce the density matrix

$$\rho^{(\kappa)}_{kl} = \big\langle \Psi^{(\kappa)}_k \big| \Psi^{(\kappa)}_l \big\rangle = \sum_{J^\kappa} A^*_{J^\kappa_k} \; A_{J^\kappa_l} \tag{3.16}$$

which, due to the orthonormality of the SPFs can be written as[1]

$$\rho^{(\kappa)}_{kl} = \sum_{J^\kappa} A^*_{J^\kappa_k} \; A_{J^\kappa_l} \tag{3.17}$$

Note that

$$\big\langle \Psi \big| \Psi \big\rangle = \sum_{J} A^*_J \; A_J = \|\boldsymbol{A}\|^2 \tag{3.18}$$

again because of the orthonormality of the SPFs. Hence

$$\mathrm{Tr}\,[\boldsymbol{\rho}^{(\kappa)}] = \sum_{j=1}^{n_\kappa} \rho^{(\kappa)}_{jj} = \|\Psi\|^2 \tag{3.19}$$

We are now ready to derive the MCTDH-EOM. But before that we will make some remarks on densities.

3.2 Remarks on densities

The density matrix of a mixed state reads

$$\hat{\rho} = \sum_n p_n \big| \Psi_n \big\rangle \big\langle \Psi_n \big|$$

where $p_n \geq 0$ denote probabilities.

[1] According to the extended notation:

$$\rho^{(\kappa)}_{kl} = \sum_{J^\kappa} A^*_{J^\kappa_k} \; A_{J^\kappa_l} = \sum_{J^\kappa} A^*_{j_1,\ldots,j_{\kappa-1},k,j_{\kappa+1},\ldots,j_f} \; A_{j_1,\ldots,j_{\kappa-1},l,j_{\kappa+1},\ldots,j_f}$$

And of a pure state is given by:

$$\hat{\rho} = |\Psi\rangle\langle\Psi|$$

A reduced density is obtained by tracing out unwanted DOFs

$$\hat{\rho}_{\rm red} = \underset{\text{unwanted dofs}}{\text{Trace}} \left\{ |\Psi\rangle\langle\Psi| \right\}$$

and the trace of an operator is given by

$$\text{Trace}\left\{\hat{A}\right\} = \sum_n \langle n|\hat{A}|n\rangle$$

for *any* complete orthonormal basis $|n\rangle$.

Choosing $|x\rangle$ as basis one obtains the one-particle reduced densities

$$\hat{\rho}^{(\kappa)}_{\rm red}(q_\kappa, q'_\kappa) = \int \Psi(q_1 \cdots q_\kappa \cdots q_f)\ \Psi^*(q_1 \cdots q'_\kappa \cdots q_f)\ dq_1 \cdots dq_{\kappa-1} dq_{\kappa+1} \cdots dq_f$$

and

$$\begin{aligned}
\langle \varphi^{(\kappa)}_j | \hat{\rho}^{(\kappa)}_{\rm red} | \varphi^{(\kappa)}_l \rangle &= \int \varphi^{(\kappa)^*}_j\ \Psi\ \Psi^*\ \varphi^{(\kappa)}_l\ \ dq_\kappa\ dq'_\kappa\ dq_1 \cdots dq_{\kappa-1} dq_{\kappa+1} \cdots dq_f \\
&= \int \Psi^{(\kappa)}_j\ \Psi^{(\kappa)^*}_l\ dq_1 \cdots dq_{\kappa-1} dq_{\kappa+1} \cdots dq_f \\
&= \langle \Psi^{(\kappa)}_l | \Psi^{(\kappa)}_j \rangle = \rho^{\rm MCTDH}_{lj} \qquad (3.20)
\end{aligned}$$

Hence

$$\left(\boldsymbol{\rho}^{(\kappa)}_{\rm red}\right) = \left(\boldsymbol{\rho}^{(\kappa)}_{\rm MCTDH}\right)^T \qquad (3.21)$$

The diagonal values, $q_\kappa = q'_\kappa$, of the reduced density are given by

$$\rho^{(\kappa)}(q_\kappa, q_\kappa) \equiv \rho^{(\kappa)}(q_\kappa) = \int \left|\Psi(q_1 \cdots q_f)\right|^2 dq_1 \cdots dq_{\kappa-1} dq_{\kappa+1} \cdots dq_f \qquad (3.22)$$

This we plot very often. The data is stored on the MCTDH `gridpop` file. Similarly, we can define 2-particle densities. Diagonal 2-particle densities can be plotted with `showsys`.[2]

Finally we note that the transformation from used SPFs to natural orbitals — in natural orbital representation the density becomes diagonal — reads:

$$\varphi^{(\kappa,\text{natorb})}_l = \sum_j \varphi^{(\kappa)}_j\ T^{(\kappa)*}_{jl} \qquad (3.23)$$

$$\varphi^{(\kappa)}_j = \sum_l T^{(\kappa)}_{jl}\ \varphi^{(\kappa,\text{natorb})}_l \qquad (3.24)$$

where $T^{(\kappa)}$ denotes the unitary eigen-vector matrix of $\rho^{(\kappa)}$, i.e. $\boldsymbol{\rho^{(\kappa)}}\ \boldsymbol{T^{(\kappa)}} = \boldsymbol{T^{(\kappa)}}\ \boldsymbol{\lambda^{(\kappa)}}$.

[2] For Hartree one can give the wavefunction for the κ-th degree, $\varphi_\kappa(q_\kappa, t)$, but for any correlated WF this is no longer possible. For correlated WFs one can only inspect the reduced densities.

3.3 MCTDH Equations of Motion

To derive the MCTDH-EOM, we first repeat the MCTDH ansatz for the wave function

$$\begin{aligned}\Psi(q_1,\dots,q_f,t) &= \sum_{j_1}^{n_1}\cdots\sum_{j_f}^{n_f} A_{j_1\dots j_f}(t)\ \varphi_{j_1}^{(1)}(q_1,t)\cdots\varphi_{j_f}^{(f)}(q_f,t)\\ &= \sum_J A_J\ \Phi_J = \sum_{j=1}^{n_\kappa}\varphi_j^{(\kappa)}\ \Psi_j^{(\kappa)}\end{aligned} \tag{3.25}$$

The variation with respect to coefficients and SPFs yields configurations and single-hole functions, respectively

$$\frac{\delta\Psi}{\delta A_J} = \Phi_J \tag{3.26}$$

$$\frac{\delta\Psi}{\delta\varphi_j^{(\kappa)}} = \Psi_j^{(\kappa)} \tag{3.27}$$

And the time derivation is given by

$$\dot\Psi = \sum_J \dot A_J\ \Phi_J + \sum_{\kappa=1}^{f}\sum_{j=1}^{n_\kappa}\ \dot\varphi_j^{(\kappa)}\ \Psi_j^{(\kappa)} \tag{3.28}$$

We first consider variations with respect to the coefficients only

$$\begin{aligned}&\delta A_J:\\ \langle\delta\Psi|H|\Psi\rangle &= \langle\Phi_J|H|\Psi\rangle = \sum_L\langle\Phi_J|H|\Phi_L\rangle\ A_L\\ &\overset{DFVP}{=} i\ \langle\delta\Psi|\dot\Psi\rangle\\ &= i\langle\Phi_J|\dot\Psi\rangle\\ &= i\sum_L\langle\Phi_J|\dot A_L\Phi_L\rangle + i\sum_\kappa\sum_l\langle\Phi_J|\dot\varphi_l^{(\kappa)}\ \Psi_l^{(\kappa)}\rangle\\ &= i\dot A_J + i\sum_\kappa\sum_l\langle\varphi_{j_\kappa}^{(\kappa)}|\dot\varphi_l^{(\kappa)}\rangle\ \langle\Phi_{J^\kappa}|\Psi_l^{(\kappa)}\rangle\\ &= i\dot A_J + i\sum_\kappa\sum_l\big(-i\ g_{j_\kappa l}^{(\kappa)}\big)\ A_{J_l^\kappa}\end{aligned} \tag{3.29}$$

Solving for $\dot A$ yields

$$\boxed{i\dot A_J = \sum_L\langle\Phi_J|H|\Phi_L\rangle\ A_L - \sum_{\kappa=1}^{f}\sum_{l=1}^{n_\kappa} g_{j_\kappa l}^{(\kappa)}\ A_{J_l^\kappa}} \tag{3.30}$$

which holds because

$$g_{j_\kappa l}^{(\kappa)} \equiv \langle\varphi_j^{(\kappa)}|\hat g^{(\kappa)}|\varphi_l^{(\kappa)}\rangle = i\ \langle\varphi_j^{(\kappa)}|\dot\varphi_l^{(\kappa)}\rangle \tag{3.31}$$

and

$$\left\langle \Phi_{J^\kappa} \middle| \Psi_l^{(\kappa)} \right\rangle = \sum_{L^\kappa} \left\langle \Phi_{J^\kappa} \middle| A_{L_l^\kappa} \Phi_{L^\kappa} \right\rangle = A_{J_l^\kappa} \tag{3.32}$$

Next we consider variations with respect to the SPFs.

$$\begin{aligned} \delta\varphi_j^{(\kappa)}: & \\ \left\langle \delta\Psi \middle| H \middle| \Psi \right\rangle &= \left\langle \Psi_j^{(\kappa)} \middle| H \middle| \Psi \right\rangle = \left\langle \Psi_j^{(\kappa)} \middle| H \middle| \sum_l \Psi_l^{(\kappa)} \varphi_l^{(\kappa)} \right\rangle \\ &= \sum_{l=1}^{n_\kappa} \left\langle H \right\rangle_{jl}^{(\kappa)} \varphi_l^{(\kappa)} \overset{DFVP}{=} i \left\langle \delta\Psi \middle| \dot{\Psi} \right\rangle \\ &= \underbrace{i \sum_L \left\langle \Psi_j^{(\kappa)} \middle| \Phi_L \right\rangle \dot{A}_L}_{\text{part 1}} + \underbrace{i \sum_L \left\langle \Psi_j^{(\kappa)} \middle| \sum_{\nu=1}^{f} \sum_{l=1}^{n_\nu} \dot{\varphi}_l^{(\nu)} \Psi_l^{(\nu)} \right\rangle}_{\text{part 2}} \end{aligned} \tag{3.33}$$

For the sake of simplicity we postpone the discussion of the general case to later and set $\hat{g}^{(\kappa)} \equiv 0$ in the following. Then Eq.(3.30) simplyfies to

$$i\dot{A}_L = \left\langle \Phi_L \middle| H \middle| \Psi \right\rangle = \sum_K \left\langle \Phi_L \middle| H \middle| \Phi_K \right\rangle A_K \tag{3.34}$$

and Eq. (3.33) part 1 reads

$$i \sum_L \left\langle \Psi_j^{(\kappa)} \middle| \Phi_L \right\rangle \dot{A}_L = \sum_L \left\langle \Psi_j^{\kappa} \middle| \Phi_L \right\rangle \left\langle \Phi_L \middle| H \middle| \Psi \right\rangle \tag{3.35}$$

which with

$$\Phi_L = \Phi_{L^\kappa} \; \varphi_{l_\kappa}^{(\kappa)} \tag{3.36}$$

and

$$\Psi_j^{(\kappa)} = \sum_{J^\kappa} A_{J_j^\kappa} \; \Phi_{J^\kappa} \tag{3.37}$$

can be turned into

$$(\text{part1}) = \sum_{L^\kappa, l_\kappa} A^*_{L_j^\kappa} \left| \varphi_{l_\kappa}^{(\kappa)} \right\rangle \left\langle \varphi_{l_\kappa}^{(\kappa)} \Phi_{L^\kappa} \middle| H \middle| \Psi \right\rangle = P^{(\kappa)} \left\langle \Psi_j^{(\kappa)} \middle| H \middle| \Psi \right\rangle \tag{3.38}$$

where we have introduced the MCTDH projector

$$P^{(\kappa)} = \sum_{j=1}^{n_\kappa} \left| \varphi_j^{(\kappa)} \right\rangle \left\langle \varphi_j^{(\kappa)} \right| \tag{3.39}$$

Hence for part 1 of Eq. (3.33) we arrive at

$$i \sum_L \left\langle \Psi_j^{(\kappa)} \middle| \Phi_L \right\rangle \dot{A}_L = P^{(\kappa)} \left\langle \Psi_j^{(\kappa)} \middle| H \middle| \Psi \right\rangle = P^{(\kappa)} \sum_{l=1}^{n_\kappa} \left\langle H \right\rangle_{jl}^{(\kappa)} \varphi_l^{(\kappa)} \tag{3.40}$$

Next we turn to part 2 of Eq. (3.33)

$$i \left\langle \Psi_j^{(\kappa)} \middle| \sum_{\nu=1}^{f} \sum_{l=1}^{n_\nu} \dot{\varphi}_l^{(\nu)} \; \Psi_l^{(\nu)} \right\rangle = i \left\langle \Psi_j^{(\kappa)} \middle| \sum_l \dot{\varphi}_l^{(\kappa)} \Psi_l^{(\kappa)} \right\rangle = i \sum_l \rho_{jl}^{(\kappa)} \dot{\varphi}_l^{(\kappa)} \tag{3.41}$$

Here we have used

$$\left\langle \varphi_j^{(\kappa)} \middle| \dot{\varphi}_l^{(\kappa)} \right\rangle = 0 \tag{3.42}$$

which holds for any j and l because $\hat{g}^{(\kappa)} \equiv 0$ is assumed. Only when $\nu = \kappa$ there is no SPF with which $\dot{\varphi}$ is to be overlapped.

Putting all parts of Eq. 3.33 together, we have

$$\sum_{l=1}^{n_\kappa} \langle H \rangle_{jl}^{(\kappa)} \ \varphi_l^{(\kappa)} = P^{(\kappa)} \sum_{l=1}^{n_\kappa} \langle H \rangle_{jl}^{(\kappa)} \ \varphi_l^{(\kappa)} + i \sum_l \rho_{jl}^{(\kappa)} \ \dot{\varphi}_l^{(\kappa)} \tag{3.43}$$

or

$$i\dot{\varphi}_j^{(\kappa)} = \sum_{k,l} \left(\boldsymbol{\rho}^{(\kappa)^{-1}}\right)_{jl} \left(1 - P^{(\kappa)}\right) \ \langle H \rangle_{lk}^{(\kappa)} \ \varphi_k^{(\kappa)} \tag{3.44}$$

Hence for $\hat{g}^{(\kappa)} \equiv 0$ we have the following set of EOM:

$$\boxed{\begin{aligned} i\dot{A}_J &= \sum_L \left\langle \Phi_J \middle| H \middle| \Phi_L \right\rangle \ A_L \\ i\dot{\varphi}_j^{(\kappa)} &= \left(1 - P^{(\kappa)}\right) \sum_{k,l=1}^{n_\kappa} \left(\boldsymbol{\rho}^{(\kappa)^{-1}}\right)_{jl} \langle H \rangle_{lk}^{(\kappa)} \ \varphi_k^{(\kappa)} \end{aligned}} \tag{3.45}$$

Introducing vectors of SPFs

$$\boldsymbol{\varphi}^{(\kappa)} = \left(\varphi_1^{(\kappa)} \cdots \varphi_{n_\kappa}^{(\kappa)}\right)^T \tag{3.46}$$

we can write the last equation more compactly

$$i\dot{\boldsymbol{\varphi}}^{(\kappa)} = \left(1 - P^{(\kappa)}\right) \ \boldsymbol{\rho}^{(\kappa)^{-1}} \left\langle \boldsymbol{H} \right\rangle^{(\kappa)} \boldsymbol{\varphi}^{(\kappa)} \tag{3.47}$$

In full generality the EOM read

$$\boxed{\begin{aligned} i\dot{A}_J &= \sum_L \left\langle \Phi_J \middle| H \middle| \Phi_L \right\rangle \ A_L - \sum_{\kappa=1}^{f} \sum_{l=1}^{n_\kappa} g_{j_\kappa l}^{(\kappa)} \ A_{J_l^\kappa} \\ i\dot{\boldsymbol{\varphi}}^{(\kappa)} &= \left(\hat{g}^{(\kappa)} \ \mathbf{1}\right) \boldsymbol{\varphi}^{(\kappa)} + \left(1 - P^{(\kappa)}\right) \left\{ \boldsymbol{\rho}^{(\kappa)^{-1}} \ \left\langle \boldsymbol{H} \right\rangle^{(\kappa)} - \hat{g}^{(\kappa)} \ \mathbf{1} \right\} \boldsymbol{\varphi}^{(\kappa)} \end{aligned}} \tag{3.48}$$

The last equation may be written as

$$i\dot{\boldsymbol{\varphi}}^{(\kappa)} = P^{(\kappa)} \ \hat{g}^{(\kappa)} \ \boldsymbol{\varphi}^{(\kappa)} + \left(1 - P^{(\kappa)}\right) \ \boldsymbol{\rho}^{(\kappa)^{-1}} \ \left\langle \boldsymbol{H} \right\rangle^{(\kappa)} \ \boldsymbol{\varphi}^{(\kappa)} \tag{3.49}$$

or

$$i\dot{\boldsymbol{\varphi}}^{(\kappa)} = \left\{ \boldsymbol{g}^{(\kappa)^T} + \left(1 - P^{(\kappa)}\right) \ \boldsymbol{\rho}^{(\kappa)^{-1}} \ \left\langle \boldsymbol{H} \right\rangle^{(\kappa)} \right\} \boldsymbol{\varphi}^{(\kappa)} \tag{3.50}$$

As

$$\begin{aligned} P^{(\kappa)} \ \hat{g}^{(\kappa)} \ \varphi_j^{(\kappa)} &= \sum_l \left| \varphi_l^{(\kappa)} \right\rangle \left\langle \varphi_l^{(\kappa)} \middle| \hat{g}^{(\kappa)} \middle| \varphi_j^{(\kappa)} \right\rangle \\ &= \sum_l \left| \varphi_l^{(\kappa)} \right\rangle \ g_{lj}^{(\kappa)} \\ &= \sum_l g_{lj}^{(\kappa)} \ \varphi_l^{(\kappa)} = \left(\boldsymbol{g}^T \ \boldsymbol{\varphi} \right)_j \end{aligned} \tag{3.51}$$

Defining

$$H_g = H - \sum_\kappa \hat{g}^{(\kappa)} \tag{3.52}$$

one arrives at the EOM

$$\boxed{\begin{aligned} i\dot{A}_J &= \sum_L \langle \Phi_J | H_g | \Phi_L \rangle \; A_L \\ i\dot{\boldsymbol{\varphi}}^{(\kappa)} &= \left\{ \hat{g}^{(\kappa)} \; \mathbf{1} + \left(1 - P^{(\kappa)}\right) \; {\boldsymbol{\rho}^{(\kappa)}}^{-1} \; \langle \boldsymbol{H}_g \rangle^{(\kappa)} \right\} \boldsymbol{\varphi}^{(\kappa)} \end{aligned}} \tag{3.53}$$

To prove Eq. (3.53), we note:

$$\langle \Phi_J | H | \Phi_L \rangle = \langle \Phi_J | H_g + \sum_\kappa \hat{g}^{(\kappa)} | \Phi_L \rangle = \langle \Phi_J | H_g | \Phi_L \rangle + \sum_\kappa \hat{g}^{(\kappa)}_{j_\kappa l_\kappa} \delta_{J^\kappa L^\kappa} \tag{3.54}$$

where the last term cancels the last term of the $i\dot{A}$ equation. And similarly

$$\begin{aligned} \langle H \rangle^{(\kappa)}_{jl} &= \langle H_g + \sum_\kappa g^{(\kappa)} \rangle^{(\kappa)}_{jl} \\ &= \langle \Psi^{(\kappa)}_j | g^{(\kappa)} | \Psi^{(\kappa)}_l \rangle + \sum_{\nu \neq \kappa} \langle \Psi^{(\kappa)}_j | g^{(\nu)} | \Psi^{(\kappa)}_l \rangle + \langle H_g \rangle^{(\kappa)}_{jl} \\ &= \hat{g}^{(\kappa)} \; \rho^{(\kappa)}_{jl} + \epsilon_{jl} + \langle H_g \rangle^{(\kappa)}_{jl} \end{aligned} \tag{3.55}$$

which defines the matrix ϵ_{jl}. The EOM for the SPF hence reads

$$\begin{aligned} i\dot{\boldsymbol{\varphi}}^{(\kappa)} &= \hat{g}^{(\kappa)} \; \boldsymbol{\varphi}^{(\kappa)} + \left(1 - P^{(\kappa)}\right) \left\{ \boldsymbol{\rho}^{-1} \; \left[\langle \boldsymbol{H}_g \rangle^{(\kappa)} + \boldsymbol{\epsilon} + \hat{g}^{(\kappa)} \; \boldsymbol{\rho} \right] - g^{(\kappa)} \right\} \boldsymbol{\varphi}^{(\kappa)} \\ &= \hat{g}^{(\kappa)} \; \boldsymbol{\varphi}^{(\kappa)} + \left(1 - P^{(\kappa)}\right) \; \boldsymbol{\rho}^{-1} \; \langle \boldsymbol{H}_g \rangle^{(\kappa)} \; \boldsymbol{\varphi}^{(\kappa)} \end{aligned} \tag{3.56}$$

as $\boldsymbol{\epsilon} \; \boldsymbol{\varphi}^{(\kappa)}$ is annihilated by the projector $(1 - P^{(\kappa)})$. This finishes the proof.

The two most obvious choices for constraint operator are either

$$\hat{g}^{(\kappa)} \equiv 0 \tag{3.57}$$

or

$$\hat{g}^{(\kappa)} = h^{(\kappa)} \tag{3.58}$$

where $h^{(\kappa)}$ denotes an operator acting on the κ-th DOF only, such that

$$H = \sum_\kappa h^{(\kappa)} + H_R \tag{3.59}$$

i.e. the $\sum h^{(\kappa)}$ term stands for the separable part of H, and H_R for the non-separable or residual part.

With the arguments just given (replacing $\hat{g}^{(\kappa)}$ with $h^{(\kappa)}$ and H_g with H_R in Eqs.(3.53,3.55)), we find for $\hat{g}^{(\kappa)} \equiv 0$

$$\boxed{\begin{aligned} i\dot{A}_J &= \sum_L \langle \Phi_J | H | \Phi_L \rangle \; A_L \\ i\dot{\boldsymbol{\varphi}}^{(\kappa)} &= \left(1 - P^{(\kappa)}\right) \; \left\{ h^{(\kappa)} \; \mathbf{1} + {\boldsymbol{\rho}^{(\kappa)}}^{-1} \; \langle \boldsymbol{H_R} \rangle^{(\kappa)} \right\} \boldsymbol{\varphi}^{(\kappa)} \end{aligned}} \tag{3.60}$$

whereas for $\hat{g}^{(\kappa)} = h^{(\kappa)}$ we arrive at

$$\boxed{\begin{aligned} i\dot{A}_J &= \sum_L \langle \Phi_J | H_R | \Phi_L \rangle \; A_L \\ i\dot{\boldsymbol{\varphi}}^{(\kappa)} &= \left\{ h^{(\kappa)} \; \mathbf{1} + \left(1 - P^{(\kappa)}\right) \boldsymbol{\rho}^{(\kappa)^{-1}} \left\langle \boldsymbol{H_R} \right\rangle^{(\kappa)} \right\} \boldsymbol{\varphi}^{(\kappa)} \end{aligned}} \tag{3.61}$$

In the MCTDH package one may switch between those two sets of EOM with the keywords `proj-h`, and `h-proj` with obvious meaning. `proj-h`, Eq.(3.60), is default in the constant mean-fields (CMF) integration scheme (cf. Chapter 4), whereas `h-proj`, Eq.(3.61), is default in the variable mean-fields (VMF) integration scheme.

It is illustrative to study the separable case $H = \sum_\kappa h^{(\kappa)}$, *i.e.* $H_R \equiv 0$.

$\hat{g}^{(\kappa)} \equiv 0$:

$$\boxed{\begin{aligned} i\dot{A}_J = \sum_L \sum_\kappa \langle \Phi_J | h^{(\kappa)} | \Phi_L \rangle \; A_L &= \sum_{\kappa=1}^{f} \sum_{l=1}^{n_\kappa} \langle \varphi_{j_\kappa}^{(\kappa)} | h^{(\kappa)} | \varphi_{l_\kappa}^{(\kappa)} \rangle \; A_{J_l^\kappa} \\ i\dot{\varphi}_j^{(\kappa)} &= \left(1 - P^{(\kappa)}\right) h^{(\kappa)} \varphi_j^{(\kappa)} \end{aligned}} \tag{3.62}$$

$\hat{g}^{(\kappa)} = h^{(\kappa)}$:

$$\boxed{\begin{aligned} i\dot{A}_J &= 0 \\ i\dot{\varphi}_j^{(\kappa)} &= h^{(\kappa)} \; \varphi_j^{(\kappa)} \end{aligned}} \tag{3.63}$$

This suggests that the choice $\hat{g}^{(\kappa)} = h^{(\kappa)}$ is of advantage, at least if H_R is small compared to the separable part $\sum h^{(\kappa)}$. However, the constant mean-field (CMF) integration scheme, which will be discussed later, is more useful with the constraint $\hat{g}^{(\kappa)} = 0$.

3.4 MCTDH-EOM for $\hat{g}^{(\kappa)} \neq 0$

We want to re-derive the EOM but this time for the general case $\hat{g}^{(\kappa)} \neq 0$. For part 1 of the Eq. (3.33) we obtain (see also (3.38)):

$$\begin{aligned} & i \sum_L \langle \Psi_j^{(\kappa)} | \Phi_L \rangle \; \dot{A}_L = \\ & \sum_L \langle \Psi_j^{(\kappa)} | \Phi_L \rangle \; \langle \Phi_L | H | \Psi \rangle - \sum_{\nu=1}^{f} \sum_{k=1}^{n_\nu} \sum_L \langle \Psi_j^{(\kappa)} | \Phi_L \rangle \; g_{l_\nu k}^{(\nu)} \; A_{L_k^\nu} = \\ & P^{(\kappa)} \; \langle \Psi_j^{(\kappa)} | H | \Psi \rangle - \sum_{l_\kappa, k} \rho_{jk}^{(\kappa)} \; g_{l_\kappa k}^{(\kappa)} \; \varphi_{l_\kappa}^{(\kappa)} - D \end{aligned} \tag{3.64}$$

where

$$D = \sum_{\nu \neq \kappa} \sum_L \sum_k \langle \Psi_j^{(\kappa)} | \Phi_L \rangle g_{l_\kappa k}^{(\nu)} \; A_{L_k^\nu} \tag{3.65}$$

The term $\nu = \kappa$ yields

$$\sum_k \sum_{L^\kappa} \sum_{l_\kappa} \langle \Psi_j^{(\kappa)} | \Phi_{L^\kappa} \ \varphi_{l_\kappa}^{(\kappa)} \rangle g_{l_\kappa k}^{(\kappa)} \ A_{L_k^\kappa} =$$
$$\sum_{k l_\kappa} \langle \Psi_j^{(\kappa)} | \Psi_k^{(\kappa)} \rangle \varphi_{l_\kappa}^{(\kappa)} \ g_{l_\kappa k}^{(\kappa)} = \sum_{k l_\kappa} \rho_{jk}^{(\kappa)} \ g_{l_\kappa k}^{(\kappa)} \ \varphi_{l_\kappa}^{(\kappa)} \tag{3.66}$$

which proves Eq. (3.64). Part 2 of Eq. (3.33) now reads

$$i \langle \Psi_j^{(\kappa)} | \sum_{\nu=1}^{f} \sum_{l=1}^{n_\nu} \dot{\varphi}_l^{(\nu)} \Psi_l^{(\nu)} \rangle = i \sum_l \rho_{jl}^{(\kappa)} \ \dot{\varphi}_l^{(\kappa)} + D' \tag{3.67}$$

where

$$D' = \sum_{\nu \neq \kappa} \sum_l \langle \Psi_j^{(\kappa)} | \dot{\varphi}_l^{(\nu)} \ \Psi_l^{(\nu)} \rangle g_{l_\kappa k}^{(\nu)} \ A_{L_k^\nu} \tag{3.68}$$

We will show later that $D = D'$. Hence adding part 1, Eq. (3.64), and part 2, Eq. (3.67), Eq. (3.33) turns into

$$\sum_l \langle H \rangle_{jl}^{(\kappa)} \ \varphi_l^{(\kappa)} =$$
$$P^{(\kappa)} \ \sum_l \langle H \rangle_{jl}^{(\kappa)} \ \varphi_l^{(\kappa)} - \sum_{l_\kappa k} \rho_{jk}^{(\kappa)} \ g_{l_\kappa k}^{(\kappa)} \ \varphi_{l_\kappa}^{(\kappa)} - D + i \sum_l \rho_{jl}^{(\kappa)} \ \dot{\varphi}_l^{(\kappa)} + D'$$

or, assuming $D = D'$

$$i \sum_l \rho_{jl}^{(\kappa)} \ \dot{\varphi}_l^{(\kappa)} = \left(1 - P^{(\kappa)}\right) \ \sum_l \langle H \rangle_{jl}^{(\kappa)} \ \varphi_l^{(\kappa)} + \sum_{l_\kappa k} \rho_{jk}^{(\kappa)} \ g_{l_\kappa k}^{(\kappa)} \ \varphi_{l_\kappa}^{(\kappa)} \tag{3.69}$$

Writing

$$\boldsymbol{\varphi}^{(\kappa)} = \left(\varphi_1^{(\kappa)} \cdots \varphi_{n_\kappa}^{(\kappa)}\right)^T \tag{3.70}$$

and multiplying by $\boldsymbol{\rho}^{-1}$ yields

$$\boxed{i \dot{\boldsymbol{\varphi}}^{(\kappa)} = \left(\boldsymbol{g}^{(\kappa)^T} + \left(1 - P^{(\kappa)}\right) \ \boldsymbol{\rho}^{(\kappa)^{-1}} \ \langle \boldsymbol{H} \rangle^{(\kappa)}\right) \ \boldsymbol{\varphi}^{(\kappa)}} \tag{3.71}$$

As

$$\left(\boldsymbol{g}^{(\kappa)^T} \boldsymbol{\varphi}^{(\kappa)}\right)_j = \sum_l |\varphi_l\rangle \langle \varphi_l | \hat{g}^{(\kappa)} | \varphi_j \rangle = P^{(\kappa)} \ g^{(\kappa)} \ \varphi_j^{(\kappa)} \tag{3.72}$$

Hence we also have

$$\boxed{i \dot{\boldsymbol{\varphi}}^{(\kappa)} = \left(P^{(\kappa)} \ \boldsymbol{g}^{(\kappa)} + \left(1 - P^{(\kappa)}\right) \ \boldsymbol{\rho}^{(\kappa)^{-1}} \ \langle \boldsymbol{H} \rangle^{(\kappa)}\right) \ \boldsymbol{\varphi}^{(\kappa)}} \tag{3.73}$$

and from this all other forms follow.

Finally, we use again the separation

$$H = \sum_\kappa g^{(\kappa)} + H_g$$

yielding

$$\langle \Phi_J | H | \Phi_L \rangle = \langle \Phi_J | H_g | \Phi_L \rangle + \sum_\kappa \sum_{l_\kappa} g^{(\kappa)}_{j_\kappa l_\kappa} \; \delta_{J^\kappa L^\kappa} \tag{3.74}$$

and

$$i\dot{A}_J = \sum_L \langle \Phi_J | H_g | \Phi_L \rangle \; A_L + \sum_\kappa \sum_{l_\kappa} g^{(\kappa)}_{j_\kappa l_\kappa} \; A_{J^\kappa_{l_\kappa}} - \sum_\kappa \sum_l g^{(\kappa)}_{j_\kappa l_\kappa} \; A_{J^\kappa_l} \tag{3.75}$$

Hence

$$\boxed{\begin{aligned} i\dot{A}_J &= \sum_L \langle \Phi_J | H_g | \Phi_L \rangle \; A_L + \sum_\kappa \sum_l g^{(\kappa)}_{j_\kappa l_\kappa} \; A_{J^\kappa_{l_\kappa}} \\ &= \sum_L \langle \Phi_J | H - \sum_\kappa \hat{g}^{(\kappa)} | \Phi_L \rangle \; A_L \end{aligned}} \tag{3.76}$$

We still have to show that $D = D'$.

$$D = \sum_{\nu \neq \kappa} \sum_L \sum_k \langle \Psi^{(\kappa)}_j | \Phi_L \rangle g^{(\nu)}_{l_\kappa k} \; A_{L^\nu_k}$$

$$D' = i \sum_{\nu \neq \kappa} \sum_l \langle \Psi^{(\kappa)}_j | \dot{\varphi}^{(\nu)}_l \; \Psi^{(\nu)}_l \rangle$$

We insert $P^{(\nu)}$ in the equation for D' and, given that $\langle \Psi^{(\kappa)}_j | P^{(\nu)} = \langle \Psi^{(\kappa)}_j |$ for $\nu \neq \kappa$, we obtain

$$\begin{aligned} D' &= i \sum_{\nu \neq \kappa} \sum_l \langle \Psi^{(\kappa)}_j | \sum_{l_\nu} | \varphi^{(\nu)}_{l_\nu} \rangle \langle \varphi^{(\nu)}_{l_\nu} | \dot{\varphi}^{(\nu)}_l \rangle \; \Psi^{(\nu)}_l \rangle \\ &= \sum_{\nu \neq \kappa} \sum_l \sum_{l_\nu} g^{(\nu)}_{l_\nu l} \langle \Psi^{(\kappa)}_j | \varphi^{(\nu)}_{l_\nu} \sum_{L^\nu} A_{L^\nu_l} \; \Phi_{L^\nu} \rangle \\ &= \sum_{\nu \neq \kappa} \sum_l \sum_L \langle \Psi^{(\kappa)}_j | \Phi_L \rangle \; g^{(\nu)}_{l_\nu l} \; A_{L^\nu_l} = D \end{aligned} \tag{3.77}$$

In summary, we again display the EOM in various forms

$$\begin{aligned} i\dot{A}_J &= \sum_L \langle \Phi_J | H | \Phi_L \rangle \; A_L - \sum_{\kappa=1}^{f} \sum_{l=1}^{n_\kappa} g^{(\kappa)}_{j_\kappa l} \; A_{J^\kappa_l} \\ &= \sum_L \langle \Phi_J | H - \sum_{\kappa=1} g^{(\kappa)} | \Phi_L \rangle \; A_L \end{aligned} \tag{3.78}$$

$$\begin{aligned} i\dot{\boldsymbol{\varphi}}^{(\kappa)} &= \left\{ g^{(\kappa)} \; \mathbf{1} + \left(1 - P^{(\kappa)}\right) \left[{\boldsymbol{\rho}^{(\kappa)}}^{-1} \; \langle \boldsymbol{H} \rangle^{(\kappa)} \; - g^{(\kappa)} \; \mathbf{1} \right] \right\} \boldsymbol{\varphi}^{(\kappa)} \\ &= P^{(\kappa)} \; g^{(\kappa)} \; \boldsymbol{\varphi}^{(\kappa)} + \left(1 - P^{(\kappa)}\right) \; {\boldsymbol{\rho}^{(\kappa)}}^{-1} \langle \boldsymbol{H} \rangle^{(\kappa)} \; \boldsymbol{\varphi}^{(\kappa)} \\ &= \left[\left(\boldsymbol{g}^{(\kappa)} \right)^T + \left(1 - P^{(\kappa)}\right) \; {\boldsymbol{\rho}^{(\kappa)}}^{-1} \; \langle \boldsymbol{H} \rangle^{(\kappa)} \right] \; \boldsymbol{\varphi}^{(\kappa)} \\ &= \left\{ g^{(\kappa)} \; \mathbf{1} + \left(1 - P^{(\kappa)}\right) \; {\boldsymbol{\rho}^{(\kappa)}}^{-1} \; \langle \boldsymbol{H} - \sum_{\kappa'} g^{(\kappa')} \rangle^{(\kappa)} \right\} \; \boldsymbol{\varphi}^{(\kappa)} \end{aligned} \tag{3.79}$$

For the separation

$$H = \sum_\kappa h^{(\kappa)} + H_R \tag{3.80}$$

one obtains for $\hat{g}^{(\kappa)} \equiv 0$

$$\boxed{\begin{aligned} i\dot{A}_J &= \sum_L \left\langle \Phi_J \middle| H \middle| \Phi_L \right\rangle \; A_L \\ i\dot{\boldsymbol{\varphi}}^{(\kappa)} &= \left(1 - P^{(\kappa)}\right)\left(h^{(\kappa)} \; \mathbf{1} + \boldsymbol{\rho}^{(\kappa)^{-1}} \; \left\langle \boldsymbol{H}_R \right\rangle\right) \; \boldsymbol{\varphi}^{(\kappa)} \end{aligned}} \tag{3.81}$$

and for $g^{(\kappa)} = h^{(\kappa)}$

$$\boxed{\begin{aligned} i\dot{A}_J &= \sum_L \left\langle \Phi_J \middle| H_R \middle| \Phi_L \right\rangle \; A_L \\ i\dot{\boldsymbol{\varphi}}^{(\kappa)} &= \left(h^{(\kappa)} \; \mathbf{1} + \left(1 - P^{(\kappa)}\right) \; \boldsymbol{\rho}^{(\kappa)^{-1}} \; \left\langle \boldsymbol{H}_R \right\rangle\right) \; \boldsymbol{\varphi}^{(\kappa)} \end{aligned}} \tag{3.82}$$

There are two sets of EOMs which are used in the Heidelberg MCTDH code.

3.5 Memory consumption

If the Hamiltonian is well structured, the memory demand to store it can be neglected. In the standard method one needs (at least) to keep 3 WF-vectors in RAM to perform propagation, setting $N_\kappa = N$ for all κ one hence needs

$$3 \times N^f \times \text{complex16} \qquad \text{bytes}$$

The MCTDH method, on the other hand, requires n^f numbers to represent the A-vector and $f \cdot n \cdot N$ numbers to represent the SPFs. Hence the storage demand is

$$12 \times \left(n^f + f \cdot n \cdot N\right) \times \text{complex16} \tag{3.83}$$

where the factor 12 accounts for the fact that one approximately needs an equivalent of about 12 WF to store all the work-arrays, mean-fields, etc.

Let us consider an example with $N = 32$ grid points and $n = 7$ SPFs for each degree of freedom.

f	St. Method	MCTDH	n^f	$f \cdot n \cdot N$
3	1.54 MB	190 KB	343	672
4	48 MB	620 KB	2401	896
6	48 GB	22 MB	$117 \cdot 10^3$	1344
9	1.54 PB	7.2 GB	$40 \cdot 10^6$	2016

Hence MCTDH shows a big advantage over the standard method. We can go to $9D$ and for small n's, *e.g.* $n = 4$, even to $12D$. However, we are still plagued by exponential scaling, n^f, although it is much smaller than the N^f scaling of the standard method, here 7^f versus 32^f.

The numerical effort is more difficult to estimate as it depends on integration step size etc. However, for one step the effort of the standard method is

$$\text{effort}_{\text{St.Method}} \approx c_0 \cdot f \cdot N^{f+1} \tag{3.84}$$

and for MCTDH

$$\text{effort}_{\text{MCTDH}} \approx c_1 \cdot s \cdot f \cdot n \cdot N^2 + c_2 \cdot s \cdot f^2 \cdot n^{f+1} \tag{3.85}$$

where c_0, c_1 and c_2 are constants of proportionality. s denotes the number of Hamiltonian terms.

If the Hamiltonian would be a full $N_{tot} \times N_{tot}$ matrix with $N_{tot} = N^f$ then the (matrix $\times$ vector) operation $H\Psi$ would take, of course, N^{2f} operations. However, we are using DVR's and for the standard method $V\Psi$ takes only N^f operations. The kinetic energy operator tensorizes, *i.e.* is of product form

$$T = \sum_{r=1}^{s'} T^{(r)} = \sum_{r=1}^{s'} T^{(1,r)} \cdots T^{(f,r)} \tag{3.86}$$

with only few terms ($s' \approx f$) and several of the $T^{(\kappa,r)}$ will be unit operators. Note that $T^{(\kappa,r)}$ operates on the κ-th degree of freedom only

$$\left(T^{(r)}\Psi\right)_{i_1,\ldots,i_f} = \sum_{j_1,\ldots,j_f} T^{(1,r)}_{i_1 j_1}\, T^{(2,r)}_{i_2 j_2} \cdots T^{(f,r)}_{i_f j_f}\, \Psi_{j_1,\ldots,j_f} \tag{3.87}$$

(Note that here we use $\Psi_{j_1,\ldots,j_f}$ for the C-vector $C_{j_1,\ldots,j_f}$ of the standard method, Eq. 2.12).

We can do the matrix multiplication successively:

Define:

$$\Psi^{(1,r)}_{i_1,j_2\cdots j_f} = \sum_{j_1} T^{(1,r)}_{i_1,j_1} \Psi_{j_1\cdots j_f} \tag{3.88}$$

For $\kappa = 2,\ldots,f$ do:

$$\Psi^{(\kappa,r)}_{i_1\cdots i_\kappa j_{\kappa+1} j_f} = \sum_{j_\kappa} T^{(\kappa,r)}_{i_\kappa,j_\kappa} \Psi^{(\kappa-1,r)}_{i_1\cdots i_{\kappa-1} j_\kappa \cdots j_f} \tag{3.89}$$

Finally:

$$\left(T\Psi\right)_{i_1\cdots i_f} = \sum_{r=1}^{s'} \Psi^{(f,r)}_{i_1\cdots i_f} \tag{3.90}$$

The matrix multiplication (3.88,3.89) takes N^{f+1} operations. There are f iterations for each r, hence the total effort is

$$s' \cdot f \cdot N^{f+1} \tag{3.91}$$

This trick is used over and over again in MCTDH. It is important to understand it clearly. It is a very powerful method as it reduces the effort from N^{2f} (or n^{2f}) to $f \cdot N^{f+1}$ (or $f \cdot n^{f+1}$), however, it requires a product form of the Hamiltonian. Since s' is usually small and since several of the $T^{(\kappa,r)}$ are unit operators (which do not require a matrix multiplication) we estimate the effort simply as

$$\text{effort}_{\text{St.Method}} = c_0 \cdot f \cdot N^{f+1} \tag{3.92}$$

For the MCTDH-effort the first term refers to the propagation of the SPFs (for potential terms N^2 is replaced by N) and the second part is the propagation of the A-vector and the build up of the mean-fields (there are f mean-fields, turning f into f^2).

$$\text{effort}_{\text{MCTDH}} = c_1 \cdot s \cdot f \cdot n \cdot N^2 + c_2 \cdot s \cdot f^2 \cdot n^{f+1} \tag{3.93}$$

For large systems the second part will dominate, both for memory and effort. This allows us to estimate the gain for large systems compactly as

$$\text{gain}_{\text{mem}} = \frac{1}{4} \left(\frac{N}{n}\right)^f \tag{3.94}$$

$$\text{gain}_{\text{CPU}} = \frac{c_0}{c_2} \frac{1}{sf} \left(\frac{N}{n}\right)^{f+1} \tag{3.95}$$

The important factor is in both cases the contraction N/n.[3] The limiting factor of large MCTDH calculations, for both memory and effort, is the A-vector length n^f. The A-vector length can be reduced by a trick called *mode-combination*. Mode-combination allows us to tackle systems with more than $12D$ with MCTDH.

3.6 Mode combination

The single-particle functions do not need to depend on one coordinate alone, they may depend on several coordinates. We group together several physical coordinates into one logical coordinate, also called *particle* or *combined mode*

$$Q_\kappa \equiv \left(q_{\kappa,1}, q_{\kappa,2}, \ldots, q_{\kappa,d}\right) \tag{3.96}$$

$$\varphi_j^{(\kappa)}(Q_\kappa, t) = \varphi_j^{(\kappa)}(q_{\kappa,1}, q_{\kappa,2}, \ldots, q_{\kappa,d}, t) \tag{3.97}$$

The MCTDH wavefunction is now expanded as

$$\Psi(q_1, \ldots, q_f, t) \equiv \Psi(Q_1, \ldots, Q_p, t) = \sum_{j_1 \cdots j_p} A_{j_1 \cdots j_p}(t) \prod_{\kappa=1}^{p} \varphi_j^{(\kappa)}(Q_\kappa, t) \tag{3.98}$$

and the SPFs themselves are expanded as:

$$\varphi_j^{(\kappa)}(Q_\kappa, t) = \sum_{i_1 \cdots i_d} C_{i_1 \cdots i_d}^{(\kappa,j)}(t)\ \chi^{(\kappa,1)}(q_{\kappa,1}) \cdots \chi^{(\kappa,d)}(q_{\kappa,d}) \tag{3.99}$$

Moreover, the number of SPFs per particle needed for convergence will increase with mode combination. If $\tilde{n} = n^d$ would hold, there would be no gain, the

[3] More general:

$$N^f \rightarrow \prod_{\kappa=1}^{f} N_\kappa$$

$$N^{f+1} \rightarrow \left(\frac{1}{f} \sum_{\kappa=1}^{f} N_\kappa\right) \cdot \prod_{\kappa=1}^{f} N_\kappa$$

and similar for n^f and n^{f+1}.

A-vector length would not change. Luckily one finds as a rule of thumb:[4]

$$\tilde{n} \approx d \cdot n \tag{3.100}$$

sometimes even less. Note that now all correlation between the DOFs within a particle is taken care of at the SPF level. Only the correlation between particles has to be accomplished by the A-vector.

The MCTDH memory requirement and effort using mode-combination reads of course

$$\begin{aligned} \text{mem} &\approx 12 \times \left(\tilde{n}^p + p \cdot \tilde{n} \cdot N^d\right) \times \text{complex16} \\ \text{effort} &\approx c_1 \cdot s \cdot p \cdot d \cdot \tilde{n} \cdot N^{d+1} + c_2 \cdot s \cdot p^2 \cdot \tilde{n}^{p+1} \end{aligned}$$

and in the gain formulas Eq. (3.94-3.95) N, n, and f are to be replaced by $\tilde{N}$, $\tilde{n}$, and p, respectively.

The great success of mode-combination is demonstrated by the following table, where we assume

$$N = 32 \quad \tilde{N} = 1024 \quad \text{or} \quad 32768 \qquad (d = 1, 2, 3)$$

grid points for uncombined and doubly or triply combined grids, respectively. Similarly, we assume

$$n = 7 \quad \tilde{n} = 15 \quad \text{or} \quad 23$$

as numbers of SPFs In realistic cases there are in general several DOFs which

Table 3.1: Comparison of memory consumption of the standard method and MCTDH with and without mode-combination $N = 32$, $\tilde{N} = 1024$ or 32768 and $n = 7$, $\tilde{n} = 15$ or 23 are assumed. The best value for each row is shown in bold face.

f	St. Method	MDTCH	2-mode	3-mode
2	**48 kB**	282 kB	-	-
4	48 MB	**620 kB**	6 MB	-
6	48 GB	22 MB	**10 MB**	290 MB
8	48 TB	1.03 GB	**22 MB**	290 MB
10	48 PB	51 GB	**160 MB**	310 MB
12	-	2.4 TB	2.2 GB	**620 MB**
15	-	-	210 GB	**1.9 GB**
18	-	-	7.38 TB	**29.3 GB**

do not couple strongly and may be represented by few grid-points (5-10, say) only. Such DOFs can be combined to a high degree (d=4 or 5, say), making it possible to treat systems with more than 30 DOFs.

[4] $\tilde{n}$ denotes the number of SPFs needed for convergence when mode-combination is used. n is the corresponding number of SPFs without mode-combination. For the sake of simplicity it is assumed that $n_\kappa = n$ for all κ, and similarly for $\tilde{n}$, N, and $\tilde{N}$.

The usefulness of mode-combination is limited by the fact that multi-dimension-al SPFs have to be propagated. If one "over combines", the propagation of the SPFs will take more effort than the propagation of the A-vector and efficiency is lost. However, we know a method which efficiently propagates multi-dimensional wavefunctions: MCTDH!

One hence may think of propagating the SPFs of an MCTDH calculation by MCTDH. This idea has lead to the development of a multi-layer MCTDH (ML-MCTDH) algorithm.

Chapter 4

The constant mean-field (CMF) integration scheme

The MCTDH equations of motion (for $g \equiv 0$ and $H = \sum_\kappa h^{(\kappa)} + H_R$) read

$$i\dot{A}_J = \sum_L \mathcal{K}_{JL}\, A_L \tag{4.1}$$

$$i\dot{\varphi}_j^{(\kappa)} = \big(1 - P^{(\kappa)}\big)\Big\{h^{(\kappa)}\varphi_j^{(\kappa)} + \sum_{k,l=1}^{n_\kappa} \big(\rho^{(\kappa)}\big)^{-1}_{jk} \sum_{r=1}^{s} \mathcal{H}^{(\kappa)}_{rlk}\, h_r^{(\kappa)}\, \varphi_l^{(\kappa)}\Big\} \tag{4.2}$$

with

$$\mathcal{K}_{JL} = \big\langle \Phi_J \big| H \big| \Phi_L \big\rangle \quad , \quad \big\langle H_R \big\rangle^{(\kappa)}_{lk} = \sum_{r=1}^{s} \mathcal{H}^{(\kappa)}_{rlk}\, h_r^{(\kappa)} \quad \text{and}$$

$$\mathcal{H}^{(\kappa)}_{rjl} = c_r \sum_{J^\kappa} A^*_{J^\kappa_j} \sum_{l_1} \langle \varphi^{(1)}_{j_1} \,|\, h^{(1)}_r \,|\, \varphi^{(1)}_{l_1} \rangle \ldots \sum_{l_f} \langle \varphi^{(f)}_{j_f} \,|\, h^{(f)}_r \,|\, \varphi^{(f)}_{l_f} \rangle A_{L^\kappa_l} \,. \tag{4.3}$$

Note that "..." does not contain a sum over l_κ.

The set of non-linear coupled differential equations (4.1, 4.2) can be solved by standard all-purpose integrators (*e.g.* Runge-Kutta, Adams-Bashforth-Moulton). This strategy is called the variable mean-field (VMF) approach. The problem is that the mean-fields matrices $\mathcal{H}^{(\kappa)}_{rlk}$ and the $\mathcal{K}$-matrix $\mathcal{K}_{JL}$ have to be built at every time step. The time-steps, however, have to be small as one has to describe an oscillating function.

Formally Ψ is given by

$$\Psi(t) = \sum_n a_n \Psi_n e^{-iE_n t}, \qquad H\Psi_n = E_n \Psi_n \tag{4.4}$$

To integrate $e^{-iE_n t}$ one needs step-sizes of the order

$$\Delta t \lesssim \frac{1}{|E_n|} \tag{4.5}$$

Hence the step-size is determined by the absolute largest eigenvalue of the matrix representation of the Hamiltonian.

The mean-fields, on the other hand, are not that strongly oscillating. It is hence tempting to set the mean-fields constant over a larger update time-step τ and to integrate the A-vector and the SPFs with much smaller time-steps. This is called the constant mean-field (CMF) approach. Keeping the mean-fields constant yields

$$i\dot{A}_J = \sum_L \bar{\mathcal{K}}_{JL}\, A_L \tag{4.6}$$

$$i\dot{\varphi}_j^{(1)} = \big(1-P^{(1)}\big)\Big\{h^{(1)}\varphi_j^{(1)} + \sum \bar{\rho}_{jk}^{(1)^{-1}} \sum_r \bar{\mathcal{H}}_{rlk}^{(1)}\, h_r^{(\kappa)}\, \varphi_l^{(1)}\Big\} \tag{4.7}$$

$$\vdots$$

$$i\dot{\varphi}_j^{(f)} = \big(1-P^{(f)}\big)\Big\{h^{(f)}\varphi_j^{(f)} + \sum \bar{\rho}_{jk}^{(f)^{-1}} \sum_r \bar{\mathcal{H}}_{rlk}^{(f)}\, h_r^{(\kappa)}\, \varphi_l^{(f)}\Big\} \tag{4.8}$$

Note that all the differential equations *decouple*! The bar indicates that the quantities are kept constant over the update time-step τ. As the equations decouple, one can use different time-steps and in fact different integrators for each set of equations. The EOM for the A-vector is *linear* and now time-independent, hence one may use an adapted integrator like Short Iterative Lanczos (SIL). The EOM for the SPFs are still non-linear because of the projector $P^{(\kappa)}$. But the main gain is of course that the mean fields need to be build less often.

The scheme outlined above is too simple. One needs at least a second order scheme, *i.e.* one in which the error scales like $\|\Psi_{ex} - \Psi\| \sim \tau^2$. In the present scheme, the error scales like τ. (For a single step the orders are τ^3 and τ^2, respectively.)

A higher-order scheme looks like:
Note that there is an additional propagation of the SPFs from $t = 0$ to $t = \tau/2$.

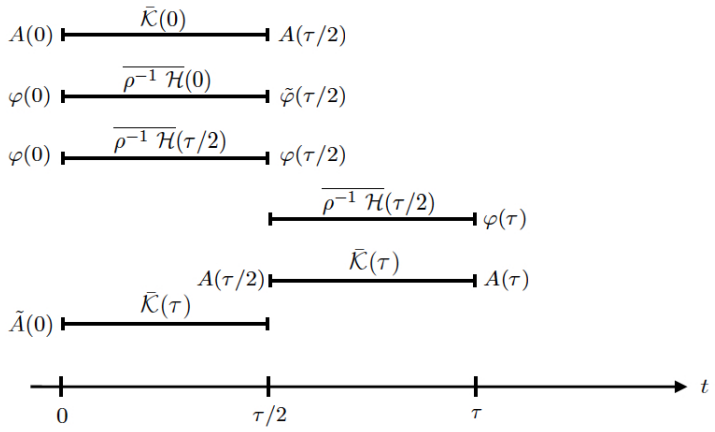

Figure 4.1: Second order CMF scheme.

The additional backward propagation of the coefficients ($A(\tau/2) \to \tilde{A}(0)$) is

done for error estimation only. This step is virtually cost free, because the Krylov-space, built for the previous forward propagation of A, is used. (The SIL integrator is used for A-propagation). A slightly different CMF-scheme has recently been discussed by Manthe (Chem. Phys. **329**, 168 (2006)).

The error of the propagation scheme of Fig. 4.1 is given in lowest order by

$$\|\Psi - \tilde{\Psi}\|^2 = \|\Delta A\|^2 + \sum_{\kappa=1}^{f} tr\big(\Delta O \cdot \rho^{(\kappa)}\big)\,, \tag{4.9}$$

where

$$\begin{aligned} \Delta A &= A(0) - \tilde{A}(0)\,, \\ \Delta O_{jl} &= \big\langle \Delta\varphi_j \big| \Delta\varphi_l \big\rangle\,, \\ \Delta\varphi_j &= \varphi_j(\tau/2) - \tilde{\varphi}_j(\tau/2)\,. \end{aligned} \tag{4.10}$$

This allows for an automatic step-size control. One sets an error limit and the algorithm searches for an appropriate value of τ.

To demonstrate that the scheme Fig. 4.1 gives an improved scaling of the error, let us consider a one-dimensional differential equation. The Taylor expansion of the solution propagated by one step reads:

$$y(\tau) = y(0) + y'(0)\cdot\tau + \frac{1}{2}\,y''(0)\cdot\tau^2 + \frac{1}{6}\,y'''(0)\cdot\tau^3 + \ldots \tag{4.11}$$

The previous scheme, Eqs.(4.6-4.8), is equivalent to an Euler integrator

$$y^{\rm app}(\tau) = y(0) + y'(0)\cdot\tau \tag{4.12}$$

which has an error

$$\text{error}: (y^{\rm app} - y)(\tau) = -\frac{1}{2}\,y''(0)\cdot\tau^2 + \ldots \tag{4.13}$$

To investigate this error introduced by the scheme Fig. 4.1 for the SPFs, we first note that the time-derivative at a half step reads

$$y'(\tau/2) = y'(0) + y''(0)\cdot\tau/2 + \frac{1}{2}y'''(0)\cdot(\tau/2)^2 \tag{4.14}$$

The one-step propagated solution, using this mid-step derivative, reads

$$y^{\rm app}(\tau) = y(0) + y'(\tau/2)\cdot\tau = y(0) + y'(0)\cdot\tau + y''(0)\cdot\tau^2/2 + y'''(0)\cdot\tau^3/8 \tag{4.15}$$

and has the error

$$\text{error}: (y^{\rm app} - y)(\tau) = \big(\frac{1}{8} - \frac{1}{6}\big)\;y'''(0)\cdot\tau^3 = -\frac{1}{24}\;y'''(0)\cdot\tau^3 \tag{4.16}$$

Similarly for the propagator of the A-vector, we obtain

$$\begin{aligned} y^{\rm app}(\tau) &= y(0) + y'(0)\cdot(\tau/2) + y'(\tau)\cdot(\tau/2) \\ &= y(0) + y'(0)\cdot\tau + y''(0)\cdot(\tau^2/2)\;\frac{1}{4}y'''(0)\cdot\tau^3 \end{aligned} \tag{4.17}$$

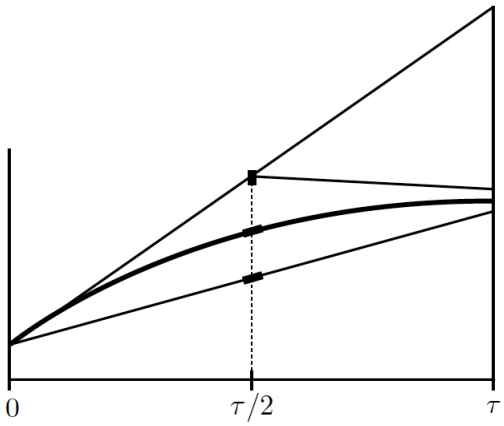

Figure 4.2: Graphical interpretation of the numerical integration. The heavy line (middle) shows an exact solution of a differential equation. Taking the initial derivative $y'(0)$ throughout the propagation leads to a rather large error at $t = \tau$. See upper straight line. Using $y'(\tau/2)$ rather than $y'(0)$ provides a much better solution. See the lowest straight line. And using $y'(0)$ for the first half-step and $y'(\tau)$ for the second half-step also provides a good approximate solution.

and the error

$$\text{error} : (\frac{1}{4} - \frac{1}{6}) y'''(0) \cdot \tau^3 = \frac{1}{12}\, y'''(0) \cdot \tau^3 \tag{4.18}$$

Hence the error done in one step scales like τ^3. The total error then scales likes τ^2 as the number of steps scales like τ^{-1}.

To understand why CMF works, let us consider a separable case

$$H = \sum_{\kappa=1}^{f} h^{(\kappa)} \tag{4.19}$$

hence $H_R = 0$ and $\boldsymbol{\mathcal{H}}^{(\kappa)} = 0$ and the mean-field $\langle \boldsymbol{H} \rangle^{(\kappa)}$ reduce to $h^{(\kappa)}$. The mean-fields are obviously constant but what is with $\mathcal{K}_{JL}$? In the following we allow for a general constraint operator $g^{(\kappa)}$, although CMF is usually performed with $g^{(\kappa)} \equiv 0$. The $\mathcal{K}$ matrix is then given (cf. Eq.(3.76,3.48)) by

$$\mathcal{K}_{JL} = \langle \Phi_J | H - \sum_{\kappa} g^{(\kappa)} | \Phi_L \rangle = \sum_{\kappa=1}^{f} \langle \varphi_{j_\kappa}^{(\kappa)} | h^{(\kappa)} - g^{(\kappa)} | \varphi_{l_\kappa}^{(\kappa)} \rangle \delta_{J^\kappa L^\kappa} \tag{4.20}$$

The EOMs for the φ's read (we drop κ for simplicity):

$$i\dot{\varphi}_j = g\ \varphi_j + \big(1 - P\big) \cdot \big(h - g\big)\ \varphi_j \tag{4.21}$$

From this follows:

$$
\begin{aligned}
&\frac{d}{dt}\langle\varphi_j|h-g|\varphi_l\rangle = \\
&i\langle g\ \varphi_j + (1-P)(h-g)\varphi_j|h-g|\varphi_l\rangle - i\langle\varphi_j|h-g|g\ \varphi_l + (1-P)(h-g)\ \varphi_l\rangle \\
&= i\langle\varphi_j|g^\dagger(h-g) + (h^\dagger - g^\dagger)(1-P)(h-g) - (h-g)g - (h-g)(1-P)(h-g)|\varphi_l\rangle \\
&\overset{\{g^\dagger=g\}}{=} i\langle\varphi_j|(h^\dagger - h)(1-P)(h-g)|\varphi_l\rangle + i\langle\varphi_j|gh - hg|\varphi_l\rangle \qquad (4.22)
\end{aligned}
$$

hence

$$
\frac{d}{dt}\mathcal{K}_{JL} = 0 \qquad \text{if} \quad h^{(\kappa)} = h^{(\kappa)^\dagger} \qquad (4.23)
$$

$$
\text{and} \quad \left[h^{(\kappa)}, g^{(\kappa)}\right] = 0\,. \qquad (4.24)
$$

The commutator vanishes for $g^{(\kappa)} \equiv 0$ and $g^{(\kappa)} = h^{(\kappa)}$, the standard choices! For non-hermitian $h^{(\kappa)}$ one may be tempted to choose $g^{(\kappa)} = h^{(\kappa)}$ as this will ensure a constant $\mathcal{K}$. However, the choice $g^{(\kappa)} = h^{(\kappa)}$ is only allowed for hermitian h because the constraint operators have to be hermitian.

The CMF integrator can take arbitrarily large update steps τ if the Hamiltonian is hermitian and separable. In a scattering problem, the Hamiltonian often becomes almost separable when the colliding partners are far from each other. However, when the scattered particle is finally absorbed by a Complex Absorbing Potential (CAP) the separable Hamiltonian becomes non-hermitian and the CMF-integrator is forced to take small steps. But our analysis has clearly shown, that the assumption of constant mean-fields is violated by the non-separable (and non-hermitian) terms of the Hamiltonian. These terms are usually much smaller than the separable ones, which justifies the assumption that the mean-fields can be taken as constant over a small update time τ, which, however, is much larger than the integration steps used to propagate the SPFs.

The CMF integrator scheme violates energy conservation which should hold for constant hermitian Hamiltonians. Only for $\tau \to 0$ energy conservation is strictly obeyed. If an MCTDH calculation shows an energy deviation which is too high to be acceptable, one must increase the integrator accuracies, in particular the CMF accuracy.

Chapter 5

Relaxation and improved relaxation

A ground state wavefunction can be obtained by a time-dependent method via relaxation, *i.e.* propagation in negative imaginary time. The Schrödinger equation is then turned into

$$\dot{\Psi} = -H\ \Psi \tag{5.1}$$

To see the effect we expand the WF in eigenstates and obtain

$$\Psi(t) = \sum_n a_n\ e^{-E_n t}\Psi_n \tag{5.2}$$

The state with the lowest energy (usually E_0) will "win". Of course the norm must be restored. To avoid this, one may change the Schrödinger equation to

$$\dot{\Psi}(t) = -\big(H - E(t)\big)\ \Psi(t) \quad \text{where} \quad E(t) = \big\langle \Psi(t)\big|H\big|\Psi(t)\big\rangle \tag{5.3}$$

Then

$$\big\langle \Psi(t)|\dot{\Psi}(t)\big\rangle = 0 \quad \Rightarrow \quad \frac{d}{dt}\|\Psi\|^2 = 0 \tag{5.4}$$

The energy E can be interpreted as a Lagrange parameter introduced to keep the norm of Ψ constant (we assume Ψ to be normalized). Differentiation of $E(t)$ leads to

$$\dot{E} = -2\big\langle \Psi(t)|(H - E(t))^2|\Psi(t)\big\rangle. \tag{5.5}$$

Hence the energy decreases with relaxation time and converges if the variance vanishes, *i.e.* if the wave function becomes an eigenstate of H. Usually this will be the ground state. Only if the initial state is orthogonal to the ground state, the algorithm may converge to an excited state.

Relaxation works well if the initial state Ψ has a reasonable overlap with the ground state and if the ground state is well separated. However relaxation may converge slowly if the energy of the first excited state, E_1, is close to the ground state energy E_0. To damp out the contribution of the excited state one needs a propagation time which satisfies $(E_1 - E_0)\cdot t \approx 10 - 30$.[1]The relaxation

[1]Note $1\ eV \cdot 1\ fs = 1.519\hbar$

can be accelerated and excited states can be computed as well, if the MCTDH A-vector is not determined by relaxation but by diagonalization. This method is called *improved relaxation*.

The algorithm can be derived via a standard time-independent variational principle $\delta\{\langle\Psi|H|\Psi\rangle - \text{constraints}\} = 0$

$$\delta\{\langle\Psi|H|\Psi\rangle - E(\sum_J A_J^* A_J - 1) - \sum_{\kappa=1}^{f}\sum_{j,l=1}^{n_\kappa}\epsilon_{jl}^{(\kappa)}(\langle\varphi_j^{(\kappa)}|\varphi_l^{(\kappa)}\rangle - \delta_{jl})\} = 0 \quad (5.6)$$

The first Lagrange parameter, E, ensures that the A-vector is normalized and the $\epsilon_{jl}^{(\kappa)}$ ensures that the SPFs are orthonormal. We note that

$$\langle\Psi|H|\Psi\rangle = \sum_{JK} A_J^*\ H_{JK}\ A_K \qquad H_{JK} = \langle\Phi_J|H|\Phi_K\rangle \quad (5.7)$$

Varying A_J^* yields

$$\sum_K H_{JK}A_K = EA_J \quad (5.8)$$

Hence the coefficient vector is obtained as an eigenvector of the Hamiltonian matrix represented in the basis of the SPFs. Using

$$\langle\Psi|H|\Psi\rangle = \langle\sum_j \Psi_j^{(\kappa)}\ \varphi_j^{(\kappa)}|H|\sum_l \Psi_l^{(\kappa)}\ \varphi_l^{(\kappa)}\rangle = \sum_{j,l}\varphi_j^{(\kappa)*}\langle H\rangle_{jl}^{(\kappa)}\varphi_l^{(\kappa)} \quad (5.9)$$

and varying with respect to $\varphi_j^{(\kappa)*}$ yields

$$\sum_{l=1}^{n_\kappa}\langle H\rangle_{jl}^{(\kappa)}\ \varphi_l^{(\kappa)} = \sum_{l=1}^{n_\kappa}\epsilon_{jl}^{(\kappa)}\ \varphi_l^{(\kappa)} \quad (5.10)$$

Projecting this equation onto $\varphi_k^{(\kappa)}$ yields

$$\epsilon_{jk}^{(\kappa)} = \sum_l \langle\varphi_k^{(\kappa)}|\langle H\rangle_{jl}^{(\kappa)}|\varphi_l^{(\kappa)}\rangle \quad (5.11)$$

and from that follows

$$(1 - P^{(\kappa)})\ \sum_{l=1}^{n_\kappa}\langle H\rangle_{jl}^{(\kappa)}\ \varphi_l^{(\kappa)} = 0 \quad (5.12)$$

As this equation holds for any j, it must hold for any linear combination as well. To arrive at a form similar to the MCTDH equations of motion we insert the inverse of the density operator

$$\dot{\varphi}_j^{(\kappa)} := -(1 - P^{(\kappa)})\ \sum_{k,l}\left(\rho^{(\kappa)^{-1}}\right)_{jk}\langle H\rangle_{kl}^{(\kappa)}\ \varphi_l^{(\kappa)} = 0 \quad (5.13)$$

with

$$\dot{\varphi} = \frac{\partial\varphi}{\partial\tau}, \quad \tau = -i\ t \quad (5.14)$$

This suggests that one can obtain the updated SPFs simply by relaxation. In fact, one can show that the energy changes during SPF-relaxation as

$$\dot{E} = -2 \sum_{\kappa=1}^{f} \sum_{l=1}^{n_\kappa} \| \sum_{j=1}^{n_\kappa} \left(\rho^{(\kappa)^{1/2}}\right)_{lj} \dot{\varphi}_j^{(\kappa)} \|^2 \leq 0 \tag{5.15}$$

From this we have that the orbital relaxation will always minimize the energy. As the energy cannot go down indefinitely it follows $\|\dot{\varphi}\| \to 0$ for $\tau \to \infty$ and hence Eq. (5.13) will be satisfied for a sufficiently long relaxation.

Proof of Eq. (5.15): The A-vector is kept constant during SPF-relaxation. The time-derivative of the energy hence reads

$$\begin{aligned}
\dot{E} &= 2\ Re\big\langle \dot{\Psi} \big| H \big| \Psi \big\rangle \\
&= 2\ Re\big\langle \sum_\kappa \sum_j \dot{\varphi}_j^{(\kappa)}\ \Psi_j^{(\kappa)} \big| H \big| \Psi \big\rangle \\
&= 2\ Re \sum_\kappa \sum_{j,l} \big\langle \dot{\varphi}_j^{(\kappa)}\ \Psi_j^{(\kappa)} \big| \varphi_l^{(\kappa)}\ \Psi_l^{(\kappa)} \big\rangle \\
&= 2\ Re \sum_\kappa \sum_{j,l} \big\langle \dot{\varphi}_j^{(\kappa)} \big| \big\langle H \big\rangle_{jl}^{(\kappa)} \big| \varphi_l^{(\kappa)} \big\rangle \\
&= 2\ Re \sum_\kappa \sum_{j,l} \big\langle \dot{\varphi}_j^{(\kappa)} \big| \big(1 - P^{(\kappa)}\big) \big\langle H \big\rangle_{jl}^{(\kappa)} \big| \varphi_l^{(\kappa)} \big\rangle
\end{aligned} \tag{5.16}$$

As

$$-\sum_k \rho_{jk}^{(\kappa)}\ \dot{\varphi}_k^{(\kappa)} = \big(1 - P^{(\kappa)}\big) \sum_l \big\langle H \big\rangle_{jl}^{(\kappa)}\ \varphi_l^{(\kappa)} \tag{5.17}$$

we have

$$\begin{aligned}
\dot{E} &= -2\ Re \sum_\kappa \sum_{j,k} \big\langle \dot{\varphi}_j^{(\kappa)} \big| \dot{\varphi}_k^{(\kappa)} \big\rangle\ \rho_{jk}^{(\kappa)} \\
&= -2\ Re \sum_\kappa \sum_{j,k,l} \big\langle \big(\rho^{(\kappa)^{1/2}}\big)_{lj} \dot{\varphi}_j^{(\kappa)} \big| \big(\rho^{(\kappa)^{1/2}}\big)_{lk} \dot{\varphi}_k^{(\kappa)} \big\rangle \\
&= -2 \sum_\kappa \sum_l \| \sum_j \rho_{lj}^{(\kappa)^{1/2}}\ \dot{\varphi}_j^{(\kappa)} \|^2
\end{aligned} \tag{5.18}$$

q.e.d.

Improved relaxation proceeds as follows: At first an initial state has to be defined. This state should have a reasonable overlap with the sought state. Then the matrix representation of the Hamiltonian H_{JK} is built and diagonalized by a Davidson routine.[2] Then the mean-fields are built and the SPFs are relaxed. After that, H_{JK} is built in the space of the new SPFs and the whole process is iterated till convergence.

If the ground state is computed, the selection of the eigenvector of the Hamiltonian is simple: one takes the eigenvector of lowest energy. When excited states

[2] Actually H_{JK} is never built as a full matrix but applied term by term to the A-vector.

are to be computed, that eigenvector is taken which corresponds to the wavefunction which has the largest overlap with the initial state.

An MCTDH always works, whatever the number of SPFs. If there are too few configurations, the propagation will be less accurate but usually still describes the overall features rather well. This is in contrast to *improved relaxation* which fails to converge when the configuration space is too small. There is never a problem in computing the ground state, but converging to excited states becomes more difficult the higher the excitation energy or, more precisely, the higher the density of states.

The *improved relaxation* algorithm may be used in block form, *i.e.* one may start with a block of initial vectors which then converge collectively to a set of eigenstates. Formally the different wave functions are treated as electronic states of one 'super wavefunction'. As the single-set algorithm is used, there is one set of SPFs for all wave functions. The mean-fields are hence state-averaged mean-fields and the Davidson routine is replaced by a block-Davidson one. The block form of *improved relaxation* is more efficient than the single vector one when several eigenstates are to be computed. However, the block form requires considerably more memory.

Improved relaxation has been applied quite succesfully to a number of problems. For 4-atoms systems (6D) it is in general possible to compute all eigenstates of interest. For a system as large as $H_5O_2^+$ (15D) it was, of course, only possible to converge few low lying states.

Chapter 6

Correlation DVR (CDVR)

6.1 TD-DVR

The correlation DVR method (CDVR) method is not implemented in the Heidelberg MCTDH package. However, as it plays a central role in the MCTDH code of Uwe Manthe, we discuss it briefly here.

The idea[1] is to use the SPFs to build a DVR. This time-dependent DVR has much less points (as $n < N$) but may still be good enough as the SPFs are optimal for representing the WF.

Hence one diagonalizes the matrix representation of the position operator

$$Q_{jl}^{(\kappa)} = \left\langle \varphi_j^{(\kappa)} \middle| \hat{q}^{(\kappa)} \middle| \varphi_l^{(\kappa)} \right\rangle \tag{6.1}$$

to obtain the eigenvalues $q_\alpha^{(\kappa)}$ $(\alpha = 1, \ldots, n_\kappa)$ and the eigenvectors which are used to transform the SPFs and the A-vector to position orbitals $\xi_j^{(\kappa)}$.

$$\left\langle \xi_j^{(\kappa)} \middle| \hat{q}^{(\kappa)} \middle| \xi_l^{(\kappa)} \right\rangle = q_i^{(\kappa)} \ \delta_{jl} \tag{6.2}$$

In this DVR, V_{JL} is given by

$$\begin{aligned} V_{JL} &= \left\langle \xi_{j_1}^{(1)} \cdots \xi_{j_f}^{(f)} \middle| V(q_1, \ldots, q_f) \middle| \xi_{l_1}^{(1)} \cdots \xi_{l_f}^{(f)} \right\rangle \\ &= V(q_{j_1}^{(1)}, \ldots, q_{j_f}^{(f)}) \cdot \delta_{j_1 l_1} \cdots \delta_{j_f l_f} \end{aligned} \tag{6.3}$$

And similarly one proceeds to compute the mean-fields.

Hence one does an "ordinary" quadrature but not over the primitive grid which has N^f points but rather over a time-dependent adaptive grid of n^f points. This is an enormous reduction in effort and the n^f scaling law is similar to the MCTDH scaling laws. So it looks very promising. However, the error introduced is too large.

[1] U. Manthe, H.-D. Meyer, L. S. Cederbaum, *J. Chem. Phys.* **97**, 3199, (1992).

6.2 CDVR

To improve the situation[2] we remark that the general MCTDH philosophy is to do the uncorrelated part correctly. Only for the correlated part one adopts an approximation (small numbers of SPFs).

To this end, one adds a correction term which ensures that one-dimensional potentials will be treated exactly, *i.e.* on the fine grid.

$$\begin{aligned} V_{JL} &= \langle \xi^{(1)}_{j_1} \cdots \xi^{(f)}_{j_f} | V(q_1 \cdots q_f) | \xi^{(1)}_{l_1} \cdots \xi^{(f)}_{l_f} \rangle \\ &= V(q^{(1)}_{j_1} \cdots q^{(f)}_{j_f}) \cdot \delta_{j_1 l_1} \cdots \delta_{j_f l_f} \\ &+ \sum_{\kappa=1}^{f} \langle \xi^{(\kappa)}_{j_\kappa} | \Delta V^{(\kappa)}(q^{(1)}_{j_1}, \ldots, q^{(\kappa-1)}_{\kappa-1}, q_\kappa, q^{(\kappa+1)}_{\kappa+1}, \ldots, q^{(f)}_{j_f}) | \xi^{(\kappa)}_{l_\kappa} \rangle \\ &\times \delta_{j_1 l_1} \cdots \delta_{j_{\kappa-1} l_{\kappa-1}} \, \delta_{j_{\kappa+1} l_{\kappa+1}} \cdots \delta_{j_f l_f} \end{aligned} \tag{6.4}$$

where

$$\begin{aligned} &\Delta V^{(\kappa)}(q^{(1)}_{j_1}, \ldots, q^{(\kappa-1)}_{\kappa-1}, q_\kappa, q^{(\kappa+1)}_{\kappa+1}, \ldots, q^{(f)}_{j_f}) = \\ &V(q^{(1)}_{j_1}, \ldots, q^{(\kappa-1)}_{\kappa-1}, q_\kappa, q^{(\kappa+1)}_{\kappa+1}, \ldots, q^{(f)}_{j_f}) - V(q^{(1)}_{j_1}, \ldots, q^{(f)}_{j_f}) \end{aligned} \tag{6.5}$$

It is easy to show that if V is separable

$$V(q_1, \ldots, q_f) = V^{(1)}(q_1) + V^{(2)}(q_2) + \cdots + V^{(f)}(q_f) \tag{6.6}$$

then V_{JL} is given "exactly", *i.e.* by quadrature over the primitive grid.

CDVR works fine and often gives good results. Its numerical effort is described by $f \cdot N \cdot n^{f-1} + n^f$ potential evaluations. This is still within MCTDH scaling laws, but the pre-factor is high as a potential evaluation will require many operations. Hence in a CDVR calculation the evaluation of the potential often takes $95 - 99.5\%$ of the total effort. That is a bit odd.

But the most important drawback of CDVR is that one cannot use mode combination, at least not straightforwardly. To arrive at two- (or multi-) dimensional grid points (x_κ, y_κ) and the associated two-dimensional localized functions one can solve the minimization problem

$$\langle \xi(x,y) | (\hat{x} - x_0)^2 + (\hat{y} - y_0)^2 | \xi(x,y) \rangle = min \tag{6.7}$$

To be varied are the numbers x_0, y_0 and the functions ξ. In $1D$ one can show that a diagonalization solves the minimum problem. With this trick one can derive a $2D$-DVR for the $2D$-SPFs. However, it seems not to work so well, as there are almost no published results. Seemingly, for multi-dimensional comined SPFs there are too few quadrature points thus deteriorating the quality of the CMF quadrature.

[2] U. Manthe, *J. Chem. Phys.* **105**, 6989 (1996).

Chapter 7

Electronic States

Some small modifications of the MCTDH algorithm are required when the WF is to be propagated on several electronic states, *i.e.* when vibronic coupling becomes important

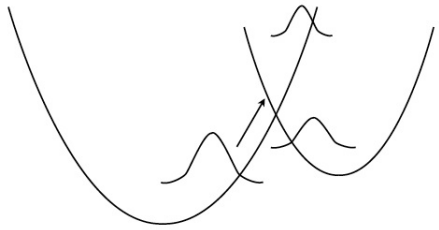

Figure 7.1: Wavepacket evolving on two coupled states.

One can modify the MCTDH ansatz straightforwardly by including the electronic state-labelling as additional coordinate

$$\Psi(q_1,\ldots,q_f,\alpha,t) = \sum_{j_1}^{n_1}\cdots\sum_{j_f}^{n_f}\sum_{s=1}^{n_s} A_{j_1\cdots j_f\ s}\ \varphi_{j_1}^{(1)}(q_1,t)\cdots\varphi_{j_f}^{(f)}(q_f,t)\varphi_s^{(f+1)}(\alpha,t) \qquad (7.1)$$

The coordinate α is discrete and $\varphi_s^{(f+1)}(\alpha,t)$ is hence a vector and not a function. But this is nothing new, all our variables are discrete, because we use DVRs.

There are usually only a few electronic states. This makes it reasonable to use a complete set of SPFs for the electronic degrees of freedom, *i.e.* as many SPFs as there are electronic states. Doing so, the SPFs become time-independent (because of the projector) and it is useful to choose

$$\varphi_s^{(f+1)}(\alpha,t) = \delta_{\alpha,s} \qquad (7.2)$$

This allows us to write the WF in a more vivid form:

$$\Psi = \sum_{j_1}^{n_1} \cdots \sum_{j_f}^{n_f} \sum_{\alpha=1}^{n_s} A_{j_1 \cdots j_f \alpha} \; \varphi_{j_1}^{(1)}(q_1,t) \cdots \varphi_{j_f}^{(f)}(q_f,t) \big| \alpha \big\rangle \tag{7.3}$$

This is the so called single set formalism. It is called "single-set" because there is one set of SPFs for all electronic states. The single-set formalism closely follows the MCTDH philosophy. In contrast, the *multi-set* formulation uses different sets of SPFs for each state

$$\Psi(q_1, \ldots, q_f, \alpha, t) = \sum_{\alpha=1}^{n_s} \Psi^{(\alpha)}(q_1, \ldots, q_f, t) \big| \alpha \big\rangle \tag{7.4}$$

where each component WF $\Psi^{(\alpha)}$ is expanded in MCTDH form

$$\Psi^{(\alpha)}(q_1, \ldots, q_f, t) = \sum_{j_1^\alpha}^{n_1^\alpha} \cdots \sum_{j_f^\alpha}^{n_f^\alpha} A^{(\alpha)}_{j_1^\alpha \cdots j_f^\alpha}(t) \; \varphi_{j_1}^{(1,\alpha)}(q_1,t) \cdots \varphi_{j_f^\alpha}^{(f,\alpha)}(q_f,t) \tag{7.5}$$

The equations of motion must be generalized

$$i \; \dot{A}_J^{(\alpha)} \;=\; \sum_{\beta=1}^{n_s} \sum_{L} \mathcal{K}_{JL}^{(\alpha,\beta)} \; A_L^{(\beta)} \tag{7.6}$$

$$i \; \dot{\varphi}_j^{(\kappa,\alpha)} \;=\; \left(1 - P^{(\kappa,\alpha)}\right) \left(\rho^{(\kappa,\alpha)}\right)^{-1}_{jl} \sum_{\beta=1}^{n_s} \sum_{k=1}^{n_\kappa^\alpha} \mathcal{H}_{lk}^{(\kappa,\alpha,\beta)} \; \varphi_k^{(\kappa,\beta)} \tag{7.7}$$

with the obvious definitions

$$\mathcal{K}_{JL}^{(\alpha,\beta)} = \big\langle \Phi_J^{(\alpha)} \big| H^{(\alpha,\beta)} \big| \Phi_L^{(\beta)} \big\rangle \tag{7.8}$$

$$\mathcal{H}_{jl}^{(\kappa,\alpha,\beta)} = \big\langle \Psi_j^{(\kappa,\alpha)} \big| H^{(\alpha,\beta)} \big| \Psi_l^{(\kappa,\beta)} \big\rangle \tag{7.9}$$

The single-set formalism is of advantage if the dynamics in the different electronic states is similar, *e.g.* when the surfaces are almost parallel. The more complicated multi-set formalism is more efficient when the dynamics on the various diabatic states is rather different. In most cases multi-set is the preferred scheme.

Chapter 8

Initial state

As emphasized several times, using a time-dependent method requires to specifiy an initial state. The simplest choice is a Hartree product. The A-vector then becomes

$$A_{j_1 \cdots j_f} = \delta_{j_1,1} \cdots \delta_{j_f,1} \tag{8.1}$$

hence a 1 at the first position and zero everywhere else. A more complicated A-vector can be specified through the keyword `A-coeff`. One specifies a few individual values of $A_{j_1 \cdots j_f}$ all remaining entries are set to zero. Next we have to specify the initial SPFs. For the Heidelberg MCTDH package, the choices are:

(1) Generalized Gaussians

$$\varphi(x) = N \, \exp(-\alpha \, (x - x_0)^2 + i p_0 x) \tag{8.2}$$

where α can be complex whereas x_0 and p_0 are real parameters.

The other SPFs of that DOF are generated by multiplying φ with x and Schmidt-orthogonalize to the lower functions. For a simple Gaussian to start with, this in fact produces the harmonic oscillator functions.

(2) Legendre functions

$$P_l(\cos\,\theta) \tag{8.3}$$

and associated Legendre functions

$$P_j^m(\cos\,\theta) \tag{8.4}$$

These functions are then $\mathcal{L}^2$ normalized and may serve as initial functions for angular degrees of freedom.

(3) Eigenfunctions of a $1D$-Hamiltonian. This $1D$-Hamiltonian has to be defined in the operator file. This operator is the diagonalised when the keyword `eigenf` is set.The eigenfunctions are taken as SPFs.

(4) Eigenfunctions of a mode-Hamiltonian. A mode (particle) Hamiltonian is diagonalised by a Lanczos algorithm when the keyword `meigenf` is set. The eigenfunctions are taken as SPFs.

Example: Inelastic $H_2 + H_2$ scattering:

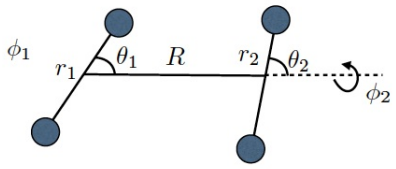

Figure 8.1: The $H_2 + H_2$ set of coordinates.

The H_4 system is described by 7 coordinates, ϕ_1, θ_1, r_1, ϕ_2, θ_2, r_2, and R. This is because we are working in a so-called E_c system rather than a body-fixed (BF) system. In BF, $\phi = 0$ by definition. The DoFs (θ_1, ϕ_1) and (θ_2, ϕ_2) are combined, because we want to use the two-dimensional DVRs KLeg or PLeg. The initial SPFs are the spherical harmonics:

$$\phi(\theta_i, \phi_i, t = 0) = Y_j^m(\theta_i, \phi_i) \sim P_j^m(cos\theta_i)\ e^{im\varphi_i} \quad \text{for } i = 1, 2 \tag{8.5}$$

where j and m denote the initial rotational quantum numbers of the diatomic subsystem. For $\varphi(r_1, t = 0)$ and $\varphi(r_2, t = 0)$ we take the eigenfunctions of the $1D$-vibrational Hamiltonian

$$H_{vib} = -\frac{1}{2m}\frac{\partial^2}{\partial r^2} + \frac{j(j+1)}{2mr^2} + V_{H_2}(r) \tag{8.6}$$

and for $\varphi(R, t = 0)$ we use a Gaussian with momentum p_0

$$\varphi(R) = e^{-\alpha(R-R_0)^2}\ e^{-ip_0R} \tag{8.7}$$

For this case this is a very appropriate initial state.

For several other applications the initial state is an eigenstate, often the ground state, of another Hamiltonian (or electronic state), *e.g.* the photodissociation of NOCl. In this case one builds a Hartree product and relaxes it to the ground state or uses improved relaxation to obtain an excited state.

Finally, one often needs to multiply a MCTDH wavefunction with an operator to get an appropriate initial state. A typical example is the IR-spectroscopy. Here the initial state is

$$\hat{\mu} \cdot \Psi_0 \tag{8.8}$$

where Ψ_0 denotes the ground state and $\hat{\mu}$ the dipole operator.

MCTDH can do such an operation, keyword "operate", but this is a complicated iterative process, because the A-vector and the SPFs have to be modified. The working equations are derived through a VP. Let $\tilde{\Psi}$ and Ψ denote the WF to be operated and the final result, respectively:

$$\Psi = \hat{D}\tilde{\Psi} \tag{8.9}$$

Then the VP reads

$$\left\langle \delta\Psi_J \middle| \Psi - \hat{D}\tilde{\Psi} \right\rangle = \delta \sum_{\kappa=1}^{f} \sum_{jl} \epsilon_{jl}^{(\kappa)} \left(\langle \varphi_j^{(\kappa)} | \varphi_l^{(\kappa')} \rangle - \delta_{jl} \right) \tag{8.10}$$

The right hand-side is introduced to ensure orthonormality of the SPFs. The $\epsilon_{jl}^{(\kappa)}$ are the so-called Lagrange multipliers.

Variation with respect to the coefficients yields ($\partial\Psi/\partial A_J = \Phi_J$)

$$\left\langle \Phi_J \middle| \Psi - D\tilde{\Psi} \right\rangle = 0 \tag{8.11}$$

or

$$\boxed{A_J = \sum_L \langle \Phi_J | D | \tilde{\Phi}_L \rangle \tilde{A}_L} \tag{8.12}$$

Variation with respect to $\langle \varphi_j^{(\kappa)} |$ yields ($\partial\Psi/\partial\varphi_j^{(\kappa)} = \Psi_j^{(\kappa)}$)

$$\left\langle \Psi_j^{(\kappa)} \middle| \Psi - \hat{D}\tilde{\Psi} \right\rangle = \sum_l \epsilon_{jl}^{(\kappa)} \ \varphi_l^{(\kappa)} \tag{8.13}$$

Since

$$\Psi = \sum_j \Psi_j^{(\kappa)} \ \varphi_j^{(\kappa)} \tag{8.14}$$

one finds

$$\left(\rho_{jl}^{(\kappa)} - \epsilon_{jl}^{(\kappa)} \right) \cdot \varphi_l^{(\kappa)} = \sum_L \langle \Psi_j^{(\kappa)} | D | \tilde{\Psi}_l^{(\kappa)} \rangle \ \tilde{\varphi}_l^{(\kappa)} \tag{8.15}$$

Rather than to determine those values of $\epsilon_{jl}^{(\kappa)}$ which keep the SPFs orthogonal, we drop the matrix $\left(\boldsymbol{\rho} - \boldsymbol{\epsilon}\right)$ and define

$$\tilde{\tilde{\varphi}}_j^{(\kappa)} = \sum_l \langle \Psi_j^{(\kappa)} | D | \tilde{\Psi}_l^{(\kappa)} \rangle \ \tilde{\varphi}_l^{(\kappa)} \tag{8.16}$$

The desired functions $\varphi_j^{(\kappa)}$ are then obtained by Schmidt orthogonalization of the $\tilde{\tilde{\varphi}}_j^{(\kappa)}$. This procedure is legitimate as only the space spanned by the SPFs matters. Orthogonal transformations among the SPFs are accounted for by the coefficients. The iteration reads:

(0)

$$\begin{aligned} \varphi_j^{(\kappa)(0)} &= \tilde{\tilde{\varphi}}_j^{(\kappa)} \\ A_j^{(0)} &= \sum_L \langle \Phi_J^{(0)} | D | \tilde{\Phi}_L \rangle \tilde{A}_L \end{aligned} \tag{8.17}$$

(1) `for` $i = 0, 1, 2, \ldots$ `do`:

$$\tilde{\tilde{\varphi}}_j^{(\kappa)(i+1)} = \sum_l \langle \Psi_j^{(\kappa)(i)} | D | \tilde{\Psi}_l^{(\kappa)} \rangle \ \tilde{\varphi}_l^{(\kappa)} \tag{8.18}$$

(2) Gram-Schmidt orthogonalization of $\tilde{\tilde{\varphi}}_j^{(\kappa)}$ to obtain $\varphi_j^{(\kappa)}$.

(3)
$$A_J^{(i+1)} = \sum_L \langle \Phi_J^{(i+1)} | D | \tilde{\Phi}_L \rangle \tilde{A}_L \tag{8.19}$$

(4) `stop if`
$$1 - \mathrm{Trace}\{ P^{(\kappa)(i)} \; P^{(\kappa)(i+1)} \; \hat{\rho}^{(\kappa)(i+1)} \} \tag{8.20}$$
is smaller than some threshold. Here $P^{(\kappa)(i)}$ denotes the MCTDH projection at the i-th iteration and $\hat{\rho}^{(\kappa)(i)}$ the density operator at the i-th iteration.

(5) `next i`

Chapter 9

Representation of the potential

9.1 The Product form

We have already mentioned the quadrature problem. At each time-step we have to compute the matrix representation of the Hamiltonian

$$H_{JK} = \langle \Phi_J | H | \Phi_K \rangle \tag{9.1}$$

and the mean-fields

$$\langle H \rangle_{jl}^{(\kappa)} = \langle \Psi_j^{(\kappa)} | H | \Psi_l^{(\kappa)} \rangle \tag{9.2}$$

If one would do these integrals by straightforward quadrature over the primitive grid, one would have to run over N^f grid points for potential like operators and N^{2f} points for non-diagonal operators. For example

$$V_{JK} = \langle \Phi_J | V | \Phi_K \rangle = \sum_{i_1=1}^{N_1} \cdots \sum_{i_f=1}^{N_f} \varphi_{j_1}^{(1)^*}(q_{i_1}^{(1)}) \cdots \varphi_{j_f}^{(f)^*}(q_{i_f}^{(f)}) V(q_{i_1}^{(1)}, \ldots, q_{i_f}^{(f)}) \varphi_{j_1}^{(1)}(q_{i_1}^{(1)}) \cdots \varphi_{j_f}^{(f)}(q_{i_f}^{(f)}) \tag{9.3}$$

And this integral has to be done for each J and K, hence n^{2f} times.

Example:

Let $f = 6$, $n = 6$ and $N = 32$.

One integral: $N^f = 32^6 = 10^9$ operations

Number of integrals: $n^{2f} = 6^{12} = 2 \cdot 10^9$ operations

hence $\approx 10^{18}$ operations in total. This is impossible!

The trick is to write the Hamiltonian as a sum of products[1]

$$H = \sum_{r=1}^{s} c_r \; h_r^{(1)} \cdots h_r^{(f)} \tag{9.4}$$

where $h_r^{(\kappa)}$ operates on the κ-th DOF only.

If we now do the integral we find:

$$H_{JK} = \sum_{r=1}^{s} c_r \langle \varphi_{j_1}^{(1)} | h_r^{(1)} | \varphi_{j_1}^{(1)} \rangle \cdots \langle \varphi_{j_f}^{(f)} | h_r^{(f)} | \varphi_{j_f}^{(f)} \rangle \tag{9.5}$$

i.e. a sum of products of *one-dimensional* integrals.[2]Doing all the H_{JK} integrals we can re-use the $\langle h_r^{(\kappa)} \rangle$ integrals. There are

$$s \cdot f \cdot n^2$$

1D integrals to be done. Hence

$$s \cdot f \cdot N \cdot n^2 \tag{9.6}$$

multiplications have to be performed.

The final summation is a negligible amount of work. This is to be compared with the work of doing the integrals directly, *i.e.* $n^{2f} \cdot N^f$. Going back to our example: $f = 6$, $n = 6$ and $N = 32$, and assumeing a rather large number of terms, $s = 14000$, we find

$$s \cdot f \cdot N \cdot n^2 \approx 10^8$$
$$n^{2f} \cdot N^f \approx 10^{18}$$

Hence we gain 10 orders of magnitude!

The question is, how realistic is a product form of the Hamiltonian? Fortunately KEOs are almost always of product form. For example NOCl (Fig.9.1):

$$\begin{aligned} T = \quad & -\frac{1}{2\mu_d} \frac{\partial^2}{\partial r_d^2} - \frac{1}{2\mu_v} \frac{\partial^2}{\partial r_v^2} \\ & -\frac{1}{2\mu_d \, r_d^2} \frac{1}{sin\theta} \frac{\partial}{\partial \theta} sin\theta \frac{\partial}{\partial \theta} \\ & -\frac{1}{2\mu_v \, r_v^2} \frac{1}{sin\theta} \frac{\partial}{\partial \theta} sin\theta \frac{\partial}{\partial \theta} \end{aligned}$$

[1]When using mode-combination and particle operators, the expression reads:

$$H = \sum_{r=1}^{s} c_r \; h_r^{(1)} \cdots h_r^{(p)}$$

where $h_r^{(\kappa)}$ operates on the κ-th particle (combined mode) only.

[2]Of course, mode-combination can be used. Then $h^{(\kappa)}$ operates on the κth particle, and the integrals in Eq.(9.5) are low-dimensional rather than one-dimensional ones.

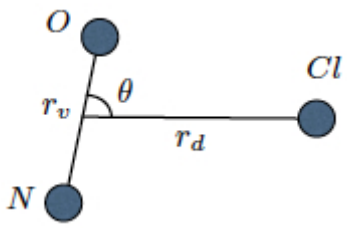

Figure 9.1: The Jacobi coordinates for NOCl.

Potentials are sometimes given as polynomials. *E.g.* in the NOCl case

$$V(r_d, r_v, \theta) = \sum_{i,j,k} C_{i,j,k} \left(r_d - r_d^e\right)^i \left(r_v - r_v^e\right)^j cos^k\theta \quad (\text{or} \quad cos(k\theta)) \tag{9.7}$$

Hence the product form is not as unusual as it may look at a first glance. For the general case, however, one needs an algorithm which brings a general potential to product form. POTFIT is such an algorithm.

9.2 The potfit algorithm

The most direct way to achieve a product form is an expansion of the potential in a product basis:

$$V^{\text{app}}(q_1, \ldots, q_f) = \sum_{j_1=1}^{m_1} \cdots \sum_{j_f=1}^{m_f} C_{j_1 \ldots j_f} \; v_{j_1}^{(1)}(q_1) \cdots v_{j_f}^{(f)}(q_f) \tag{9.8}$$

(Looks like a MCTDH expansion of a WF!) The expansion orders, m_κ, have to be chosen such that the representation of the "potfitted" potential, V^{app}, is on the one hand as small as possible but on the other hand of sufficient accuracy.

As we use DVRs we need to know the potential only at the grid points. Let $q_i^{(\kappa)}$ denote the position of the i-th grid point of the κ-th grid. Then we define

$$V_{i_1,\ldots,i_f} = V(q_{i_1}^{(1)}, \ldots, q_{i_f}^{(f)}) \tag{9.9}$$

i.e. $V_{i_1,\ldots,i_f}$ denotes the value of the potential on the grid points.
The approximate potential on the grid is given by

$$V_{i_1,\ldots,i_f}^{\text{app}} = \sum_{j_1=1}^{m_1} \cdots \sum_{j_f=1}^{m_f} C_{j_1 \ldots j_f} \; v_{i_1\, j_1}^{(1)} \cdots v_{i_f\, j_f}^{(f)} \tag{9.10}$$

where

$$v_{i_\kappa\, j_\kappa}^{(\kappa)} = v_{j_\kappa}^{(\kappa)}(q_{i_\kappa}^{(\kappa)}) \tag{9.11}$$

The single particle potentials (SPPs) are assumed to be orthogonal on the grid

$$\sum_{i=1}^{N_\kappa} v_{ij}^{(\kappa)} v_{il}^{(\kappa)} = \delta_{jl} \tag{9.12}$$

Throughout this chapter i and k label grid-points and j and l label SPPs. We can, of course, use mode combination. Then the SPPs are defined on multi-dimensional grids and f is to be replaced by p. The generalization is obvious.

To find the optimal coefficients and the optimal SPPs, we minimize

$$\Delta^2 = \sum_{i_1=1}^{N_1} \cdots \sum_{i_f=1}^{N_f} \left(V_{i_1 \ldots i_f} - V^{\mathrm{app}}_{i_1 \ldots i_f} \right)^2 = \sum_I (V_I - V_I^{\mathrm{app}})^2 \tag{9.13}$$

Minimizing Δ^2 by varying only the coefficients yields:

$$C_{j_1 \cdots j_f} = \sum_{i_1=1}^{N_1} \cdots \sum_{i_f=1}^{N_f} V_{i_1 \ldots i_f} \; v^{(1)}_{i_1 \; j_1} \cdots v^{(f)}_{i_f \; j_f} \tag{9.14}$$

hence the coefficients are given by overlap (as expected).

Plugging this into the expression for Δ^2 yields:

$$\Delta^2 = \|\boldsymbol{V}\|^2 - \|\boldsymbol{C}\|^2 = \sum_I V_I^2 - \sum_I C_I^2 \tag{9.15}$$

Therefore, one has to optimize the (orthonormal) SPPs such that $\|\boldsymbol{C}\|^2$ becomes maximal. The solution of this variational problem is difficult. It is numerically very demanding and likely to converge to a local minimum.

We take a shortcut and define potential density matrices as:

$$\rho^{(\kappa)}_{kk'} = \sum_{I^\kappa} V_{I^\kappa_k} V_{I^\kappa_{k'}} \tag{9.16}$$

We then diagonalize the densities $\boldsymbol{\rho}^{(\kappa)}$ and take the eigenvectors with the largest eigenvalues as SPPs. (Note $\boldsymbol{\rho}^{(\kappa)}$ is positive semi-definite. Hence all eigenvalues $\lambda_j \geq 0$). The procedure is known to yield the optimal SPPs for a two dimensional case. For higher dimensions the error is not optimal but sufficiently close to optimal.

9.2.1 Contraction

Contraction over one mode is another very useful trick to reduce the numerical effort. We can perform one sum once for all. Let us, for the sake of simplicity, contract over the first DOF:

$$D_{i_1 j_2 \cdots j_f} := \sum_{j_1=1}^{N_1 \not= m_1} C_{j_1 \cdots j_f} \; v^{(1)}_{i_1 j_1} \tag{9.17}$$

The potential is then given by

$$V^{\mathrm{app}}_{i_1, \ldots, i_f} = \sum_{j_2=1}^{m_1} \cdots \sum_{j_f=1}^{m_f} D_{i_1 j_2 \ldots j_f} \; v^{(2)}_{i_2 \; j_2} \cdots v^{(f)}_{i_f \; j_f} \tag{9.18}$$

Hence, rather than m^f terms we have only $m^{(f-1)}$ terms. Moreover, if we increase m_1 to N_1, which increases the accuracy, one notices that C of that index is a unitary transformation of V which is then transformed back. Hence there is no transformation at all and D is given by

$$D_{i_1 j_2 \ldots j_f} = \sum_{i_2 \cdots i_f} V_{i_1 \cdots i_f} \; v^{(2)}_{i_2 \; j_2} \cdots v^{(f)}_{i_f \; j_f} \tag{9.19}$$

Turning to a coordinate representation, we write the contracted potential more vividly

$$V^{\text{app}}(q_1, \ldots, q_f) = \sum_{j_2=1}^{m_2} \cdots \sum_{j_f=1}^{m_f} D_{j_2 \ldots j_f}(q_1) v^{(2)}_{j_2}(q_2) \cdots v^{(f)}_{j_f}(q_f) \tag{9.20}$$

Of course we can contract over any degree of freedom, not necessarily over the first one. In general one will contract over that mode which otherwise has the largest m. Note that when using contraction the coefficient vector C and the SPPs of the contracted mode are not computed, see Eq. (9.19).

9.2.2 Error estimate

Letting ν denote the contracted mode, the error can be bounded by

$$\frac{\Lambda}{f-1} \leq \Delta^2_{opt} \leq \Delta^2 \leq \Lambda \tag{9.21}$$

where

$$\Lambda = \sum_{\substack{\kappa=1 \\ \kappa \neq \nu}}^{f} \sum_{j=m_\kappa+1}^{N_\kappa} \lambda^{(\kappa)}_j \tag{9.22}$$

and where Δ^2 denotes the potfit $\mathcal{L}^2$-error and Δ^2_{opt} the $\mathcal{L}^2$-error one would obtain after a full optimization of the SPPs. Note that the error is determined by the eigenvalues of the neglected SPPs. In particular, for $m_\kappa = N_\kappa$ one recovers the exact potential on the grid.

The last inequality of Eq. (9.21) tells us how to choose the expansion orders, m_κ, for a given error to be tolerated. The inequality in the middle is trivial and the last inequality shows that the error bound Λ is at most $(f-1)$ times larger than the optimal error Δ^2_{opt}.

Proof of Eq. (9.21)

In appendix D of the MCTDH review[3] is shown that

$$\begin{aligned}\Delta^2 &= \sum_{\substack{\text{neglected}\\ \text{terms}}} |C_J|^2 = \sum_{j_1=m_1+1}^{N_1}\sum_{j_2=1}^{N_2}\cdots\sum_{j_f=1}^{N_f}|C_{j_1\ldots j_f}|^2 \\ &+ \sum_{j_1=1}^{m_1}\sum_{j_2=m_2+1}^{N_2}\cdots\sum_{j_f=1}^{N_f}|C_{j_1\ldots j_f}|^2 \\ &+ \cdots + \\ &+ \sum_{j_1=1}^{m_1}\sum_{j_2=1}^{m_2}\cdots\sum_{j_f=m_f+1}^{N_f}|C_{j_1\ldots j_f}|^2 \end{aligned} \tag{9.23}$$

where we have assumed that the coefficients $C_{j_1\ldots j_f}$ are evaluated for $1 \le j_\kappa \le N_\kappa$ although in potfit they are used only for $1 \le j_\kappa \le m_\kappa$. We can enlarge the sum by letting j_κ always run up to N_κ. Hence

$$\Delta^2 \le \sum_{\kappa=1}^{f}\sum_{I^\kappa}\sum_{j=m_\kappa+1}^{N_\kappa}|C_{I_j^\kappa}|^2 = \sum_{\kappa=1}^{f}\sum_{j=m_\kappa+1}^{N_\kappa}\lambda_j^{(\kappa)} \tag{9.24}$$

because

$$\tilde{\rho}_{jj'}^{(\kappa)} = \sum_{J^\kappa}^{\{N\}} C_{I_j^\kappa} C_{I_{j'}^\kappa} = \delta_{jj'}\ \lambda_j^{(\kappa)} \tag{9.25}$$

Here J runs up to N. Note that the C's are just the unitarily transformed V's.[4]

This proves the right-hand-side inequality. Because we use contraction and we are complete in the contracted mode, we may restrict the sums over κ in Eq. (9.24) to $\kappa \neq \nu$, where ν denotes the contracted mode. Next, we set all $m_\nu = N_\nu$ except for the κ-th degree of freedom. The $\mathcal{L}^2$-error is then

$${}^{(\kappa)}\Delta^2 = \sum_{j=m_\kappa+1}^{N_\kappa}\lambda_j^{(\kappa)} \tag{9.26}$$

and as we may collect all DOFs $\neq \kappa$ into one mode, we are essentially treating a 2-mode problem which is optimal

$${}^{(\kappa)}\Delta^2 = {}^{(\kappa)}\Delta^2_{\text{opt}} \tag{9.27}$$

[3] M. H. Beck, A. Jäckle, G. A. Worth and H.-D. Meyer, Physics Reports **324**, 1 (2000).

[4] To show this

$$\begin{aligned}\tilde{\rho}_{jj'}^{(\kappa)} &= \sum_{J^\kappa}^{\{N\}} C_{I_j^\kappa} C_{I_{j'}^\kappa} \\ &= \sum_{J^\kappa} \left(\boldsymbol{\Omega}^T \boldsymbol{V}\right)_{J_j^\kappa} \left(\boldsymbol{\Omega}^T \boldsymbol{V}\right)_{J_{j'}^\kappa} \\ &= \sum_{I^\kappa}\sum_{i,i'} V_{I_i^\kappa}\ v_{ij}^{(\kappa)}\ V_{I_{i'}^\kappa}\ v_{i'j'}^{(\kappa)} \\ &= \sum_{i,i'} v_{ij}^{(\kappa)}\ \rho_{ii'}^{(\kappa)}\ v_{i'j'}^{(\kappa)} = \left(\boldsymbol{v}^{(\kappa)^T}\ \boldsymbol{\rho}^{(\kappa)}\ \boldsymbol{v}^{(\kappa)}\right)_{j,j'} \\ &= \rho_{jj'}^{\text{diag}} = \delta_{jj'}\ \lambda_j^{(\kappa)}\end{aligned}$$

where the orthogonality of the SPPs along the grid has been used.

On the other hand, we have

$$ {}^{(\kappa)}\Delta^2_{\rm opt} \leq \Delta^2_{\rm opt} \tag{9.28} $$

because for ${}^{(\kappa)}\Delta^2$ we keep more terms. Finally, as κ is arbitrary, we arrive at

$$ \frac{1}{f-1} \sum_{\substack{\kappa=1 \\ \kappa\neq\nu}}^{f} \sum_{j=m_\kappa+1}^{N_\kappa} \lambda_j^{(\kappa)} \leq \max_{\kappa\neq\nu} \sum_{j=m_\kappa+1}^{N_\kappa} \lambda_j^{(\kappa)} \leq \max_{\kappa} {}^{(\kappa)}\Delta^2_{opt} $$

$$ \leq \Delta^2_{opt} \leq \Delta^2 \leq \sum_{\substack{\kappa=1 \\ \kappa\neq\nu}}^{f} \sum_{j=m_\kappa+1}^{N_\kappa} \lambda_j^{(\kappa)} \tag{9.29} $$

where ν denotes the contracted mode.

9.2.3 Weights

The inclusion of weights is often very important, because one does not need a uniform accuracy. The accuracy may be low when the potential is high, simply because the WF does not go there. On the other hand, we need a high accuracy near the minimum and at transition states (saddle points). Hence, we want to minimise:

$$ \Delta^2_w = \sum_I w_I^2 \, (V_I - V_I^{\rm app})^2 \tag{9.30} $$

The inclusion of separable weights

$$ w_I = w_{i_1}^{(1)} \ldots w_{i_f}^{(f)} \tag{9.31} $$

is very simple. One simply potfits $w_I \cdot V_I$ and then divide the SPPs by the weights

$$ v_i^{(\kappa)} \;\rightarrow\; v_i^{(\kappa)} / w_i^{(\kappa)} \tag{9.32} $$

However, separable weights are in general not very helpful. The inclusion of non-separable weights is very difficult. There appear matrices like

$$ \left\langle v_{j_1}^{(1)} \ldots v_{j_f}^{(f)} \middle| w \middle| v_{j_1}^{(1)} \ldots v_{j_f}^{(f)} \right\rangle \tag{9.33} $$

which have to be inverted. As their dimension is the full total grid size, this is impossible.

There is a nice trick to emulate non-separable weights. Assume there is a reference potential $V^{\rm ref}$ such that

$$ (V_I - V_I^{\rm app})\, w_I^2 = V_I^{\rm ref} - V_I^{\rm app} \tag{9.34} $$

holds. Then, we simply potfit $V^{\rm ref}$ and hence minimize

$$ \sum_I \left(V_I^{\rm ref} - V_I^{\rm app}\right)^2 \tag{9.35} $$

which in turn is equal to

$$ \sum_I w_I^2 \, (V_I - V_I^{\rm app})^2 \tag{9.36} $$

i.e. the weighted sum which we want to minimize! Obviously, V^{ref} is given by

$$V_I^{\text{ref}} = w_I^2 V_I + (1 - w_I^2) V_I^{\text{app}} \tag{9.37}$$

However, as V_I^{app} is unknown, we have to use an iterative process:[5]

(1) $V_I^{app\ (0)} = \texttt{potfit}(\text{V})$

(2) `for` $n = 1, ..., n_{\max}$ `do`

$$V_I^{\text{ref}\ (n)} = w_I^2\ V_I + (1 - w_I^2)\ V_I^{\text{app}\ (n-1)}$$
$$V^{\text{app}\ (n)} = \texttt{potfit}(V_I^{\text{ref}\ (n)})$$

(3) `next n`

The question is, of course, does this process converge? In fact, one may multiply w_I by some positive constant. The final converged result must not change. One can show that for sufficiently small w_I the iteration will always converge and for sufficiently large w_I it will always diverge.

For defining the weights adopt the concept of a relevant region, *i.e.*

$$w_I = w(q_I) = \begin{cases} 1 & \text{if } q_I \in \text{relevant region}, \\ 0 & \text{else.} \end{cases}$$

The relevant region is often defined by an energy criterium

$$w_I = w(q_I) = \begin{cases} 1 & \text{if } V_I \leq E_{rel}, \\ 0 & \text{if } V_I > E_{rel}. \end{cases}$$

but it may contain restrictions on the coordinate as well. We also tried to replace w_I by $\alpha \cdot w_I$. The iterative process always converges for $0 < \alpha \leq 1$ and always diverges for $\alpha > 2$. The convergence is slower for smaller α. An improved convergence speed can be obtained for $\alpha \approx 1.5, 1.6, \ldots$

9.2.4 Computational effort

Doing the integrals

$$\langle \Phi_J \,|V|\, \Phi_L \rangle \tag{9.38}$$

directly requires N^f multiplications. Using potfit one needs $s \cdot f \cdot N$ multiplications with $s = m^{f-1}$. Hence the gain is[6]

$$\text{gain}_{\text{CPU}} = \frac{1}{f} \left(\frac{N}{m} \right)^{f-1}$$

This is already a considerable gain if $m \leq N/3$ and $f \geq 3$. If we have to perform the integrals for all J and L we have to do n^{2f} such integrals because J and

[5] Actually, we loop over the modes and update V^{ref} after each new SPP(m).

[6] When using mode combination

$$\text{gain}_{\text{CPU}} = \frac{1}{p} \left(\frac{N}{m} \right)^{p-1}$$

L can take n^f different values. With potfit, however, we need to do $f \cdot n^2$ 1D integrals, store them, and finally do the sum of products of these integrals. The effort for the latter operation is negligible. Doing all the 1D integrals takes:

$$m^{f-1} \cdot f \cdot N \cdot n^2 \tag{9.39}$$

multiplications. Comparing this to $N^f \cdot n^{2f}$ yields the gain:

$$\text{gain}_{\text{CPU}} = \frac{1}{f} \left(\frac{N}{m} \right)^{f-1} n^{2(f-1)} \tag{9.40}$$

which is a large number already for $f \geq 3$. Example, for $f = 4$, $N = 21$, $m = 7$, and $n = 6$, $\text{gain}_{\text{CPU}} = 315000$.

9.2.5 Memory consumption

As the potential is diagonal (we always assume a DVR), it consumes N^f data points. A potfit with contraction reads

$$V^{\text{app}}_{i_1 \cdots i_f} = \sum_{j_2=1}^{m_2} \cdots \sum_{j_f=1}^{m_f} D_{j_2 \ldots j_f}(q_1) v^{(2)}_{j_2}(q_2) \cdots v^{(f)}_{j_f}(q_f) \tag{9.41}$$

Hence there are

$$\underbrace{m^{f-1} \cdot N}_{D} + \underbrace{(f-1) \cdot m \cdot N}_{v's} \tag{9.42}$$

data points. For $f \geq 3$ the second part is negligible. Hence

$$\text{gain}_{\text{mem}} = \frac{N^f}{m^{f-1} \cdot N} = \left(\frac{N}{m} \right)^{f-1} \tag{9.43}$$

For the small example system we have just discussed ($f = 4$, $N = 21$, $m = 7$), we have a memory gain of 27. But turning to a slightly larger system: $f = 6$, $N = 24$, $m = 6$, we find

$$\begin{aligned} \text{gain}_{\text{mem}} &= 1024 \\ \text{Full potential} &= 1.5\text{GB} \\ \text{Potfit} &= 1.5\text{MB} \end{aligned}$$

This is a very considerable reduction in memory demand!

Let us go even further and assume a really large system with $f = 12$, $N = 12$. Here we adopt mode-combination and combine 3 DOF into one particle: $d = 3$, $p = 4$, $N_{\text{particle}} = N^3_{\text{DOF}} = 1728$.

Let us assume we need $m = 45$ for convergence. Then there are

$$s = m^{p-1} = 45^3 = 91125 \quad \text{terms} \tag{9.44}$$

and the memory consumption is

$$m^{p-1} \cdot N_{\text{particle}} = 1.575 \times 10^8 \text{points} = 1.17\text{GB} \tag{9.45}$$

The full potential, however, requires

$$N^f = 12^{12} = 8.9 \cdot 10^{12} \text{ points} = 65\text{TB} \tag{9.46}$$

65 TB is impossible, but 1.17 GB is doable. Hence potfit solves also a memory problem! This is crucial for larger systems.

Unfortunately, we cannot potfit a $12D$ system. In potfit we have to run over the full product grid to determine the coefficients or the density matrices. This limits the use of potfit to systems with less than 10^9 grid points (*e.g.* 6D or 7D)

9.2.6 Summary

(i) POTFIT, although not fully optimal, is a variational method. If the number of terms increases, the error has to go down. For $m_\kappa = N_\kappa$ one recovers the exact potential at the grid points. Defining (cf. Eq.(9.29)):

$$\Lambda = \sum_{\substack{\kappa=1 \\ \kappa\neq\nu}}^{f} \sum_{j=m_\kappa+1}^{N_\kappa} \lambda_j^{(\kappa)} \tag{9.47}$$

we can bound the potfit error by

$$\frac{1}{f-1}\Lambda \leq \Delta^2_{\text{opt}} \leq \Delta^2 \leq \Lambda \tag{9.48}$$

(ii) The inclusion of weights is often important. It can significantly lower the rms error[7], which in this case is the error within the relevant region. However, due to the iterative character this makes potfit slow.

(iii) The operation

$$\sum_I V_{JI} \cdot A_I \tag{9.49}$$

which is part of

$$i\dot{A}_J = \sum_I H_{JI}\ A_I \tag{9.50}$$

requires $s \cdot f \cdot n^{f+1}$ operations for a potfitted potential rather than n^{2f} operations. This is another advantage of the product structure.

9.3 Cluster expansion

One way out of the potfit dilemma, (potfit can handle only total grid sizes up to 10^9), is an expansion called n-mode representation, or cut-HDMR or cluster

[7] The rms is defined as

$$\text{rms} = \sqrt{\Delta^2 / \sum_I w_I^2} = \sqrt{\Delta^2/N_{tot}} \qquad \text{if } w_I = 1 \qquad N_{tot} = \prod_\kappa N_\kappa$$

expansion. The potential is represented by a hierarchical expansion of one-body terms, two-body terms, etc.

$$V(q_1, q_2, \ldots, q_f) = V^{(0)} + \sum_{j=1}^{f} V_j^{(1)}(q_j) + \sum_{j<k} V_{jl}^{(2)}(q_j, q_k) + \sum_{j<k<l} V_{jkl}^{(2)}(q_j, q_k, q_l) + \ldots \quad (9.51)$$

The expansion is exact if we include all clusters up to the f-th order. The hope is, of course, that the series can be truncated after few terms.

The clusters $V^{(n)}$ can be determined in different ways, the easiest one is with respect to a reference point

$$\boldsymbol{q}^{(0)} = (q_1^{(0)}, q_2^{(0)}, \ldots, q_f^{(0)}) \quad (9.52)$$

usually the GS geometry. Then

$$V^{(0)} = V(\boldsymbol{q^{(0)}}) \quad (9.53)$$

$$V_j^{(1)}(q_j) = V(q_1^{(0)}, \ldots, q_{j-1}^{(0)}, q_j, q_{j+1}^{(0)}, \ldots, q_f^{(0)}) - V^{(0)} \quad (9.54)$$

$$V_{j,k}^{(2)}(q_j, q_k) = V(q_1^{(0)}, \ldots, q_j, \ldots, q_l, \ldots, q_f^{(0)}) - (V^{(0)} + V_j^{(1)}(q_j) + V_k^{(1)}(q_k)) \quad (9.55)$$

Note that the cluster vanishes, if at least one of the coordinates is at the reference point.

$$V_j^{(1)}(q_j^{(0)}) = 0$$
$$V_{jk}^{(2)}(q_j, q_k^{(0)}) = V_{jk}^{(2)}(q_j^{(0)}, q_k) = 0$$
$$V_{jkl}^{(3)}(q_j, q_k, q_l^{(0)}) = V_{jkl}^{(3)}(q_j, q_k^{(0)}, q_k) = V_{jkl}^{(3)}(q_j^{(0)}, q_k, q_l) = 0$$

From that follows that the n-th order cluster expansion

$$V_n(q_j, \ldots, q_f) = V^{(0)} + \ldots \sum_j V_{j\ldots}^{(n)} \quad (9.56)$$

is *exact* if at most n coordinates are not at the reference point.

The clusters can then be potfitted as they are usually smaller than 6D. One problem is that there are so many clusters. There are

$$\begin{pmatrix} f \\ n \end{pmatrix} = \frac{f!}{n!(f-n)!} \quad (9.57)$$

clusters of n-th order. For f=12 we obtain

n	0	1	2	3	4	5	6
$\begin{pmatrix} f \\ n \end{pmatrix}$	1	12	66	220	495	792	924

A way out of this dilemma is mode combination. We do the cluster expansion in combined modes

$$V(Q_1,\ldots,Q_p) = V^{(0)} + \sum_{j=1}^{p} V_j^{(1)}(Q_p) + \ldots + \sum V_{jl}^{(n)} + \ldots \tag{9.58}$$

with $f = 12$, $d = 2$ and $p = 6$, we could go to second or third order in the particles which would be up to 4th or 6th order in the DOFs. However, we have only a selection of the high order DOF clusters. With

$$Q_1 = (q_1, q_2),\ Q_2 = (q_3, q_4),\ Q_3 = (q_5, q_6) \tag{9.59}$$

and second order mode expansion one obtains

$$\begin{aligned} V(q_1,q_2,\ldots,q_f) = V^{(0)} + V^{(1)}(q_1,q_2) + V^{(1)}(q_3,q_4) + V^{(1)}(q_5,q_6) + \\ V^{(2)}(q_1,q_2,q_3,q_4) + V^{(2)}(q_1,q_2,q_5,q_6) + V^{(2)}(q_3,q_4,q_5,q_6) \end{aligned} \tag{9.60}$$

we do not miss any second order DOF term, *e.g.* $V(q_1, q_5)$ is contained in $V(q_1, q_2, q_5, q_6)$. In second order we are complete! However, we miss the 3rd order DOF terms $V(q_1, q_3, q_5)$, *i.e.* all terms where each coordinate is out of a different particle. Similarly, we miss $V(q_1, q_2, q_3, q_5)$, etc. If the mode combination scheme is good, *i.e.* combines the strongly correlated DOFs, the neglected terms will be small. The neglected terms will, of course, be recovered when including high orders in expansion (9.58). This, however is often out of the reach for numerical reasons. One usually takes all second order particle based clusters and a selection of third order clusters into account.

Chapter 10

Complex absorbing potentials (CAPs)

When dealing with a bound system, there is no problem with the grids. Turning to study dissociation or scattering processes one notices that some of the grids may become very long. The minimal propagation time is determined by the time needed for the slow components of the WF to leave the interaction region. Within this time interval the fast components of the WP may have travelled a long distance requiring a long grid.

A solution to this problem is provided by complex absorbing potentials (CAP). A CAP is a negative imaginary potential, usually written as

$$-i\eta W(r) = -i\eta\big(r - r_c\big)^n \; \theta\big(r - r_c\big)$$

where $W(r)$ is a non-negative real function, often of the indicated monomial form, n is 2,3, or 4, η is a strength parameter, r_c denotes the position where the CAP is switched on, and θ denotes a step function which ensures that the CAP vanishes for $r < r_c$.

Let us investigate how a CAP changes the norm

$$\begin{aligned}
\frac{d}{dt}\|\Psi\|^2 &= \frac{d}{dt}\big\langle\Psi\big|\Psi\big\rangle = \big\langle\dot\Psi\big|\Psi\big\rangle + \big\langle\Psi\big|\dot\Psi\big\rangle && (10.1)\\
&= \big\langle -iH\Psi\big|\Psi\big\rangle + \big\langle\Psi\big| -iH\Psi\big\rangle && (10.2)\\
&= i\big\langle\Psi\big|H^\dagger - H\big|\Psi\big\rangle && (10.3)
\end{aligned}$$

with

$$\begin{aligned}
H &= H_0 - i\eta W \qquad H_0 = H_0^\dagger && (10.4)\\
H^\dagger &= H_0 + i\eta W \qquad W = W^\dagger && (10.5)
\end{aligned}$$

follows

$$\begin{aligned}
\frac{d}{dt}\|\Psi\|^2 &= -2\eta\,\big\langle\Psi\big|W\big|\Psi\big\rangle && (10.6)\\
\frac{d}{dt}\|\Psi\| &= -\eta\,\frac{\big\langle\Psi\big|W\big|\Psi\big\rangle}{\|\Psi\|} && (10.7)
\end{aligned}$$

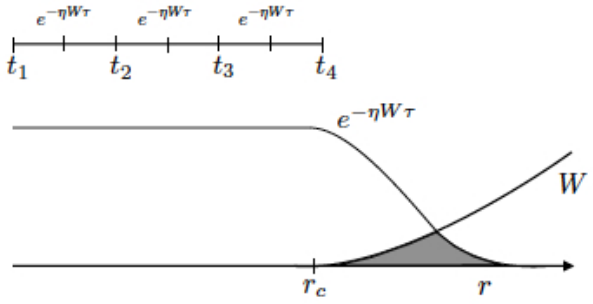

Figure 10.1: Decrease of the norm of a wavepacket being annihilated by a complex absorbing potential starting at r_c.

Hence the norm of the WF decreases when the wavepacket enters the CAP. We want to inspect in more detail how the CAP annihilates the wavepacket. We know the formal solution of the Schrödinger equation

$$\begin{aligned} \Psi(t+\tau) &= e^{(-iH_0-\eta W)\tau}\ \Psi(t) \\ &= e^{-iH_0\frac{\tau}{2}}\ e^{-\eta W\tau}\, e^{-iH_0\frac{\tau}{2}}\ \Psi(t) + O(\tau^3) \end{aligned} \tag{10.8}$$

i.e. in the middle of each time step, the WF is multiplied by $e^{-\eta W\tau}$, a half Gaussian when $W \sim r^2$ (Fig. 10.1).

When is it legitimate to use a CAP? Of course, it is legitimate to annihilate the outgoing parts when they do not enter the computation of desired observables. For instance, when computing the autocorrelation function

$$a(t) = \big\langle \Psi(0) \big| \Psi(t) \big\rangle \tag{10.9}$$

then it is clear that those parts of $\Psi(t)$ which do not overlap with $\Psi(0)$ and will never return to overlap with $\Psi(0)$ may be annihilated (Fig. 10.2).

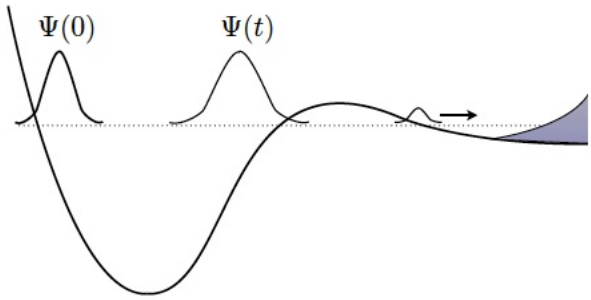

Figure 10.2: Example of the correct location of a CAP.

What happens, if we do not introduce a CAP but still work with a small grid? At the end of the grid one automatically introduces a wall, *i.e.* a grid or

a finite basis set puts the system into a box. Due to the wall, the outgoing part of the WP will be reflected and will again overlap with $\Psi(0)$. This destroys the correctness of the autocorrelation function. Hence a CAP is a great invention. However, it does not only annihilate a WF, but also reflects. The reflection is a non-ideal behaviour of a CAP.

The origin of the reflection is easy to understand. It is related to the Heisenberg uncertainty principle. We change the form of the WF, *i.e.* its coordinate distribution. But this implies that one also changes the momentum distribution which is just the Fourier-transform of the coordinate representation and this means reflection. To see this, let us turn to the time-independent picture.

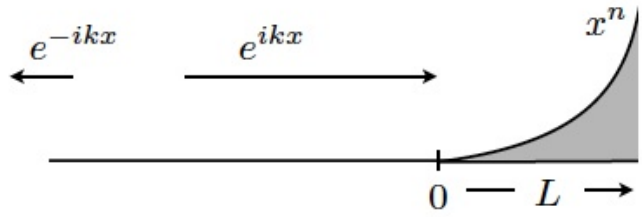

Figure 10.3: Undesired behaviour of a CAP.

At energy E the WF must be a linear combination of e^{ikx} and e^{-ikx} where $E = k^2/2m$. Hence

$$\Psi(x) \sim e^{ikx} - Re^{-ikx} \qquad \text{for} \quad x < 0\,, \tag{10.10}$$

and

$$\Psi(x) \sim Te^{ikx} \qquad \text{for} \quad x > L\,, \tag{10.11}$$

where R and T denote the reflection and transmission coefficients, respectively. If we put an infinite wall at $x = 0$, we have total reflection ($R = 1$) and zero transmission ($T = 0$):

$$\Psi(x) \sim e^{ikx} - e^{-ikx} \sim \sin\ kx \qquad \text{for} \quad x \leq 0\,. \tag{10.12}$$

The wavefunction, which when undisturbed is a plane wave, e^{ikx}, has thus completely lost its form by reflection from the end of the grid.

Using scattering theory and semiclassical arguments, approximate but very reliable formulas for the transmission and reflection coefficients of a CAP have been derived in Ref. "Riss and Meyer, J. Phys. B **26**, 4503 (1993)". (These formulas are evaluated when running the MCTDH script placp.) For the following discussion, we give a simplified form of the lengthy equations which are derived in the above reference.

$$|R|^2 \;=\; \big|\frac{n!}{2^{n+2}}\big|^2 \cdot \frac{\eta^2}{E^2 \cdot k^{2n}} = \big|\frac{n!}{2^{n+2}}\big|^2 \cdot \big(\frac{1}{2m}\big)^n \cdot \frac{\eta^2}{E^{n+2}} \tag{10.13}$$

$$|T|^2 \;=\; \exp\big(-\frac{\eta L^{n+1} \cdot 2m}{k(n+1)}\big) = \exp\big(-\frac{\eta W(L)}{E} \cdot \frac{k \cdot L}{n+1}\big)\,. \tag{10.14}$$

Of course one wants to acheive $|T|^2 + |R|^2 \ll 1$. To keep the reflection small, one needs a weak CAP (small η), in particular when the energy is low. To achieve a small transmittion, for a given CAP-strangth η, one needs a long CAP (L large).

Note that $k \cdot L = 2\pi$ is equivalent to saying that L equals one de-Broglie wavelength. A CAP should be at least two de-Broglie wavelengths long. Hence, when a particle enters the CAP with very low energy, e.g. at a threshold for opening a new channel, then the CAP is likely to produce unwanted reflections.

Chapter 11

Flux analysis

In general there is not much interest in the propagated wavefunction $\Psi(t)$ as such, the quantities of interest are observables like spectra or cross-sections. Spectra are conveniently generated by a Fourier transform of the autocorrelation function, and cross-sections can be computed by a flux-analysis of the time evolved wavefunction.

Consider a reactive scattering event, *e.g.* A + BC $\rightarrow$ AB + C. There are hence two reaction channels, the educt channel A + BC and the product channel C + AB. We assume that the scattering energy is small enough such that a three-body breakup is not possible, AB must be bound when the distance between AB and C becomes large. For simplicity we also ignore the reaction channel AC + B.

We want to know the probability with which an initial wavepacket, which starts in the educt channel, ends up in the product channel. This reaction probability is defined as

$$P_{\text{react}} = \lim_{t\to\infty} \int_{R_c}^{\infty} dR \int d\boldsymbol{q}\, |\Psi(R, \boldsymbol{q}, t)|^2 \,, \tag{11.1}$$

where R denotes the dissociative coordinate and $\boldsymbol{q}$ all remaining coordinates, the latter describing bound motion. The separation, reaction coordinate *vs.* bound coordinates, depends on the reaction channel considered.[1] The interpretation of Eq.(11.1) is clear. The reaction probability is given by that part of the probability density $|\Psi|^2$ which for large times is separated from the AB fragment by a distance larger than R_c. The value of R_c must be large enough to ensure that a particle, which has passed the coordinate space dividing surface defined by $R = R_c$, will never again assume distances smaller than R_c. The limes can be replaced by a time integral over a time derivative[2] and the lower bound of

[1] Actually, we are considering the wavefunction of a particular total angular momentum J (that makes the dissociate coordinate R one-dimensional). Hence Ψ should be replaced with Ψ^J, but for sake of simplicity we suppress the total angular momentum label J.

[2] The initial state has no density beyond R_c, *i.e.* $\theta(R - R_c)|\Psi(R, \boldsymbol{q}, t = 0)|^2 \equiv 0$

the R-integration by a step function θ

$$\begin{aligned} P_{\text{react}} &= \int_0^\infty dt \int\int \theta(R-R_c)\,\frac{\partial}{\partial t}\big(\Psi^*(R,\boldsymbol{q},t)\Psi(R,\boldsymbol{q},t)\big)\,dR\,d\boldsymbol{q} \\ &= i\int_0^\infty dt \int\int (H\Psi^*)\theta\Psi - \Psi^*\theta H\Psi\; dR\,d\boldsymbol{q} \\ &= i\int_0^\infty dt\; \big(\langle H\Psi|\theta|\Psi\rangle - \langle\Psi|\theta H|\Psi\rangle\big) \\ &= i\int_0^\infty \langle\Psi|[H,\theta]|\Psi\rangle\,dt \\ &= \int_0^\infty \langle\Psi(t)|F|\Psi(t)\rangle\,dt \end{aligned} \tag{11.2}$$

where we have introduced the flux operator

$$F = i[H,\theta]\;. \tag{11.3}$$

The reaction probability is hence defined by summing the quantum flux passing through the plane defined by the step function, *i.e.* by $R = R_c$. As the step function commutes with the potential, the Hamiltonian H in Eq.(11.3) can be replaced with the KEO. When the KEO assumes for the dissociative coordinate the simple form $-1/2\mu\cdot\partial^2/\partial R^2$, the flux operator becomes

$$F = \frac{-i}{2\mu}\left(\frac{\partial}{\partial R}\,\delta(R-R_c) + \delta(R-R_c)\,\frac{\partial}{\partial R}\right)\;. \tag{11.4}$$

The flux through a surface is independent of the detailed shape of the surface. This is an important point because it allows us to choose the dividing surface (i.e. the surface where θ jumps from zero to one) quite arbitrarily as long as it separates the educt from the product channel. All following equations involving the flux operator remain valid for any such dividing surface.

It is now convenient to switch to a time-independent picture for a short while. For each reaction channel γ there exist a separate set of coordinates $(R_\gamma, \boldsymbol{q_\gamma})$, where R_γ is the distance between the center of mass of the molecular fragment and the leaving atom (or, for larger systems, the distance between the centers of mass of the two molecular fragments of channel γ). The Hamiltonian is separated into

$$H = -\frac{1}{2\mu_{R_\gamma}}\frac{\partial^2}{\partial R_\gamma^2} + H_\gamma(\boldsymbol{q}_\gamma) + V_\gamma(R_\gamma,\boldsymbol{q}_\gamma) \tag{11.5}$$

where H_γ is the internal Hamiltonian of the separated fragments, and the interaction potential V_γ vanished for $R_\gamma\to\infty$.

The exact scattering wavefunction with outgoing scattering boundary con-

ditions reads

$$\Psi^{+}_{E\alpha\nu}(R_\gamma, \boldsymbol{q}_\gamma) \overset{R_\gamma\to\infty}{\longrightarrow} \Phi^{-}_{E\alpha\nu}(R_\alpha, \boldsymbol{q}_\alpha)\,\delta_{\alpha\gamma} - \sum_{\nu'} S_{\gamma\nu',\alpha\nu}(E)\,\Phi^{+}_{E\gamma\nu'}(R_\gamma, \boldsymbol{q}_\gamma) \tag{11.6}$$

$$\Phi^{\pm}_{E\gamma\nu}(R_\gamma, \boldsymbol{q}_\gamma) = \chi^{\pm}_{E\gamma\nu}(R_\gamma)\,\xi_{\gamma\nu}(\boldsymbol{q}_\gamma) \tag{11.7}$$

$$\chi^{\pm}_{E\gamma\nu}(R_\gamma) = \sqrt{\frac{\mu_{\gamma R}}{2\pi k_{\gamma\nu}}}\, e^{\pm i k_{\gamma\nu} R_\gamma}\ , \tag{11.8}$$

where $\xi_{\gamma\nu}$ is a ro-vibrational eigenstate of the fragment Hamiltonian H_γ, and ν denotes collectively all quantum numbers of this state. The channel momentum $k_{\gamma\nu}$, which appears in the definition of the plane waves $\chi^{\pm}_{E\gamma\nu}(R_\gamma)$, is given by

$$k_{\gamma\nu} = \sqrt{2\mu_{\gamma R}(E - E_{\gamma\nu})} \tag{11.9}$$

with $E_{\gamma\nu}$ being the energy eigenvalue of the fragment Hamiltonian H_γ for the wavefunction $\xi_{\gamma\nu}$. $S_{\gamma\nu',\alpha\nu}$ denotes the S-matrix describing a transition from the initial reaction channel α and initial quantum numbers ν to a final reaction channel γ and final quantum numbers ν'. The upper indices + and - refer to outgoing and ingoing scattering boundary conditions, respectively. The fragment states ξ are L^2 normalized eigenfunctions of the internal fragment Hamiltonian, and the scattering states are normalized to δ-functions.

$$\begin{aligned} \langle \chi^{\pm}_{E\gamma\nu} | \chi^{\pm}_{E'\gamma\nu} \rangle &= \delta(E - E') \\ \langle \Phi^{\pm}_{E\gamma\nu} | \Phi^{\pm}_{E'\gamma\nu'} \rangle &= \delta(E - E')\,\delta_{\nu\nu'} \end{aligned} \tag{11.10}$$

It is now easy to compute the expectation value of the flux operator with respect to the exact scattering state. For $\gamma \neq \alpha$ follows

$$\langle \Psi^{+}_{E\alpha\nu} \,|\, F_\gamma \,|\, \Psi^{+}_{E\alpha\nu} \rangle = \frac{1}{2\pi} \sum_{\nu'} |S_{\gamma\nu',\alpha\nu}(E)|^2\ , \tag{11.11}$$

where we have used, cf. Eq. (11.4), that

$$\langle \chi^{\pm}_{E\gamma\nu} | F_\gamma | \chi^{\pm}_{E\gamma\nu} \rangle = \pm \frac{1}{2\pi} \tag{11.12}$$

holds. The sum over the internal states may be removed by employing projectors onto these states,

$$P_{\gamma\nu} = |\,\xi_{\gamma\nu}\rangle\langle\xi_{\gamma\nu}\,|\,, \tag{11.13}$$

yielding[3]

$$\langle \Psi^{+}_{E\alpha\nu} \,|\, P_{\gamma\nu'} F_\gamma P_{\gamma\nu'} \,|\, \Psi^{+}_{E\alpha\nu} \rangle = \frac{1}{2\pi}\, |\, S_{\gamma\nu',\alpha\nu}(E)\,|^2\ . \tag{11.14}$$

The integral cross-section can be computed from the $|S|^2$ elements. For this we have to remember that, for sake of simplicity, we have suppressed the total

[3] Actually $P_{\gamma\nu}$ commutes with F_γ. Thus $P_{\gamma\nu} F_\gamma = F_\gamma P_{\gamma\nu} = P_{\gamma\nu} F_\gamma P_{\gamma\nu}$. The extra projector is added for symmetry reasons only.

angular momentum index J from wavefunctions and S-matrix.[4] All equations above are diagonal in J. Re-introducing J we can write the integral cross-section as

$$\sigma_{\gamma\nu'\leftarrow\alpha\nu} = \frac{\pi}{k^2_{\alpha\nu}} \sum_{J=0}^{\infty} (2J+1) |S^J_{\gamma\nu',\alpha\nu}(E)|^2 \,, \tag{11.15}$$

where $k_{\alpha\nu}$ denotes the initial momentum with which the two fragments collide. Summing over all final quantum numbers ν' one obtains the initial state selected total cross section

$$\begin{aligned} \sigma_{\gamma\leftarrow\alpha\nu} &= \sum_{\nu'} \sigma_{\gamma\nu'\leftarrow\alpha\nu} \\ &= \frac{2\pi^2}{k^2_{\gamma\nu}} \sum_{J=0}^{\infty} (2J+1) \langle \Psi^{J+}_{E\alpha\nu} \,|\, F_\gamma \,|\, \Psi^{J+}_{E\alpha\nu} \rangle \,. \end{aligned} \tag{11.16}$$

Note that the flux formalism automatically sums over all final states if there is no projection.

Turning to a time-dependent approach one starts with an initial wave packet Ψ_0 which is a superposition of infinitely many exact scattering states. Formally Ψ_0 is written as

$$\Psi_0 = \sum_\nu \int c_\nu(E)\, \Psi^+_{E\alpha\nu}\, dE \tag{11.17}$$

This wavepacket may then be propagated. But in the end one is not interested in the time evolved wavepacket $\Psi(t)$, not even in its reaction probability Eq. (11.1), in general one is interested to compute *energy resolved* quantities. For this we define the flux function

$$F_\gamma(E,\Psi_0) = 2\pi \langle \Psi_0 | \delta(H-E)\, F_\gamma\, \delta(H-E) | \Psi_0 \rangle \,, \tag{11.18}$$

or, state resolved

$$F_\gamma(E,\nu,\Psi_0) = 2\pi \langle \Psi_0 | \delta(H-E)\;\; P_{\gamma\nu} F_\gamma P_{\gamma\nu}\, \delta(H-E) | \Psi_0 \rangle \,. \tag{11.19}$$

Before we continue with the flux analysis, let us study the action of the δ-function on the initial wavepacket

$$\delta(H-E)\,\Psi_0 = \sum_\nu \int c_\nu(E)\, \delta(H-E)\, \Psi^+_{E'\alpha\nu}\, dE' = \sum_\nu c_\nu(E)\, \Psi^+_{E\alpha\nu} \,, \tag{11.20}$$

and introduce the energy density function

$$|\Delta(E)|^2 := \langle \Psi_0 |\, \delta(H-E)\, | \Psi_0 \rangle = \sum_\nu |c_\nu(E)|^2 \,, \tag{11.21}$$

where the last equation follows from Eqs. (11.10,11.20).

Next we want to discuss the flux analysis of a direct dissociation process, *e.g* photodissociation of NOCl. Then there is only one channel and we suppress

[4] We have also suppressed some J-dependent phase factors in Eqs (11.6,11.8). They are irrelevant, because here we consider only the modulus of the S-matrix elements.

the channel index γ in the following discussion. Using Eq. (11.20,11.12), the flux-function takes the form

$$\begin{aligned} F(E,\Psi_0) &= 2\pi \sum_{\nu} \sum_{\nu'} c^*_{\nu}(E)\, c_{\nu'}(E)\, \langle \Psi^+_{E\alpha\nu}|\, F\, |\Psi^+_{E\alpha\nu'}\rangle \\ &= 2\pi \sum_{\nu} |c_{\nu}(E)|^2\, \langle \chi^+_{E\nu}|F|\chi^+_{E\nu}\rangle \\ &= \sum_{\nu} |c_{\nu}(E)|^2\,, \end{aligned} \tag{11.22}$$

or, state resolved

$$F(E,\nu,\Psi_0) = |c_{\nu}(E)|^2\,. \tag{11.23}$$

Hence, in this case the unprojected flux reproduces the energy density function, *i.e.* the power spectrum. The latter is more easily computed by a Fourier transform of the autocorrelation function. However, the projected flux provides more information, namely the dissociation probability for leaving the fragment molecule (here NO) in a particular ro-vibrational state ν.

Turning back to reactive scattering, it is now easy to show that

$$F_{\gamma}(E,\Psi_0) = \sum_{\nu,\nu'} |c_{\nu}(E)|^2\, |S_{\gamma\nu',\alpha\nu}(E)|^2\,, \tag{11.24}$$

and

$$F_{\gamma}(E,\nu',\Psi_0) = \sum_{\nu} |c_{\nu}(E)|^2\, |S_{\gamma\nu',\alpha\nu}(E)|^2\,. \tag{11.25}$$

When the initial state, as usual for reactive scattering calculations, is pure in the initial quantum number ν, the sum over ν drops out. In this case the modulus of the S-matrix element is given by

$$|S_{\gamma\nu',\alpha\nu}(E)|^2 = F_{\gamma}(E,\nu',\Psi_{0\nu})/|\Delta(E)|^2 \tag{11.26}$$

where we have replaced Ψ_0 with $\Psi_{0\nu}$ to indicate that this initial state is a pure state with quantum number ν with respect to the internal degrees of freedom.

What is left to be done is to define a stable and efficient method to evaluate the flux-function. After the wavepacket has passed the surface defined by $R = R_c$ it is no longer needed and can be absorbed by a CAP which starts at $R = R_c$. The R-grid then ends at R_c+L, where L is the length of the CAP. We know from Eq. (10.6) that the speed of annihilation is proportional to the matrix element of the CAP, hence it should be possible to express the flux by such a matrix element. Indeed, let us introduce the CAP augmented Hamiltonian

$$\tilde{H} = H - iW\,, \tag{11.27}$$

where H is Hermitian and W a real, non-negative, continuous function[5] of R, which vanishes for $R \le R_c$. Hence W commutes with the flux defining step function, *i.e.* $\theta W = W\theta = W$. The flux operator may now be written as (cf. Eq. (11.3)

$$F = iH\theta - i\theta H = 2W + i\tilde{H}^{\dagger}\theta - i\theta\tilde{H}\,. \tag{11.28}$$

[5]Here the strength parameter η is included in the definition of W, in contrast to Chapter 10.

Turning to the reaction probability $P_{\rm react}$ of Eqs. (11.1,11.2) one obtains

$$\begin{aligned} P_{\rm react} &= \int_0^\infty \langle\Psi(t)|F|\Psi(t)\rangle\, dt \\ &= \int_0^\infty \langle\Psi(t)|2W|\Psi(t)\rangle\, dt \\ &\quad + \int_0^\infty \frac{d}{dt}\langle\Psi(t)|\theta|\Psi(t)\rangle\, dt\ , \end{aligned} \tag{11.29}$$

where the last term can be understood by noting that $\partial_t\langle\Psi(t)| = i\langle\Psi(t)|\tilde{H}^\dagger$, and $\partial_t|\Psi(t)\rangle = -i\tilde{H}|\Psi(t)\rangle$. This last line vanishes, because $\langle\Psi(t)|\theta|\Psi(t)\rangle = 0$ for both $t = 0$ and $t = \infty$. Initially Ψ has no contributions for $R \geq R_c$ and finally that part of Ψ, which has entered the reaction channel, has vanished because of the CAP. However, in practice one does not propagate to infinite times but stops the propagation at some final time T. In this case it is useful to keep the second term, which is trivial to integrate. The working equation thus reads

$$P_{\rm react} = 2\int_0^T \langle\Psi(t)|W|\Psi(t)\rangle\, dt \ + \ \langle\Psi(T)|\theta|\Psi(T)\rangle\ . \tag{11.30}$$

The first part accounts for the density which is annihilated by the CAP and the second part stands for the density which still exist on the interval $[R_c, R_c + L]$. If one runs `flux84` of the MCTDH package, then these two terms and their sum are written to the file `iwtt` at every output time step.

We want to use the technique developed here to derive working equations for the flux function $F_\gamma(E, \Psi_0)$. We re-introduce the channel index γ, there will be a CAP, $-iW_\gamma$, in each reaction channel. The δ-functions are expressed in Fourier representation

$$\delta(H - E) = \frac{1}{2\pi}\int_{-\infty}^{\infty} e^{-i(H-E)t}\, dt \tag{11.31}$$

Inserting this equation into Eq. (11.18), replacing H with $\tilde{H}$, and making use of Eq. (11.28) one obtains

$$\begin{aligned} F_\gamma(E, \Psi_0) &= \frac{1}{2\pi}\int_{-\infty}^{\infty} dt \int_{-\infty}^{\infty} dt' \langle\Psi_0|e^{i(\tilde{H}^\dagger - E)t} F_\gamma e^{-i(\tilde{H}-E)t'}|\Psi_0\rangle \\ &= \frac{1}{2\pi}\int_0^\infty dt \int_0^\infty dt' \langle\Psi(t)|2W_\gamma|\Psi(t')\rangle e^{-iE(t-t')} \\ &\quad + (\frac{d}{dt} + \frac{d}{dt'})\langle\Psi(t)|\theta_\gamma|\Psi(t')\rangle e^{-iE(t-t')}\ , \end{aligned} \tag{11.32}$$

where $\Psi(t) = \exp(-i\tilde{H}t)\Psi_0$ is used and where again the lower limits of the integrals could be safely replaced with zero, because for negative times the wavepacket cannot reach the CAP region of the γ's reaction channel. We now replace the upper integral limits with the final propagation time T and first

evaluate the second term

$$\begin{aligned} F_{\gamma,\theta}(E,\Psi_0) &= \frac{1}{2\pi}\int_0^T dt\,\langle\Psi(t)|\theta_\gamma|\Psi(T)\rangle e^{iE(T-t)} \\ &\quad +\frac{1}{2\pi}\int_0^T dt'\,\langle\Psi(T)|\theta_\gamma|\Psi(t')\rangle e^{-iE(T-t')} \\ &= \frac{1}{\pi}\mathrm{Re}\int_0^T dt\,\langle\Psi(t)|\theta_\gamma|\Psi(T)\rangle e^{iE(T-t)} \\ &= \frac{1}{\pi}\mathrm{Re}\int_0^T d\tau\,\langle\Psi(T-\tau)|\theta_\gamma|\Psi(T)\rangle e^{iE\tau}\ , \end{aligned} \tag{11.33}$$

where we used the substitution $\tau = T - t$. To evaluate the first term of Eq. (11.32) we substitute $t' = t + \tau$

$$\begin{aligned} F_{\gamma,W}(E,\Psi_0) &= \frac{1}{\pi}\int_0^T d\tau\int_0^{T-\tau} dt\,\langle\Psi(t)|W_\gamma|\Psi(t+\tau)\rangle e^{iE\tau} \\ &\quad +\frac{1}{\pi}\int_{-T}^0 d\tau\int_{-\tau}^T dt\,\langle\Psi(t)|W_\gamma|\Psi(t+\tau)\rangle e^{iE\tau}\ . \end{aligned} \tag{11.34}$$

With the substitutions $\tau \to -\tau$ and then $t \to t + \tau$ the second integral turns into

$$\frac{1}{\pi}\int_0^T d\tau\int_0^{T-\tau} dt\,\langle\Psi(t+\tau)|W_\gamma|\Psi(t)\rangle e^{-iE\tau} \tag{11.35}$$

which is just the complex conjugate of the first integral of Eq. (11.34). Hence

$$F_{\gamma,W}(E,\Psi_0) = \frac{2}{\pi}\mathrm{Re}\int_0^T d\tau\int_0^{T-\tau} dt\,\langle\Psi(t)|W_\gamma|\Psi(t+\tau)\rangle\, e^{iE\tau}\ . \tag{11.36}$$

In practice we define the auxiliary function $g(\tau)$

$$g(\tau) = \int_0^{T-\tau}\langle\Psi(t)|W_\gamma|\Psi(t+\tau)\rangle\,dt\ +\ \frac{1}{2}\langle\Psi(T-\tau)|\theta_\gamma|\Psi(T)\rangle\ . \tag{11.37}$$

The flux, $F_\gamma = F_{\gamma,W} + F_{\gamma,\theta}$, is then given by the Fourier integral

$$F_\gamma(E,\Psi_0) = \frac{2}{\pi}\mathrm{Re}\int_0^T g(\tau)\,e^{iE\tau}d\tau\ . \tag{11.38}$$

Of course one can make use of projectors here as well. For this one merely replaces W_γ and θ_γ in Eq. (11.37) with $P_{\gamma\nu}W_\gamma P_{\gamma\nu}$ and $P_{\gamma\nu}\theta_\gamma P_{\gamma\nu}$, respectively.

Finally we note that if no projectors are used, the dissociative coordinate may be any coordinate which separates the fragments, it does not need to be Jacobian-like. If projectors are used one needs a Jacobian-like dissociate coordinate, because otherwise an internal channel Hamiltonian H_γ cannot be defined.

Chapter 12

Filter-Diagonalization (FD)

We know that the exact autocorrelation function of a bound system is given by (see Chapter 1):

$$a(t) = \sum_n \left|c_n\right|^2 \, e^{-iE_n t} \tag{12.1}$$

with

$$c_n = \left\langle \Psi_n \middle| \Psi(0) \right\rangle \text{ and } H\Psi_n = E\Psi_n \tag{12.2}$$

The intensities $\left|c_n\right|^2$ and the eigenenergies E_n can be obtained by a Fourier transform of $a(t)$, but this requires that $a(t)$ is given for all times, otherwise we have a finite resolution.

But if there is only a finite number, say 100 or less, of lines with noticeable intensity, then one may simply fit the right hand side of Eq. (12.1) to the first short period of the autocorrelation function $a(t)$. However, this is a non-linear fit, which complicates the analysis.

The FD-method accomplishes such a fit by linear algebra. Within some energy window one defines a usually equally spaced energy grid $\epsilon_1 < \epsilon_2 < \cdots \epsilon_n$ (Fig. 12.1). For each point of the energy grid one computes the filtered states: [1]

$$\Psi_{E_k} = \int g(t) \; \tilde{\Psi}(t) \; e^{i\epsilon_k} \; dt \tag{12.4}$$

Such a state is a superposition of exact eigenstates with energy near ϵ_k, $g(t)$ is a window function introduced in Section 1.3.1. We take the filtered states as basis set and compute the Hamiltonian matrix

$$H_{jk} = \left\langle \Psi_{E_j} \middle| H \middle| \Psi_{E_k} \right\rangle \tag{12.5}$$

as well as the overlap matrix

$$\Theta_{jk} = \left\langle \Psi_{E_j} \middle| \Psi_{E_k} \right\rangle \tag{12.6}$$

which is needed because the filtered states are not orthonormal.

[1] Note that

$$\Psi_E \sim \delta(H - E) \; \Psi(0) \sim \int_{-\infty}^{\infty} e^{iEt} \Psi(t) dt \tag{12.3}$$

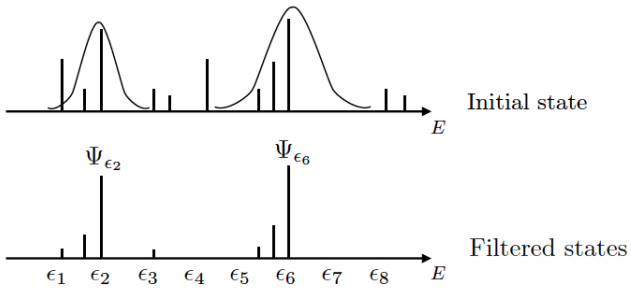

Figure 12.1: Filter diagonalization. The upper picture shows a spectral decomposition (Power Spectrum) of an initial state and, symbolically, the filtering envelopes. The lower figure shows the spectral decomposition of two filtered states.

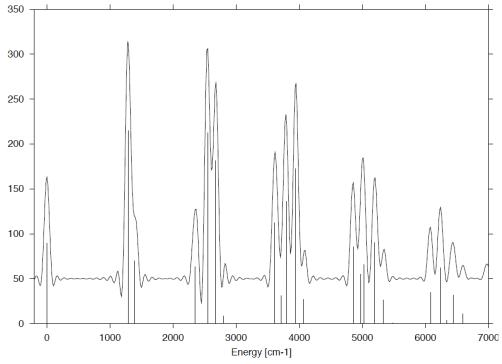

Figure 12.2: The vibrational spectrum of CO_2 as obtained by Fourier transform of the autocorrelation function and by FD using the same autocorrelation function. For better visibility, the Fourier spectrum is shifted upwards by 50 units.

Then we solve the generalized eigenvalue problem

$$\boldsymbol{H}\boldsymbol{b_n} = \tilde{E}_n \boldsymbol{\Theta}\boldsymbol{b_n} \tag{12.7}$$

where $\tilde{E}_n$ is our approximation to the exact eigenenergy E_n. The approximate eigenvectors are given by

$$\Psi_{E_n} = \sum_j b_{j_n}\ \Psi_{\epsilon_j} \tag{12.8}$$

The method works because in practice one never computes the filtered states Ψ_{ϵ_j}. The overlap-matrix $\boldsymbol{\Theta}$ and the Hamiltonian matrix $\boldsymbol{H}$ can be directly calculated from the autocorrelation function $a(t)$

$$\Theta_{jk} = Re \int_0^T G(E_j - E_k, \tau)\ a(\tau)\ e^{i\frac{E_j+E_k}{2}\tau}\ d\tau \tag{12.9}$$

$$H_{jk} = Re \int_0^T i\ \dot{G}(E_j - E_k, \tau)\ a(\tau)\ e^{i\frac{E_j+E_k}{2}\tau}\ d\tau \tag{12.10}$$

where G is a known but complicated function which depends on the window function g (see J. Chem. Phys.,**109**,3730 (1998)). Hence FD is just another but more efficient form to extract the information from the autocorrelation function $a(t)$. The FD algorithm is more efficient than the Fourier transform of the autocorrelation function, because it "knows" that the spectra consist of discrete lines of positive intensity.

The usefulness of the filter-diagonalization approach is demonstrated in Fig. 12.2 where a spectrum obtained by Fourier-transform of the autocorrelation function is compared with the stick spectrum obtained by filter-diagonalization using the same autocorrelation function.

Appendix A

Discrete Variable Representation (DVR)

A.1 Introduction

On a computer a function has to be represented by a *finite* set of numbers, *i.e.* by a vector. To achieve this discretization, one may use basis sets representations (Spectral methods)

$$\Psi = \sum_{j=1}^{N} a_j \phi_j, \;\; a_j = \langle \phi_j | \Psi \rangle$$

$$\Psi \to \boldsymbol{a} = (a_1, a_2, \ldots, a_N)^T$$

or grid representations

$$x_\alpha, \alpha = 1, \ldots, N \text{ grid points}$$

$$\Psi(x) \to (\Psi(x_1), \ldots, \Psi(x_N))^T = (\Psi_1, \ldots, \Psi_N)^T = \{\Psi_\alpha\}$$

The great advantage of grid methods is that the application of the in general complicated potential operator is very simple

$$(\hat{V}\Psi)_\alpha = (\hat{V}\Psi)(x_\alpha) = V(x_\alpha) \cdot \Psi(x_\alpha) \tag{A.1}$$

For doing matrix-elements by quadrature over the grid, we need weights in addition

$$\langle \Psi | \Phi \rangle = \sum_{\alpha=1}^{n} w_\alpha \Psi^*(x_\alpha) \Phi(x_\alpha) \tag{A.2}$$

But the most difficult problem are the differential operators, because there is no differentiable function anymore. If one interpolates the points *locally*, one arrives at the finite-difference formulas, *e.g.*

$$\Psi''(x_\alpha) \approx \frac{1}{h^2} \left(\Psi(x_{\alpha+1}) - 2\Psi(x_\alpha) + \Psi(x_{\alpha-1}) \right) \tag{A.3}$$

(local quadratic interpolation of an equidistant grid, where h is the grid spacing). Unfortunately, the finite differences are not too accurate!

A.2 Discrete Variable Representation

A DVR, like a basis representation, is a global approximation of high accuracy. To arrive at a DVR we diagonalize the matrix representation of the coordinate operator

$$\begin{aligned} Q_{jk} &= \langle \varphi_j | \hat{x} | \varphi_k \rangle && \text{(A.4)} \\ \boldsymbol{Q} &= \boldsymbol{U}\ \boldsymbol{X}\ \boldsymbol{U}^{\dagger} \quad \text{Eigenvector matrix} && \text{(A.5)} \\ \boldsymbol{X}_{\alpha\beta} &= x_\alpha^2\ \delta_{\alpha\beta} \quad \text{Eigenvalue matrix} && \text{(A.6)} \end{aligned}$$

If $\boldsymbol{Q}$ is tri-diagonal, then the weights are given as

$$w_\alpha^{1/2} = \frac{U_{k,\alpha}}{\varphi_k^*(x_\alpha)} \tag{A.7}$$

independent of k![1]

Hence we have a quadrature rule, and the matrix elements

$$\begin{aligned} \big\langle \varphi_j \big| \varphi_k \big\rangle &= \sum_{\alpha=1}^{N} w_\alpha\ \varphi_j^*(x_\alpha)\ \varphi_k(x_\alpha) = \delta_{\alpha\beta} && \text{(A.8)} \\ \big\langle \varphi_j \big| \hat{x} \big| \varphi_k \big\rangle &= \sum_{\alpha=1}^{N} w_\alpha\ \varphi_j^*(x_\alpha)\ x_\alpha\ \varphi_k(x_\alpha) = Q_{jk} && \text{(A.9)} \end{aligned}$$

are *exact* in quadrature.

Next we introduce DVR-functions defined as

$$\chi_\alpha(x) = \sum_{j=1}^{N} \varphi_j(x)\ U_{j\alpha} \tag{A.10}$$

The DVR functions are, of course, orthonormal

$$\big\langle \chi_\alpha \big| \chi_\beta \big\rangle = \delta_{\alpha\beta} \tag{A.11}$$

and they behave like δ-functions on the grid

$$\chi_\alpha\big(x_\beta\big) = w_\alpha^{-1/2}\ \delta_{\alpha\beta} \tag{A.12}$$

Potential matrix elements are now simple

$$\begin{aligned} \big\langle \chi_\alpha \big| V \big| \chi_\beta \big\rangle &= \sum_{\gamma=1}^{N} w_\gamma\ \chi_\alpha^*(x_\gamma)\ V(x_\gamma)\ \chi_\beta(x_\gamma) \\ &= \sum_{\gamma=1}^{N} w_\gamma\ w_\alpha^{-1/2}\ w_\beta^{-1/2}\ \delta_{\alpha\gamma}\ \delta_{\beta\gamma}\ V(x_\gamma) \\ &= V(x_\gamma)\ \delta_{\alpha\beta} && \text{(A.13)} \end{aligned}$$

[1] This is called a proper DVR. The quadrature is then of Gaussian quality. If Q is not tri-diagonal one speaks of an improper DVR. An improper DVR does not provide weights. Here we assume proper DVRs, but the CDVR method (see Chapter 6) as well as the well known "potential optimized DVR" (PODVR) method are built on improper DVRs.

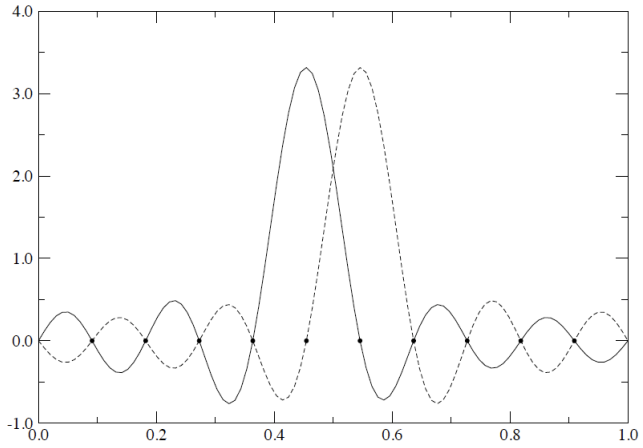

Figure A.1: Two sine DVR functions (solid and dashed lines) centred at two consecutive DVR points. Note that the functions are strictly zero at all DVR points (black dots) but one, which labels the function.

This is the DVR approximation. It is an approximation because the matrix element is done by quadrature, not exactly. Similarly

$$\langle \chi_\alpha | \Psi \rangle = \sum_{\gamma=1}^{N} w_\gamma \; \chi_\alpha^*(x_\gamma) \; \Psi(x_\gamma) = w_\alpha^{-1/2} \; \Psi(x_\alpha) \tag{A.14}$$

connecting grid and basis set representations.

We represent the WF by its values at the grid points times square root of weights

$$\Psi(x) \to \mathbf{\Psi} = \left(w_1^{1/2} \Psi(x_1), \ldots, w_N^{1/2} \Psi(x_N) \right)^T \tag{A.15}$$

which is both, a grid and a spectral representation (see Eq. A.14, pseudo-spectral methods). Integrals are now simple

$$\langle \Psi | \Phi \rangle = \sum_{\alpha=1}^{N} w_\alpha \; \Psi_\alpha^*(x_\alpha) \; \Phi(x_\alpha) = \sum_{\alpha=1}^{N} \Psi_\alpha^* \; \Phi_\alpha = \mathbf{\Psi}^* \cdot \mathbf{\Phi} \tag{A.16}$$

In fact, one almost never needs the weights, as they are build into the WF. Only for plotting a WF or generating an initial WF from an analytic expression, weights are needed.

To derive the kinetic energy operator for the DVR-grid representations, we start considering its basis set representation (finite basis representation, FBR).

$$T_{jk}^{\mathrm{FBR}} = \langle \varphi_j | \hat{T} | \varphi_k \rangle \tag{A.17}$$

where we assume that the matrix elements can be done analytically.

The DVR-representation is then given by a unitary transformation

$$T^{\mathrm{DVR}}_{\alpha\beta} = \langle \chi_\alpha | \hat{T} | \varphi_\beta \rangle = \left(\boldsymbol{U}^\dagger \, \boldsymbol{T}^{\mathrm{FBR}} \, \boldsymbol{U} \right)_{\alpha\beta} \tag{A.18}$$

Remarks:

(i) a DVR must be consistent with the the volume element used: dr, $r^2 dr$, $sin\theta \; d\theta$, etc.

(ii) a DVR must be consistent with the boundary conditions applied.

(iii) the potential should be smoother than the WF to ensure that the DVR error is small, (no hard walls). The variational property is destroyed because the potential matrix elements are not evaluated exactly, *i.e.* computed eigenvalues are not necessarily upper bounds to the exact ones.

(iv) for smooth potentials and not too few grid points, the DVR error (*cf.* Eq. (A.13)) is in general smaller or of the same order than the basis set truncation error.

For a more comprehensive discussion on DVRs see Appendix B of the MCTDH review (Phys.Rep. **324**, 1 (2000)).

Appendix B

Lagrangian, McLachlan, and Dirac-Frenkel variational principles

B.1 Time-Dependent Variational Principles

A model wave function Ψ can be considered to depend on parameters λ_j. There may be a finite or a countable infinite number of parameters. Examples for parameters are the expansion coefficients of a basis set expansion of a wave function, the Fourier coefficients of a Fourier series of a periodic function (or one restricted to a finite support), or the parameters of a Heller-Gaussian.

The space of allowed variations $\{\delta\Psi\}$ is the linear space spanned by the partial derivatives $\frac{\partial\Psi}{\partial\lambda_j}$. Hence,

$$\delta\Psi = \sum_j \frac{\partial\Psi}{\partial\lambda_j}\delta\lambda_j \tag{B.1}$$

and

$$\dot{\Psi} = \sum_j \frac{\partial\Psi}{\partial\lambda_j}\dot{\lambda}_j \tag{B.2}$$

which shows that $\dot{\Psi} \in \{\delta\Psi\}$. If all parameters are complex and if Ψ is analytic in its parameters, then the variation $i\delta\Psi$ is an allowed one if $\delta\Psi$ is allowed.

B.1.1 Lagrangian variational principle

The Lagrangian variational principle (VP) reads

$$L = \langle\Psi|i\frac{\partial}{\partial t} - H|\Psi\rangle \tag{B.3}$$

$$\delta\int_{t_1}^{t_2} L dt = 0 \tag{B.4}$$

subject to the boundary conditions $\delta L(t_1) = \delta L(t_2) = 0$
Writing the equation more explicitly yields

$$
\begin{aligned}
0 &= \int_{t_1}^{t_2} dt \int dx\ \delta\big(\Psi^* i\frac{\partial}{\partial t}\Psi - \Psi^* H\Psi\big) && \text{(B.5)}\\
&= \int_{t_1}^{t_2} dt \int dx\ \delta\Psi^*\, i\frac{\partial}{\partial t}\Psi - \delta\Psi^* H\Psi \\
&\quad + \Psi^*\, i\frac{\partial}{\partial t}\delta\Psi - \Psi^* H\delta\Psi && \text{(B.6)}\\
&= \int_{t_1}^{t_2} dt \int dx\ \delta\Psi^*\, i\frac{\partial}{\partial t}\Psi - \delta\Psi^* H\Psi \\
&\quad - i\frac{\partial}{\partial t}\Psi^*\,\delta\Psi - \Psi^* H\delta\Psi && \text{(B.7)}\\
&= \int_{t_1}^{t_2} dt\ \langle\delta\Psi|i\frac{\partial}{\partial t} - H|\Psi\rangle + \langle\Psi| - i\frac{\partial}{\partial t} - H|\delta\Psi\rangle && \text{(B.8)}\\
&= \int_{t_1}^{t_2} dt\ 2\,\mathrm{Re}\,\langle\delta\Psi|i\frac{\partial}{\partial t} - H|\Psi\rangle && \text{(B.9)}
\end{aligned}
$$

As the integration limits t_1 and t_2 are arbitrary, one obtains

$$\mathrm{Re}\,\langle\delta\Psi|i\frac{\partial}{\partial t} - H|\Psi\rangle = 0 \qquad \text{(B.10)}$$

Note that δ and $\partial/\partial t$ commute, as partial derivatives commute. Remember that $\delta\Psi$ can be viewed as a partial derivative of Ψ with respect to some parameter. The step (B.6) $\rightarrow$ (B.7) uses partial integration.

B.1.2 McLachlan variational principle

The McLachlan VP reads

$$\delta||i\frac{\partial}{\partial t}\Psi - H\Psi||^2 = 0 \qquad \text{(B.11)}$$

where only the time derivative is to be varied. We write the norm-squared term as a scalar product and vary bra and ket side of this product.

$$
\begin{aligned}
0 &= \delta\langle i\frac{\partial}{\partial t}\Psi - H\Psi|i\frac{\partial}{\partial t}\Psi - H|\Psi\rangle && \text{(B.12)}\\
&= \langle i\delta\frac{\partial}{\partial t}\Psi|i\frac{\partial}{\partial t} - H|\Psi\rangle\ +\ \langle(i\frac{\partial}{\partial t} - H)\Psi|i\delta\frac{\partial}{\partial t}\Psi\rangle && \text{(B.13)}\\
&= -i\,\langle\delta\Psi|i\frac{\partial}{\partial t} - H|\Psi\rangle\ +\ i\,\langle(i\frac{\partial}{\partial t} - H)\Psi|\delta\Psi\rangle && \text{(B.14)}\\
&= 2\,\mathrm{Im}\,\langle\delta\Psi|i\frac{\partial}{\partial t} - H|\Psi\rangle && \text{(B.15)}
\end{aligned}
$$

In step (11) $\rightarrow$ (12) we have used the fact, that $\{\delta\frac{\partial}{\partial t}\Psi\}$ and $\{\delta\Psi\}$ span the same linear space.

B.1.3 Dirac-Frenkel variational principle

If for each variation $\delta\Psi$, $i\delta\Psi$ is also an allowed variation, then both the Lagrangian and the McLachlan VP turn into the Dirac-Frenkel VP

$$\langle\delta\Psi|i\frac{\partial}{\partial t} - H|\Psi\rangle = 0 \tag{B.16}$$

As the Dirac-Frenkel VP is the simplest of the three VPs discussed, we prefer to use the Dirac-Frenkel VP when deriving the MCTDH-EOM.